

2011

# The effect of exopolymers on the compressibility and shear strength of kaolinite

Rick Alton Nugent

*Louisiana State University and Agricultural and Mechanical College, rnugen2@lsu.edu*

Follow this and additional works at: [https://digitalcommons.lsu.edu/gradschool\\_dissertations](https://digitalcommons.lsu.edu/gradschool_dissertations)



Part of the [Civil and Environmental Engineering Commons](#)

---

## Recommended Citation

Nugent, Rick Alton, "The effect of exopolymers on the compressibility and shear strength of kaolinite" (2011). *LSU Doctoral Dissertations*. 1130.

[https://digitalcommons.lsu.edu/gradschool\\_dissertations/1130](https://digitalcommons.lsu.edu/gradschool_dissertations/1130)

This Dissertation is brought to you for free and open access by the Graduate School at LSU Digital Commons. It has been accepted for inclusion in LSU Doctoral Dissertations by an authorized graduate school editor of LSU Digital Commons. For more information, please contact [gradetd@lsu.edu](mailto:gradetd@lsu.edu).

**THE EFFECT OF EXOPOLYMERS ON THE COMPRESSIBILITY AND SHEAR  
STRENGTH OF KAOLINITE**

A Dissertation

Submitted to the Graduate Faculty of the  
Louisiana State University and  
Agricultural and Mechanical College  
in partial fulfillment of the  
requirements for the degree of  
Doctor of Philosophy

in

The Department of Civil and Environmental Engineering

By

Rick Alton Nugent  
B.S., Louisiana State University, 2007  
May, 2011

## **ACKNOWLEDGEMENTS**

I would like to thank my advisor, Dr. Guoping Zhang, whose wise counsel has been so instrumental to my success. I also would like to thank the other members of my Advisory Committee: Dr. Robert Gambrell, Dr. Khalid Alshibli, and Dr. Zhi-Qiang Deng. I greatly appreciate their guidance and the time and energy that they have expended in providing me with the help that I needed to complete my research.

Additionally, I thank the many professors at Louisiana State University who taught me numerous lessons that I shall never forget and who helped prepare me for my future endeavors. I especially thank the professors with whom I worked while an undergraduate at LSU: Dr. Guoping Zhang, Dr. William Henk, Dr. Marc Levitan, and Dr. W. Todd Monroe. Not to be forgotten, are the secretaries and administrative staff in the Department of Engineering who were always ready to assist me when I needed help.

I would also like to recognize the many friends that I have made while studying at LSU. It has been a pleasure studying alongside my fellow students and working with other team and club members. In particular, I would like to thank Yeimi Soler and Jacques Boudreaux for their comradeship and help in my research.

In addition, I am thankful for the awards that I have received that provided me with financial support, especially the Donald Clayton Graduate Scholarship award. I also thank the Coastal Restoration and Enhancement through Science and Technology (CREST) program and NOAA for their financial support for my research.

Last, but not least, I would like to thank my family who encouraged me throughout my studies. This includes my brother Ross, my mother Ouida, and my father Dennis, who recently passed away. To each and every one, I extend heartfelt thanks.

## TABLE OF CONTENTS

ACKNOWLEDGEMENTS .....	ii
LIST OF TABLES .....	vi
LIST OF FIGURES .....	vii
ABSTRACT .....	x
CHAPTER 1. INTRODUCTION .....	1
1.1 Dissertation Objectives .....	3
1.2 Dissertation Layout .....	4
CHAPTER 2. LITERATURE REVIEW .....	6
2.1 Exopolymers and Erosion .....	6
2.2 Exopolymers and Shear Strength .....	7
2.3 Guar Gum .....	7
2.4 Xanthan Gum .....	8
2.5 Kaolinite .....	9
CHAPTER 3. THE EFFECT OF EXOPOLYMERS ON THE LIQUID LIMIT OF KAOLINITE AND ITS ENGINEERING IMPLICATIONS .....	12
3.1 Introduction .....	12
3.2 Materials and Methods .....	14
3.2.1 Materials .....	14
3.2.2 Xanthan Gum .....	14
3.2.3 Guar Gum .....	15
3.2.4 Preparation of Biopolymer Solutions .....	16
3.2.5 Liquid Limit Test .....	17
3.2.6 ESEM Imaging .....	18
3.3 Results and Discussion .....	19
3.3.1 Biopolymer Solution Viscosity .....	19
3.3.2 Biopolymer Mediated Aggregation .....	23
3.3.3 Biopolymer Cross-linking .....	25
3.3.4 Biopolymer Adsorption on Kaolinite .....	27
3.3.5 Engineering Implications .....	30
3.4 Conclusions .....	31
CHAPTER 4. THE EFFECT OF EXOPOLYMERS, VOID RATIO, AND CATIONS ON THE EROSIONAL RESISTANCE OF KAOLINITE .....	33
4.1 Introduction .....	33
4.2 Materials and Methods .....	35
4.2.1 Guar Gum .....	36
4.2.2 Xanthan Gum .....	37
4.2.3 Preparation of Biopolymer and Clay Mixtures .....	37

4.2.4 Cohesive Strength Meter Methodology and Data Analysis .....	40
4.3 Results and Discussion .....	42
4.3.1 Biopolymer Mixtures with DI Water and 180% Initial Water Content ....	45
4.3.2 Guar Gum Mixtures with DI Water and Varying Initial Water Content ..	47
4.3.3 Xanthan Gum Mixtures with Calcium and Sodium Background Cations.	48
4.3.4 Guar Gum Mixtures with Sodium and Potassium Background Cations ...	49
4.4 Practical Applications .....	50
4.5 Conclusions .....	51
 CHAPTER 5. THE EFFECT OF EXOPOLYMERS ON THE COMPRESSIBILITY OF KAOLINITE .....	
5.1 Introduction .....	53
5.2 Materials and Methods .....	55
5.2.1 Guar Gum .....	56
5.2.2 Xanthan Gum .....	56
5.2.3 Preparation of Biopolymer and Clay Mixtures .....	57
5.2.4 Test Apparatus and Methods .....	59
5.3 Results and Discussion .....	60
5.3.1 Guar Gum and Kaolinite Mixtures .....	67
5.3.2 Xanthan Gum and Kaolinite Mixtures .....	70
5.3.3 Comparison between Guar Gum and Xanthan Gum Results .....	72
5.4 Practical Applications .....	75
5.5 Conclusions .....	76
 CHAPTER 6. DIRECT SHEAR MEASUREMENT OF THE EFFECT OF EXOPOLYMERS ON THE SHEAR STRENGTH OF KAOLINITE .....	
6.1 Introduction .....	79
6.2 Materials and Methods .....	79
6.2.1 Direct Shear Test Apparatus and Methods .....	79
6.3 Results and Discussion .....	81
6.3.1 Guar Gum and Kaolinite Mixtures .....	84
6.3.2 Xanthan Gum and Kaolinite Mixtures .....	85
6.4 Conclusions .....	87
 CHAPTER 7. TRIAXIAL MEASUREMENT OF THE EFFECT OF EXOPOLYMERS ON THE SHEAR STRENGTH OF KAOLINITE .....	
7.1 Introduction .....	89
7.2 Materials and Methods .....	90
7.2.1 Preparation of Triaxial Specimens .....	90
7.2.2 Triaxial Test Apparatus and Methods .....	92
7.3 Results and Discussion .....	94
7.4 Practical Applications .....	104
7.5 Conclusions .....	105

CHAPTER 8. EMPIRICAL MODELING OF THE IMPROVEMENT IN COMPRESSIBILITY AND UNDRAINED SHEAR STRENGTH DUE TO EXOPOLYMER ADDITION .....	107
8.1 Introduction .....	107
8.2 Materials and Methods .....	107
8.2.1 Consolidation Test Method .....	107
8.2.2 Direct Shear Test Method .....	108
8.2.3 Empirical Modeling Method .....	108
8.3 Results and Discussion .....	110
8.4 Practical Applications .....	114
8.5 Conclusions .....	115
CHAPTER 9. CONCLUSIONS AND RECOMMENDATIONS .....	117
9.1 Conclusions .....	117
9.2 Practical Applications .....	118
9.3 Recommendations for Future Research .....	119
REFERENCES .....	121
APPENDIX A: LETTER OF PERMISSION FROM THE TRANSPORTATION RESEARCH BOARD .....	127
APPENDIX B: LETTER OF PERMISSION FROM THE AMERICAN SOCIETY OF CIVIL ENGINEERS .....	129
VITA .....	132

## LIST OF TABLES

Table 5.1: Fitted line data for guar gum and kaolinite mixtures and xanthan gum and kaolinite mixtures .....	60
Table 6.1: Fitted line data for guar gum and kaolinite mixtures and xanthan gum and kaolinite mixtures .....	81
Table 7.1: Summary of data for all triaxial tests performed .....	95
Table 8.1: Additional test results for guar gum and kaolinite mixtures .....	110
Table 8.2: Results for the empirical models .....	112

## LIST OF FIGURES

Figure 3.1: Liquid limit of kaolinite and xanthan gum solution viscosity as a function of xanthan gum concentration .....	20
Figure 3.2: Liquid limit of kaolinite and guar gum solution viscosity as a function of guar gum concentration .....	20
Figure 3.3: Liquid limit of kaolinite and xanthan gum solution viscosity as a function of xanthan gum concentration with emphasis on low concentration behavior .....	22
Figure 3.4: Liquid limit of kaolinite and guar gum solution viscosity as a function of guar gum concentration with emphasis on low concentration behavior .....	22
Figure 3.5: ESEM images of kaolinite at the liquid limit for (a) DI water, (b) 1 wt. % xanthan gum, and (c) 2 wt. % guar gum .....	25
Figure 3.6: Liquid limit of kaolinite as a function of xanthan gum concentration and background ion .....	26
Figure 3.7: Liquid limit of kaolinite as a function of guar gum concentration and background ion .....	28
Figure 3.8: ESEM images of kaolinite at the liquid limit for 2 wt. % guar gum solution made with (a) DI water, (b) 0.01 M KCl, and (c) 0.01 M NaCl .....	29
Figure 4.1: (a) Picture of CSM sensor head and (b) schematic of CSM sensor head cross section inserted into a sediment surface .....	38
Figure 4.2: Representative raw CSM data and data analysis .....	42
Figure 4.3: Erosional resistance as a function of biopolymer concentration .....	43
Figure 4.4: Erosional resistance as a function of guar gum concentration and initial $w$ .....	43
Figure 4.5: Erosional resistance as a function of xanthan gum concentration and background cation .....	44
Figure 4.6: Erosional resistance as a function of guar gum concentration and background cation .....	44
Figure 5.1: Strain vs. time for a 0.020 $R_{bm}$ xanthan gum mixture under 23.94 kPa (500 psf) vertical load by ring height .....	61
Figure 5.2: Void ratio vs. vertical effective stress for guar gum and kaolinite mixtures .....	61



Figure 5.3: Void ratio vs. coefficient of consolidation for guar gum and kaolinite mixtures ....	62
Figure 5.4: Coefficient of secondary compression vs. biopolymer mass ratio for guar gum and kaolinite mixtures .....	62
Figure 5.5: Strain vs. time for two load increments of a 0.015 $R_{bm}$ guar gum mixture .....	63
Figure 5.6: Void ratio vs. hydraulic conductivity for guar gum and kaolinite mixtures .....	63
Figure 5.7: Void index vs. vertical effective stress for guar gum and kaolinite mixtures .....	64
Figure 5.8: Void ratio vs. vertical effective stress for xanthan gum and kaolinite mixtures .....	64
Figure 5.9: Void ratio vs. coefficient of consolidation for xanthan gum and kaolinite mixtures .....	65
Figure 5.10: Coefficient of secondary compression vs. biopolymer mass ratio for xanthan gum and kaolinite mixtures .....	65
Figure 5.11: Strain vs. time for two load increments of a 0.015 $R_{bm}$ xanthan gum and kaolinite mixture .....	66
Figure 5.12: Void ratio vs. hydraulic conductivity for xanthan gum and kaolinite mixtures ....	66
Figure 5.13: Void index vs. vertical effective stress for xanthan gum and kaolinite mixtures. .	67
Figure 5.14: Void ratio vs. vertical effective stress for biopolymer and kaolinite mixtures .....	73
Figure 5.15: Coefficient of secondary compression vs. biopolymer mass ratio by vertical load and biopolymer .....	74
Figure 5.16: Void ratio vs. hydraulic conductivity by biopolymer .....	75
Figure 6.1: Undrained shear strength vs. pre-shear vertical effective stress for guar gum and kaolinite mixtures .....	82
Figure 6.2: Void index vs. undrained shear strength for guar gum and kaolinite mixtures .....	82
Figure 6.3: Undrained shear strength vs. pre-shear vertical effective stress for xanthan gum and kaolinite mixtures .....	83
Figure 6.4: Void index vs. undrained shear strength for xanthan gum and kaolinite mixtures .....	83
Figure 7.1: Images of the triaxial specimen preparation apparatus .....	91

Figure 7.2: Images of a representative triaxial specimen (a) after trimming and (b) after shearing .....	92
Figure 7.3: MIT stress paths for tests performed on just kaolinite by OCR .....	95
Figure 7.4: Stress vs. strain curves for tests performed on just kaolinite by OCR .....	96
Figure 7.5: Excess pore water pressure during shear for tests performed on just kaolinite by OCR .....	96
Figure 7.6: SHANSEP model determination for just kaolinite and 0.0050 $R_{bm}$ guar gum mixtures .....	98
Figure 7.7: Cambridge stress paths and modified Cam clay predicted yield loci for tests performed on just kaolinite by OCR .....	98
Figure 7.8: MIT stress paths for tests performed on 0.0050 $R_{bm}$ mixtures by OCR .....	100
Figure 7.9: Stress vs. strain curves for tests performed on 0.0050 $R_{bm}$ mixtures by OCR .....	100
Figure 7.10: Excess pore water pressure during shear for tests performed on 0.0050 $R_{bm}$ mixtures by OCR .....	101
Figure 7.11: MIT stress paths for tests performed on 2.7 OCR specimens by $R_{bm}$ .....	101
Figure 7.12: Stress vs. strain curves for tests performed on 2.7 OCR specimens by $R_{bm}$ .....	102
Figure 7.13: Excess pore water pressure during shear for tests performed on 2.7 OCR specimens by $R_{bm}$ .....	102
Figure 7.14: Normalized $C_c^{-1}$ and $s_u/\sigma_{vo}'$ ratios vs. guar gum concentration .....	104
Figure 8.1: Void ratio vs. vertical effective stress for additional guar gum and kaolinite mixtures .....	111
Figure 8.2: Undrained shear strength vs. pre-shear vertical effective stress for additional guar gum and kaolinite mixtures .....	111
Figure 8.3: Second empirical model plotted against all collected data .....	113

## ABSTRACT

Erosion and subsidence threaten coastal infrastructure and natural habitats throughout the coastal United States, and this threat is especially significant along the Louisiana coastline since wetland clays are generally weak and highly compressible. Hydraulic pumping of dredged sediment is a common method for combating damage caused by erosion and subsidence, but the high water content slurry deposited is very compressible with low shear strength. Although conventional soil amendments are effective for reducing compressibility and increasing shear strength, these stabilizers are often caustic or toxic, making them too risky to use. Exopolymers, however, have the potential to improve sediment stability without the environmental risks of typical soil stabilizers.

Exopolymers are high molecular weight polysaccharides produced by soil microorganisms. While there have been some studies that correlate soil exopolymer content with improved erosional resistance, there has been no work that measures changes in compressibility and shear strength and relates these changes to Stress History And Normalized Soil Engineering Properties (SHANSEP) models. This dissertation describes methods for using two exopolymer analogues, guar gum and xanthan gum, to change the properties of a pure kaolinite.

Changes in the compressibility of biopolymer and kaolinite mixtures were measured using 1D consolidation and triaxial tests. Also, modifications of shear strength were measured using direct shear and triaxial tests. Results from these tests were used to develop SHANSEP and empirical models.

The statistically strongest empirical model demonstrated that guar gum produces a 19% mean increase in the inverse of compressibility with a 3% standard deviation at the optimum concentration. It also produces a 9.6% mean increase in undrained shear strength with a 5%

standard deviation. Further, cohesive strength meter (CSM) tests showed that guar gum can increase erosional resistance by nine times over the kaolinite on its own.

Speculative mechanisms were proposed to aid in interpretation of liquid limit, CSM, 1D consolidation, direct shear, and triaxial test results and to guide future research. This study seeks to advance the understanding needed to develop biological methods of sediment stabilization. It also specifically demonstrates the potential of guar gum amendment for possible use in hydraulically pumped dredged sediment.

## **CHAPTER 1. INTRODUCTION**

Interest has been growing in investigating the influence of soil biota on engineering properties of soils and in exploring biological processes for soil treatment and improvement, such as biocementation and bioclogging (Ivanov and Chu 2008; Mitchell and Santamarina 2005). The wide occurrence of microorganisms in soil environments has been well recognized. An important product formed by micro-communities of bacteria, or biofilms, is exopolymers, or extracellular polymeric substances (EPS) (Sutherland 2001), which are exuded by microorganisms for protection and to make the environment more hospitable for the micro-community (Maier et al. 2000). Most exopolymers are high molecular weight polysaccharides containing chemically active groups with electrical charges (Sutherland 2001), and hence they interact very actively with soil particles, particularly clay minerals. Therefore, it is expected that exopolymers affect soil behavior and engineering properties in a variety of ways. Specifically, these exopolymers should improve the stiffness and shear strength of a clay to reduce damage due to erosion and subsidence.

Every 24 minutes, the state of Louisiana loses one acre of land due to erosion (Fischetti 2001). Erosion refers to the gradual removal of particles from the soil surface by currents or flows (Plummer et al. 2003). Of bridge failures between 1989 and 2000, 15.51% were caused by scouring of bridge foundations (Wardhana and Hadipriono 2003). Additionally, both external and internal erosion, such as erosion from piping, can cause failures of river banks, levees, and dams, and this threatens coastal infrastructure throughout the United States (Parker and Jenne 1967; Sherard et al. 1972).

Subsidence, the reduction in surface elevation due to soil consolidation, also threatens many estuaries in the United States. Coastal wetlands and cities in Louisiana are especially

vulnerable, with subsidence reducing land elevation by 5-10 mm per year (Tornqvist et al. 2008). This loss of elevation is in addition to changes in sea level.

One common engineering method for rapidly rebuilding wetlands lost through erosion and subsidence is hydraulic pumping of dredged sediment. However, the high water content slurry deposited by dredging is very compressible with low shear strength. This poor stability makes freshly deposited slurry susceptible to erosion and subsidence.

Although there are many soil amendments that can reduce compressibility and improve shear strength, these soil stabilizers are often caustic or toxic. Specifically, ASTM standard D 6276 (ASTM 2006) states that  $\text{Ca(OH)}_2$  or  $\text{CaO}$  must be added to a soil at a concentration that raises soil pH to 12.4, and the standard also states that agricultural lime, crushed limestone, will not produce any improvement. Many grouts, such as acrylamide, are toxic, and human exposure must be minimized. The large scale and environmentally sensitive nature of wetland restoration projects makes these traditional amendments too risky to use. Additionally, Tengbeh (1993) demonstrated that grass roots can provide a five-fold increase in shear strength over a wide range of water contents, and de Baets et al. (2007) showed that plant roots can increase surface erosion resistance. Therefore, any compound used for improving slurry stability must not inhibit or slow plant growth, since plants are also important for increasing sediment stability.

The World Health Organization (1975; 1987) performed toxicity studies for guar gum and xanthan gum and found that they do not represent a hazard to health and that there was no need to establish an acceptable daily intake of the substances. Further, Sandford et al. (1984) established that both guar gum and xanthan gum are used in agricultural fertilizers and feed supplements with no harm to the environment. With this in mind, these two exopolymer analogs show little evidence in causing environmental harm should they be used for wetland stabilization

and could enhance the growth of plants (Wallace 1986), while improving sediment stability. However, it must be proved that application of these two polymers at the concentrations recommended in this dissertation will be environmentally benign, and this study is currently being conducted at Louisiana State University.

The purpose of this dissertation is to characterize how exopolymers change the compressibility and shear strength of clay and to provide geotechnical models to aid practitioners in using the materials. Emphasis is placed on cohesive soils, since the Lower Mississippi River Basin and the Northern Gulf Coast are covered extensively by fine-grained, mostly cohesive sediments. Methods for mixing exopolymer with clay and quantifying exopolymer concentration in soil will be developed, and compressibility and shear strength will be measured using Casagrande cup, 1D consolidation, direct shear, cohesive strength meter (CSM), and triaxial tests. This program will lay the foundation for developing an environmentally benign technology for bioengineered coastal sediment stabilization and erosion control.

## **1.1 Dissertation Objectives**

This dissertation will describe how exopolymers change the compressibility and shear strength of kaolinite and will relate these changes to the Stress History And Normalized Soil Engineering Properties (SHANSEP) (Ladd and Foott 1974) model. Methods for mixing exopolymer with clay and quantifying exopolymer concentration in soil will also be described. Compressibility and shear strength will be measured using Casagrande cup, 1D consolidation, direct shear, CSM, and triaxial tests. Results from these tests, relating to compressibility and shear strength, will be used to develop SHANSEP models along with empirical correlations. Additionally, speculative mechanisms will be proposed to aid in interpretation of results and to help guide future research. This work will provide the basic understanding needed to develop a

technology for bioengineered coastal sediment stabilization and erosion control, and it will suggest further areas of research needed to make the technology mature.

## **1.2 Dissertation Layout**

Nine chapters make up this dissertation. Literature review is provided in Chapter 2. It focuses on the potential for exopolymers to reduce erosion and gives a description of the initial studies of exopolymer effects on soil shear strength. Guar gum and xanthan gum, two exopolymer analogs that will be used in this dissertation, and kaolinite, the clay mineral used, are also described.

Chapter 3 describes the results of a study on how guar gum and xanthan gum change the liquid limits of kaolinite. Cations are also used in the study to better understand how the biopolymers influence the liquid limit. Results from a CSM study on how guar gum and xanthan gum improve the erosional resistance of kaolinite are presented in Chapter 4. This study also uses cations to more thoroughly comprehend the speculative mechanisms of interaction and incorporates information from Chapter 2.

The fifth and sixth chapters, respectively, show the outcome of 1D consolidation and direct shear tests performed on guar gum and kaolinite mixtures, as well as xanthan gum and kaolinite mixtures. These chapters contain direct measurements of the compressibility and shear strength of biopolymer and kaolinite mixtures. Patterns of improvement and weakening of compressibility and shear strength parameters are discussed and related to speculative mechanisms proposed in the third and fourth chapters.

Triaxial tests and empirical models are provided in Chapters 7 and 8, respectively. Both of these chapters focus on the behavior of low concentration guar gum and kaolinite mixtures, since these mixtures produced the greatest improvement in compressibility and shear strength.



The triaxial tests produce both measurements of compressibility and shear strength, and the results from the tests are used to produce SHANSEP models. Empirical models that use the data from Chapters 5, 6, and 7, along with additional replicate 1D consolidation and direct shear test data, are proposed in Chapter 8.

Chapter 9 gives the conclusion of all of the studies performed as part of this dissertation. Potential practical applications are proposed. Also, areas of future work are recommended.

## CHAPTER 2. LITERATURE REVIEW

To date, there has been very little research regarding how exopolymers change the geotechnical properties of a clay, and there is no research that relates these changes to the SHANSEP model. Thus, the literature review provides background on the potential for exopolymers to reduce erosion, and gives a description of the initial studies of exopolymer effects on soil shear strength. Guar gum and xanthan gum, two exopolymer analogues that will be used in this dissertation, and kaolinite, the clay mineral used, are also characterized in this section.

### 2.1 Exopolymers and Erosion

The general understanding is that the presence of exopolymers on sediment surfaces significantly increases the erosional resistance of the sediments (Widdows et al. 2006; Yallop et al. 2000). It has been demonstrated that a biofilm built by *Alteromonas atlantica* in sand substantially increases the critical shear velocity required to start erosion of the sand (Dade et al. 1990). Widdows et al. (2006) conducted a field study showing that the stability of newly placed sediments in intertidal mudflats has a strong correlation with the production and quantity of EPS in the sediment. Gerbersdorf et al. (2007) showed that sediment EPS is positively correlated with erosional resistance and that humic acids are negatively correlated.

Along with results from Hernandez and Mitsch (2007), Gerbersdorf et al. (2007) demonstrates why high organic wetland sediment is not already stabilized by the preexisting organic material. In an Ohio wetland, Hernandez and Mitsch (2007) found that a large fraction of the soil organic material is humic acid. Most of the remaining organic material is fulvic acid, and aside from having a lower molecular weight and being more soluble in water, fulvic acid is

similar to humic acid. Thus, one cannot assume that a high organic content sediment is already benefiting from EPS stabilization.

## **2.2 Exopolymers and Shear Strength**

In addition to erosional stability, a few pilot studies have explored the application of exopolymers to soil treatment and improvement. For instance, artificially added EPS dramatically increased the tensile strength of air-dried strips of the common clay minerals kaolinite and montmorillonite (Chenu and Guérif 1991). Çabalar and Çanakci (2005) performed direct shear tests to measure how the average shear strength of Leighton Buzzard sand changed with the addition of xanthan gum. They found that the addition of xanthan gum significantly increases the shear strength of the sand. Martin et al. (1996) also found that the addition of xanthan gum to a low plasticity clayey silt increases the shear strength of the soil.

## **2.3 Guar Gum**

Guar gum is a neutral polysaccharide found in the seeds of *Cyamopsis tetragonoloba* (Risica et al. 2005). Although guar gum is not a microbially produced biopolymer, it possesses the ability to produce viscous, pseudoplastic aqueous solutions representative of neutral microbial EPS. This ability is the result of its high molecular weight and extensive, hydrogen bonding promoted chain hyperentanglements (Goycoolea et al. 1995; Cheng et al. 2002). Hyperentanglements are a type of intermolecular association (Rao 2007). Guar gum's availability and inexpensiveness also make it potentially useful in practice.

The polymer backbone of guar gum consists of mannose linked with  $\beta$ -1,4 bonds, and a single galactose is bonded to every second mannose (Whistler and Smart 1953). Carboxylic acid groups (-COOH) are absent from the structure of guar gum, and the lack of ionizable functional groups causes guar gum to have no electrical charge. Numerous hydroxyl (-OH) groups allow

guar gum to form hydrogen bonds. Although it is possible for the hydrogen in hydroxyl groups to dissociate, this process requires a surrounding solution with very high pH (Bruice 2004). In addition, guar gum has a high molecular weight of up to  $2 \times 10^6$  Da (Risica et al. 2005).

Guar gum also maintains a commercial significance. This is because of its ability to increase the viscosity of aqueous systems (Whitcomb et al. 1980). Additionally, guar gum solutions are pseudoplastic, which means that the viscosity of a guar gum solution decreases with an increased shear rate.

## **2.4 Xanthan Gum**

Xanthan gum is an anionic polysaccharide produced by *Xanthomonas campestris* (Sutherland 1994). Its polymer backbone consists of glucose linked with  $\beta$ -1,4 bonds, and every second glucose possesses a mannose-glucuronic acid-mannose side chain (Hassler and Doherty 1990). The two mannoses are typically modified with an *O*-acetyl group added to the mannose closest to the glucose backbone, while the mannose furthest from the backbone contains a pyruvate ketal. However, the exact proportion of mannose modified depends on the bacterial strain and the physiological environment in which the bacteria grow (Sutherland 1994). The carboxylic acid groups (-COOH) on the glucuronic acid and pyruvate bestow the xanthan gum its anionic charge, since the hydrogen can easily dissociate from a carboxylic acid group and form a carboxylate (-COO<sup>-</sup>) anion (Bruice 2004).

Being naturally produced, xanthan gum's exact molecular weight depends on the bacterial strain and the physiological environment used for production. Typical molecular weights range from 0.9 to  $1.6 \times 10^6$  Da (Sutherland 1994). Its ability to increase the viscosity of aqueous systems makes it commercially significant (Hassler and Doherty 1990). Since small

concentrations of xanthan gum can greatly increase the viscosity of a solution, it is a commonly used substance. The solutions made with xanthan gum are also pseudoplastic (Milas et al. 1985).

## **2.5 Kaolinite**

Kaolinite is a 1:1 clay mineral, which means each particle has one tetrahedral silica layer and one octahedral alumina layer (Mitchell and Soga 2005). Individual particles of kaolinite form stacks with hydrogen bonds and van der Waals forces holding together successive particles (Mitchell and Soga 2005). The strength of these bonds prevents water from entering the interlayer spaces and causing swelling (Mitchell and Soga 2005). Cation exchange capacity (CEC) values for kaolinite typically range between 3 to 15 meq / 100 g (Mitchell and Soga 2005).

Although Ma and Eggleton (1999) suggest that kaolinite's permanent negative charge due to isomorphic substitution is insignificant, zeta potential tests on kaolinite by Tombácz and Szekeres (2006), Alkan et al. (2005), and Li and Xu (2008) show that kaolinite possesses an overall negative charge over most pH values. Zeta potential data have the same sign as the excess charge of a particle, and zeta potential magnitude is roughly proportional to particle charge (Hunter 1981). Tombácz and Szekeres (2006) demonstrated that kaolinite does have permanent negative charges that are the result of isomorphic substitution, but variable charge sites, such as along particle edges, can balance this permanent negative charge at low enough pH. However, over the pH range Tombácz and Szekeres (2006) tested (pH 3 to 11), their kaolinite was negatively charged. Li and Xu (2008) had similar results where kaolinite had a net negative charge over the 3 to 7 pH range. Alkan et al. (2005) found that kaolinite lost its net negative charge at a pH of about 2.35. These results, however, show that kaolinite generally possesses a net negative charge.

South Louisiana wetland clays are not largely composed of kaolinite. Other minerals, such as smectites and illites, also make up the mineral portion of south Louisiana wetland sediments (Aslan and Autin 1998). In addition, certain wetland soils, like peats, contain large quantities of organic material (Plummer et al. 2003). As this is the first investigation to model the effects of exopolymers on a clay, a relatively pure kaolinite was chosen to minimize effects caused by the sediment alone.

Pure bentonite, for example, would have a much higher CEC of 80 to 150 meq / 100 g (Mitchell and Soga 2005), and these cations can have significant influence on exopolymer and clay interactions (Nugent et al. 2009; Nugent et al. 2011a). Specifically, Nugent et al. (2011a) showed that  $\text{Na}^+$  and  $\text{Ca}^{2+}$  counter electrostatic repulsion effects for xanthan gum. Additionally,  $\text{K}^+$  increases the adsorption of guar gum on kaolinite (Ma and Pawlik 2007). Kaolinite, on the other hand, has a much smaller CEC, which helps to eliminate sorbed cation effects (Mitchell and Soga 2005).

Bentonite also significantly shrinks and swells depending on the water content and the type and concentration of cations in the pore fluid (Budhu 2000; Mitchell and Soga 2005). This activity would mask exopolymer effects that are of interest. However, kaolinite is largely free from these effects (Budhu 2000; Mitchell and Soga 2005). A pure illite would also not have problems with shrinking and swelling (Budhu 2000; Mitchell and Soga 2005), but bulk pure illite is too expensive to perform the number of geotechnical tests needed.

Since sampled wetland sediments would have a mix of different clay minerals along with organic material, it would be extremely difficult to adequately control for variance produced by natural organic material. This is because humic substances, which make up a large portion of wetland organic carbon (Hernandez and Mitsch 2007), have significant variation in chemical

functional groups, molecular weight, and other chemical properties (Maier et al. 2000). Thus, kaolinite provides the best starting point for quantifying exopolymer effects.

## CHAPTER 3. THE EFFECT OF EXOPOLYMERS ON THE LIQUID LIMIT OF KAOLINITE AND ITS ENGINEERING IMPLICATIONS\*

### 3.1 Introduction

Interest has been growing in understanding the influence of soil biota on engineering properties of soils and in exploring biological processes for soil treatment and improvement, such as biocementation and bioclogging (Ivanov and Chu 2008; Mitchell and Santamarina 2005). The wide occurrence of microorganisms in soil environments has been well recognized. An important product formed by micro-communities of bacteria associated with a surface, also known as biofilms, is exopolymers, or extracellular polymeric substances (EPS) (Sutherland 2001), which are exuded by microorganisms for protection and to make the environment more hospitable for the micro-community (Maier et al. 2000). Most exopolymers are high molecular weight polysaccharides containing chemically active groups with electrical charges (Sutherland 2001), and hence they interact very actively with soil particles, particularly clay minerals. Therefore, it is expected that exopolymers affect soil behavior and engineering properties in a variety of ways.

The general understanding is that the presence of exopolymers on sediment surfaces significantly increases the erosional resistance of the sediments (Widdows et al. 2006; Yallop et al. 2000). There have been studies to substantiate this. For example, it has been demonstrated that a biofilm built by *Alteromonas atlantica* in sand substantially increases the critical shear velocity required to start erosion of the sand (Dade et al. 1990). Additionally, Widdows et al. (2006) conducted a field study showing that the stability of newly placed sediments in intertidal mudflats has a strong correlation with the production and quantity of EPS in the sediment.

---

\*Material reprinted from Nugent et al. (2009) with permission from the Transportation Research Board on behalf of the National Academy of Sciences.



Besides erosional stability, there have been a few pilot studies exploring the application of exopolymers for soil treatment and improvement. For instance, artificially added EPS dramatically increased the tensile strength of air-dried strips of the common clay minerals kaolinite and montmorillonite (Chenu and Guérif 1991). Çabalar and Çanakci (2005) performed direct shear tests to measure how the average shear strength of Leighton Buzzard sand changed with the addition of xanthan gum. They found that the addition of xanthan gum significantly increases the shear strength of the sand. Martin et al. (1996) also found that the addition of xanthan gum to a low plasticity clayey silt increases the strength of the soil.

An extensive investigation is being conducted at Louisiana State University to study and understand how exopolymers interact with soils and affect their engineering properties. This is due to the fact that every 24 minutes the state of Louisiana loses one acre of land due to erosion (Fischetti 2001). Erosion refers to the gradual removal of particles from the soil surface by currents or flows (Plummer et al. 2003). This threatens coastal transportation infrastructure (e.g., highways, bridges). Also, the erosion or scouring of bridge piers, piles, and abutments is one of the major factors for bridge failures in the United States (Wardhana and Hadipriono 2003). Moreover, erosion, including internal erosion, can cause failures of embankments and dams (Parker and Jenne 1967; Sherard et al. 1972), and thus it affects waterway transportation.

Emphasis of this study is placed on cohesive soils, since the Lower Mississippi River Basin and the Northern Gulf Coast are covered exclusively by fine-grained, mostly cohesive sediments. In the US, cohesive soils and sediments are also prevalent in several major estuaries and bays, such as Boston Harbor, San Francisco Bay, the Delaware River estuary, and New York City Hudson River estuary. This investigation aims to develop an environmentally benign technology for bioengineered coastal sediment stabilization and erosion control.

Preliminary results of this study pertinent to the liquid limit measurement of a kaolinite clay are presented in this chapter. Xanthan gum, an anionic bacterial extracellular polysaccharide, and guar gum, a neutral plant polysaccharide, are two biopolymers used as EPS analogs. Both biopolymer concentrations and the types of background cations, including  $\text{Ca}^{2+}$ ,  $\text{Na}^+$ , and  $\text{K}^+$ , in the pore fluid were varied in the clay sample to study the various molecular or nanoscale interactions among biopolymers, cations, and clay particles. The macroscopic index property (i.e., liquid limit) is interpreted along with the hypothesized nanoscale interactions within the biopolymer-clay system. Furthermore, this interpretation is reinforced with imaging of the microstructure of the system under environmental scanning electron microscopy (ESEM).

## **3.2 Materials and Methods**

### **3.2.1 Materials**

The clay sample used in this study is a relatively pure kaolinite purchased from Thiele Kaolin Co. Particles smaller than 2  $\mu\text{m}$  make up 98 percent by weight (wt.%) of the sample. The average specific surface area is 20-26  $\text{m}^2/\text{g}$  (Flick 1989). The as-received sample was used without further treatment. Three inorganic salts were used as the background ions: calcium nitrate ( $\text{Ca}(\text{NO}_3)_2$ , ACS Grade) was purchased from EMD Chemicals Inc., while both ACS grade potassium chloride (KCl) and sodium chloride (NaCl) were purchased from Mallinckrodt Chemicals. Two exopolymers that were used, xanthan gum (NF Grade) and guar gum (Laboratory Grade), were purchased from Spectrum Chemical Manufacturing Corp. and Fisher Scientific, respectively. Some basic information about these two EPS analogs is provided below.

### **3.2.2 Xanthan Gum**

Xanthan gum is an anionic polysaccharide produced by *Xanthomonas campestris* (Sutherland 1994). Its polymer backbone consists of glucose linked with  $\beta$ -1,4 bonds, and every

second glucose possesses a mannose-glucuronic acid-mannose side chain (Hassler and Doherty 1990). The two mannoses are typically modified with an *O*-acetyl group added to the mannose closest to the glucose backbone, while the mannose furthest from the backbone contains a pyruvate ketal. However, the exact proportion of mannose modified depends on the bacterial strain and the physiological environment in which the bacteria grow (Sutherland 1994). The carboxylic acid groups (-COOH) on the glucuronic acid and pyruvate bestow the xanthan gum its anionic charge, since the hydrogen can easily dissociate from a carboxylic acid group and form a carboxylate (-COO<sup>-</sup>) anion (Bruice 2004).

Because xanthan gum is naturally produced, its exact molecular weight depends on the bacterial strain and the physiological environment used for production. Typical molecular weights range from 0.9 to  $1.6 \times 10^6$  Da (Sutherland 1994). Xanthan gum's ability to increase the viscosity of aqueous systems makes it commercially significant (Hassler and Doherty 1990). Since small concentrations of xanthan gum can greatly increase the viscosity of a solution, it is a commonly used substance. Additionally, xanthan gum solutions are pseudoplastic, which means that the viscosity of a xanthan gum solution decreases with an increased shear rate (Milas et al. 1985).

### **3.2.3 Guar Gum**

Guar gum is a neutral polysaccharide found in the seeds of *Cyamopsis tetragonoloba* (Risica et al. 2005). Although guar gum is not a microbially produced biopolymer, it possesses the ability to produce viscous, pseudoplastic aqueous solutions representative of neutral microbial EPS. Its availability and inexpensiveness also make it potentially useful in practice.

The polymer backbone of guar gum consists of mannose linked with  $\beta$ -1,4 bonds, and a single galactose is bonded to every second mannose (Whistler and Smart 1953). Carboxylic acid

groups (-COOH) are absent from the structure of guar gum, and the lack of ionizable functional groups provides guar gum its neutral charge. Numerous hydroxyl (-OH) groups allow guar gum to form hydrogen bonds. Although it is possible for the hydrogen in hydroxyl groups to dissociate, this process requires a surrounding solution with very high pH (Bruice 2004). In addition, guar gum has a high molecular weight of up to  $2 \times 10^6$  Da (Risica et al. 2005). Similar to xanthan gum, guar gum also maintains a commercial significance because of its ability to increase the viscosity of aqueous systems (Whitcomb et al. 1980).

#### **3.2.4 Preparation of Biopolymer Solutions**

Since xanthan gum and guar gum are both high molecular weight biopolymers with variable molecular weights, the biopolymer solutions were measured using weight percent instead of molarity, where weight percent is the ratio of the weight of biopolymer to that of biopolymer solution. Biopolymer solutions of a desired concentration were prepared by dissolving biopolymer powder into deionized (DI) water. To prevent the powder from clumping, two measures were used: (1) for low concentration solutions, the water was stirred using a stir bar, and the biopolymer powder was very slowly added to the liquid vortex over several minutes; and (2) for high concentration solutions, an immersion blender was used to break down any remaining clumps of biopolymer powder and to homogenize the solution.

All freshly prepared biopolymer solutions were either used immediately after mixing or were stored in a refrigerator at 4 °C to minimize the effect of biological degradation. Those refrigerated solutions were allowed to warm to room temperature (approximately 20 °C) before being used in subsequent tests.

There are other means of making homogenous biopolymer solutions that involve the addition of chemicals, such as glycol and alcohol (Phillips and Williams 2000). It seems,

however, that direct physical means of mixing the solutions would be preferred for large scale application in the field. This is because it would save on costs, since additional chemicals would not have to be purchased. Therefore, these tests used physical mixing.

Xanthan gum solutions with concentrations ranging from 0.25 to 10 wt.% were used to examine the effect of xanthan gum on the liquid limit of kaolinite. Similarly, guar gum solutions with concentrations ranging from 0.25 to 3 wt.% were also used. Note that some concentrations were specifically chosen in order to better define the curve formed by plotting the liquid limit against biopolymer concentration, as described below.

Biopolymer solutions with background salt concentrations were utilized to investigate how biopolymer cross-linking and the adsorption of biopolymers onto clay particle surfaces influence the liquid limit. In order to produce a biopolymer solution with a background salt concentration, 0.1 M  $\text{Ca}(\text{NO}_3)_2$ , 0.01 M KCl, and 0.01 M NaCl salt solutions were prepared, and those salt solutions were used instead of DI water to make the biopolymer solutions. The effect of cross-linking was studied using xanthan gum solutions with concentrations ranging from 1 to 5 wt.% and with 0.1 M  $\text{Ca}(\text{NO}_3)_2$  as the background salt solution. The effect of biopolymer adsorption was examined using two sets of guar gum solutions with concentrations ranging from 0.5 to 2 wt.%. One set of guar gum solutions used 0.01 M KCl as the background salt solution, while the other set used 0.01 M NaCl.

### **3.2.5 Liquid Limit Test**

Liquid limit tests were performed using the Casagrande cup method following the procedures specified in the ASTM standard D 4318 (ASTM 2006). For most of the liquid limit tests, biopolymer solutions or salt solutions were used instead of deionized water. The tests were performed by adding a small amount of biopolymer solution to dry kaolinite powder and hand

mixing the clay and biopolymer solution together until a homogenous paste was formed. Next, the clay and biopolymer mixture was tested in a Casagrande cup. Some of the mixture in the Casagrande cup was used to measure the water content of the mixture, according to ASTM standard D 2216 (ASTM 2006). Following this, more biopolymer solution was added to the clay-biopolymer mixture that was again hand-mixed until it was homogenous. The Casagrande cup test was then repeated, and six points were collected to determine each liquid limit.

Note that the addition of biopolymer solution to a constant mass of clay results in a mixture with a constant biopolymer concentration in the pore fluid, but the clay to biopolymer mass ratio varies during the experiment. Since the biopolymers are high molecular weight polysaccharides, they do not volatilize at  $110 \pm 5$  °C in the drying oven. As an example of how high molecular weight polysaccharides resist volatilization, wood that largely consists of high molecular weight polysaccharides (Sjötröm 1993) does not appreciably volatilize until the temperature is above 300 °C (U.S. 2007). Because of the biopolymers' lack of volatilization, they contribute to the weight of the solids when determining water content or liquid limit.

### **3.2.6 ESEM Imaging**

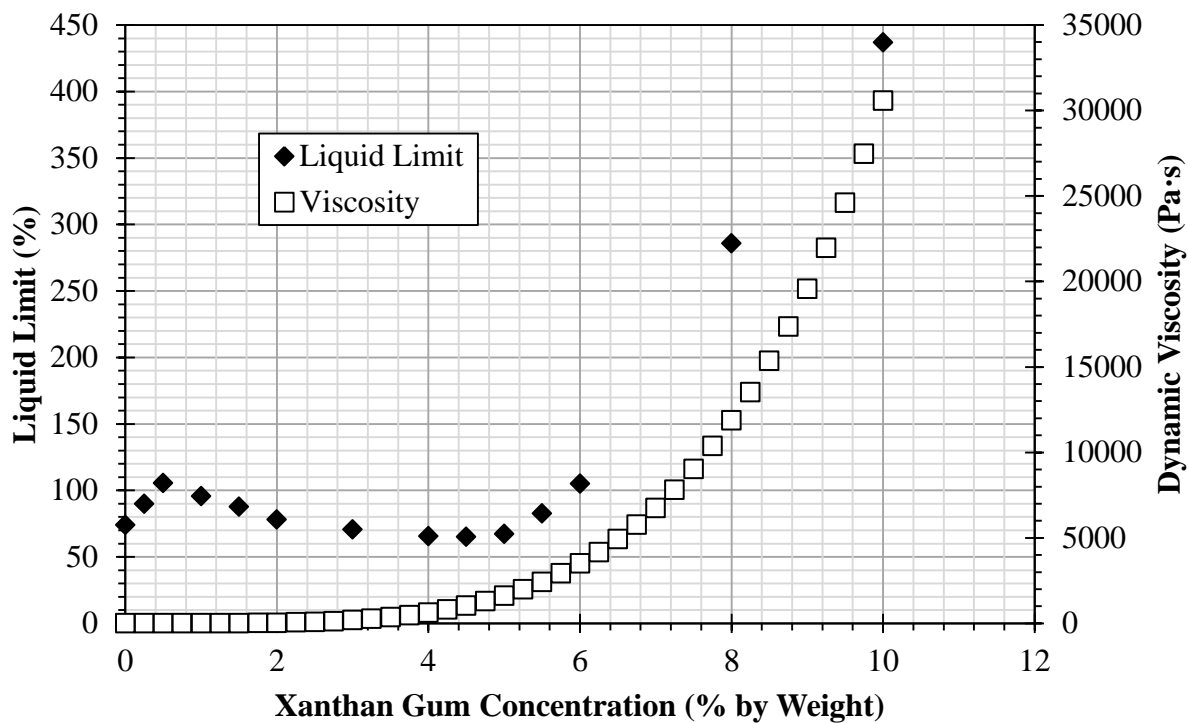
After determining the liquid limits of the kaolinite and biopolymer mixtures, samples of kaolinite and biopolymer mixtures at the measured liquid limits were prepared for selected biopolymer solutions. These samples were observed and imaged using an FEI Quanta 200 ESEM under a constant relative humidity of 95-100%, which essentially prevents samples from drying during imaging. Observation of samples under ESEM does not require pre-processing of samples (e.g., drying, coating, fixing). Special attention was paid to the presence of biopolymer gels within pores, clay particle aggregation, and aggregate sizes.

### 3.3 Results and Discussion

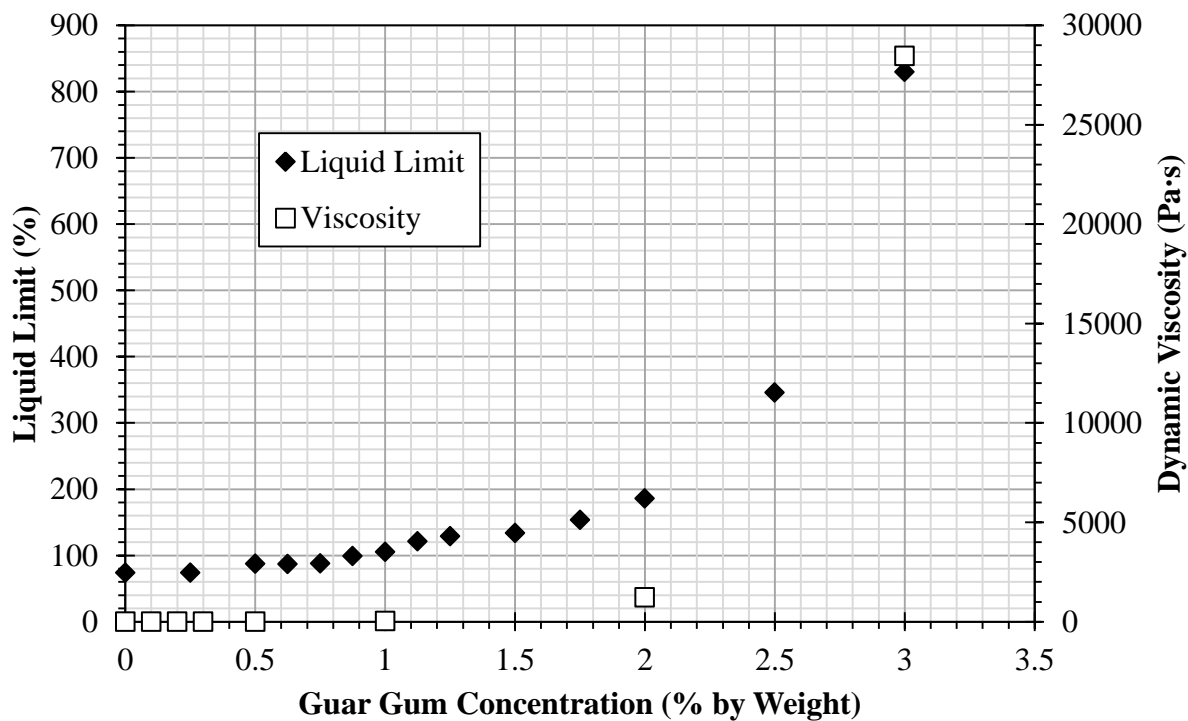
#### 3.3.1 Biopolymer Solution Viscosity

Figure 3.1 plots the liquid limit of kaolinite against the concentration of xanthan gum solution as the pore fluid, while Figure 3.2 shows the respective results for guar gum. For comparison, the zero shear rate dynamic viscosities of xanthan gum (with a molecular weight of  $1.25 \times 10^6$  Da) (Milas et al. 1985) and guar gum solutions (Whitcomb et al. 1980) are also shown in Figures 3.1 and 3.2, respectively. One striking feature observed from these two figures is the rapid, non-linear increase of the liquid limit with increasing biopolymer concentration in the pore fluid. Furthermore, the rate of change in the liquid limit follows the rate of change in viscosity, especially at higher concentrations. These features seem to indicate that the biopolymer solution viscosity in the pore fluid is significantly related to the increase of the liquid limit of the kaolinite, particularly for higher concentrations (e.g., >5 wt.% for xanthan gum and >2 wt.% for guar gum). For lower concentrations, the influence of the two biopolymers is slightly different. An obvious peak is observed around 0.5 wt.% xanthan gum concentration, while only a small hump is found around 1.25 wt.% guar gum concentration. The appearance of the peaks is believed to be caused by the biopolymer-induced aggregation at low concentrations.

The liquid limit is a measure of how much fluid must be added to a soil in order to reduce its undrained shear strength to 1.7-2.0 kPa (Sharma and Bora 2003). Since water has a dynamic viscosity of about 0.001 Pa·s (Bolz and Tuve 1973), and viscosity is a measure of how well a fluid resists shear stress (Crowe et al. 2001), water contributes little to the ability of the kaolinite to resist shear stresses. However, a 4.5 wt.% xanthan gum solution and a 2 wt.% guar gum solution possess zero shear rate viscosities of 1037 Pa·s (Milas et al. 1985) and 1220 Pa·s (Whitcomb et al. 1980), respectively. These viscosities are six orders of magnitude greater than



**Figure 3.1: Liquid limit of kaolinite and xanthan gum solution viscosity (Milas et al. 1985) as a function of xanthan gum concentration.**



**Figure 3.2: Liquid limit of kaolinite and guar gum solution viscosity (Whitcomb et al. 1980) as a function of guar gum concentration.**



water. Therefore, it must take more biopolymer solution to reach the liquid limit than it would take for water to do so, since biopolymer solutions contribute to the shear resistance of the clay-biopolymer system when sheared with a high rate of strain, such as with the impact of a Casagrande cup.

It is also worth discussing the difference resulting from the two biopolymers. Although 3 wt.% guar gum and 10 wt.% xanthan gum solutions have nearly equal viscosity (i.e., 30000 Pa·s) (Milas et al. 1985; Whitcomb et al. 1980), the liquid limits of kaolinite with these two concentrations are different: 436.8% for 10 wt.% xanthan gum solution, but 829.5% for 3 wt.% guar gum solution. This appears to indicate that other mechanisms in addition to pore fluid biopolymer viscosity and aggregation (which is discussed later) also contribute to the liquid limit of kaolinite.

Figures 3.3 and 3.4 highlight the low concentration behavior of xanthan gum and guar gum solutions and further illustrate the differences between the two biopolymers. Both 0.25 wt.% xanthan gum and 0.25 wt.% guar gum have similar viscosities of 0.015 Pa·s (Milas et al. 1985; Whitcomb et al. 1980). However, the liquid limit of kaolinite with 0.25 wt.% xanthan gum is 89.9%, while the liquid limit is 73.8% for 0.25 wt.% guar gum solution.

It is believed that these differences are caused by different types of clay-biopolymer interactions involved for the two biopolymers. Anionic xanthan gum molecules may be linked to the adsorbed cations on the kaolinite particle surfaces (Dontsova and Bigham 2005). However, kaolinite has limited cation exchange capacity (Mitchell and Soga 2005) and has a net negative charge for pH values greater than 3 (Tombácz and Szekeres 2006; Alkan et al. 2005; Li and Xu 2008), so the degree of linking is limited. On the other hand, guar gum is a neutral

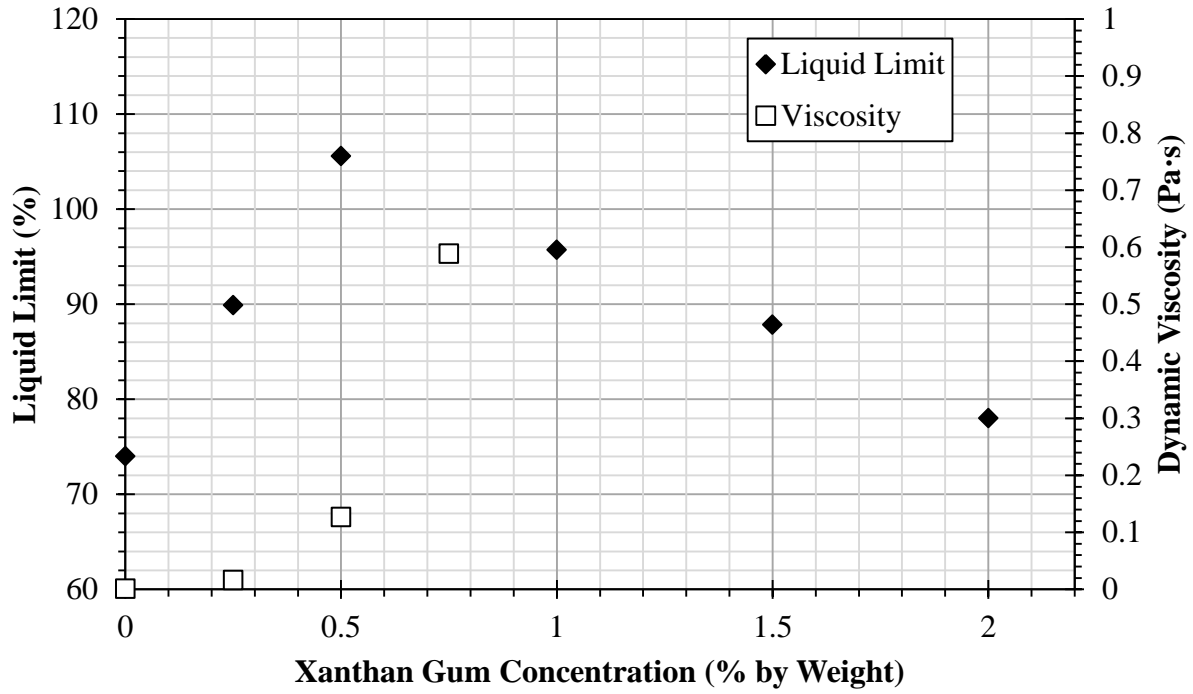


**Figure 3.3: Liquid limit of kaolinite and xanthan gum solution viscosity (Milas et al. 1985) as a function of xanthan gum concentration with emphasis on low concentration behavior.**

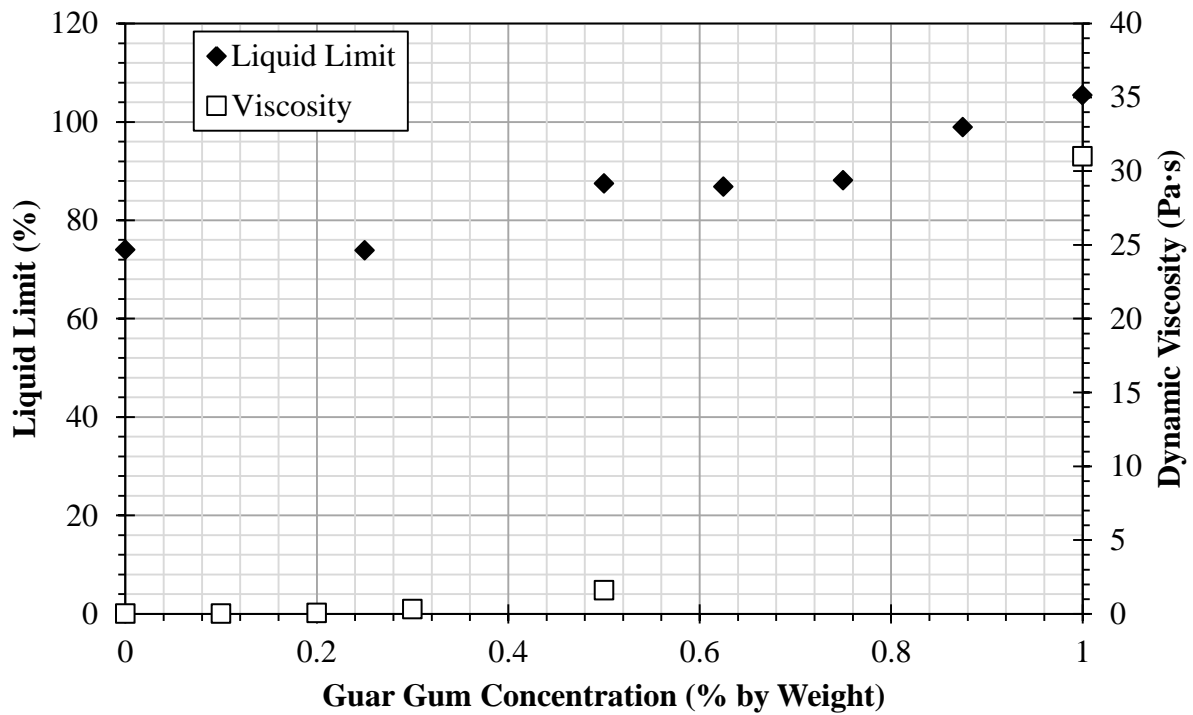


**Figure 3.4: Liquid limit of kaolinite and guar gum solution viscosity (Whitcomb et al. 1980) as a function of guar gum concentration with emphasis on low concentration behavior.**

polysaccharide with numerous hydroxyl (-OH) groups (Risica et al. 2005) that can form hydrogen bonds (Bruice 2004).

Additionally, kaolinite has asymmetrical surfaces with one face surface consisting of oxygen (O) and the other consisting of hydroxide (OH) (Mitchell and Soga 2005). Both the oxygen and hydroxide face surfaces are capable of forming hydrogen bonds with other compounds. For example, kaolinite particles can form stacks with hydrogen bonds making up the interlayer bond (Mitchell and Soga 2005). Podsiadlo et al. (2007) showed that organic polymers can form a highly linked clay-polymer network through hydrogen bonding between the polymer and clay particles. Further, Ma and Pawlik (2007) demonstrated that hydrogen bonding was the dominant mechanism of interaction between guar gum and kaolinite surfaces. Since the kaolinite surfaces readily interact with guar gum molecules to form numerous hydrogen bonds, they form a highly linked, extensive clay-polymer network within the clay-polymer mixture.

Based on this discussion, it can be concluded that, even if 3 wt.% guar gum and 10 wt.% xanthan gum solutions have nearly the same viscosity, the molecular scale interactions between biopolymer and clay particles are different. Since guar gum interacts more extensively with kaolinite than xanthan gum, the 3 wt.% guar gum solution seems to have a more profound influence on liquid limit than even 10 wt.% xanthan gum solution. The mechanisms of biopolymer mediated aggregation, biopolymer cross-linking, and biopolymer adsorption on kaolinite further help to describe these deviations. Additional mechanisms for interaction are likely to exist, and more investigation is needed.

### **3.3.2 Biopolymer Mediated Aggregation**

Although the viscosity of 4.5 wt.% xanthan gum solutions and 2 wt.% guar gum solutions are similar, the liquid limits for kaolinite when these solutions are used measure 65.1% and

185.9%, respectively. Aggregation of the clay particles seems to account for the difference. Ouhadi and Goodarzi (2006) demonstrated that adding a coagulant to clay reduces the liquid limit of the clay. By causing the clay particles to aggregate, the specific surface area of the clay is decreased, and less liquid is required to fully hydrate the surfaces of the soil particles. The liquid limit for the kaolinite and 4.5 wt.% xanthan gum mixture is less than the liquid limit for the kaolinite and 2 wt.% guar gum mixture because xanthan gum causes more aggregation than guar gum.

The maximum liquid limit that occurs in Figures 3.1 and 3.3 at 0.5 wt.% xanthan gum is caused by the interaction of viscosity and aggregation for xanthan gum and kaolinite. For xanthan gum concentrations less than 0.5 wt.%, the increase in the liquid limit caused by increases in pore fluid viscosity outpaces the decrease caused by aggregation of the kaolinite particles. For concentrations greater than 0.5 wt.% and less than 5 wt.%, the decrease in the liquid limit caused by the xanthan gum aggregating the kaolinite particles was stronger than the increase caused by viscosity.

Figure 3.5 shows ESEM images of kaolinite at the liquid limit for DI water, 1 wt.% xanthan gum, and 2 wt.% guar gum. The images for the biopolymer solutions show significant aggregation compared to the image for kaolinite with just DI water. The mechanism for aggregation could be provided by strands of biopolymer binding multiple clay particles together. The pseudoplastic nature of xanthan gum and guar gum solutions, even at very low concentrations, prohibited the use of particle size distribution tests that depend on Stokes' law since Stokes' law requires exact knowledge of the viscosity of the fluid that resists the movement of individual particles.

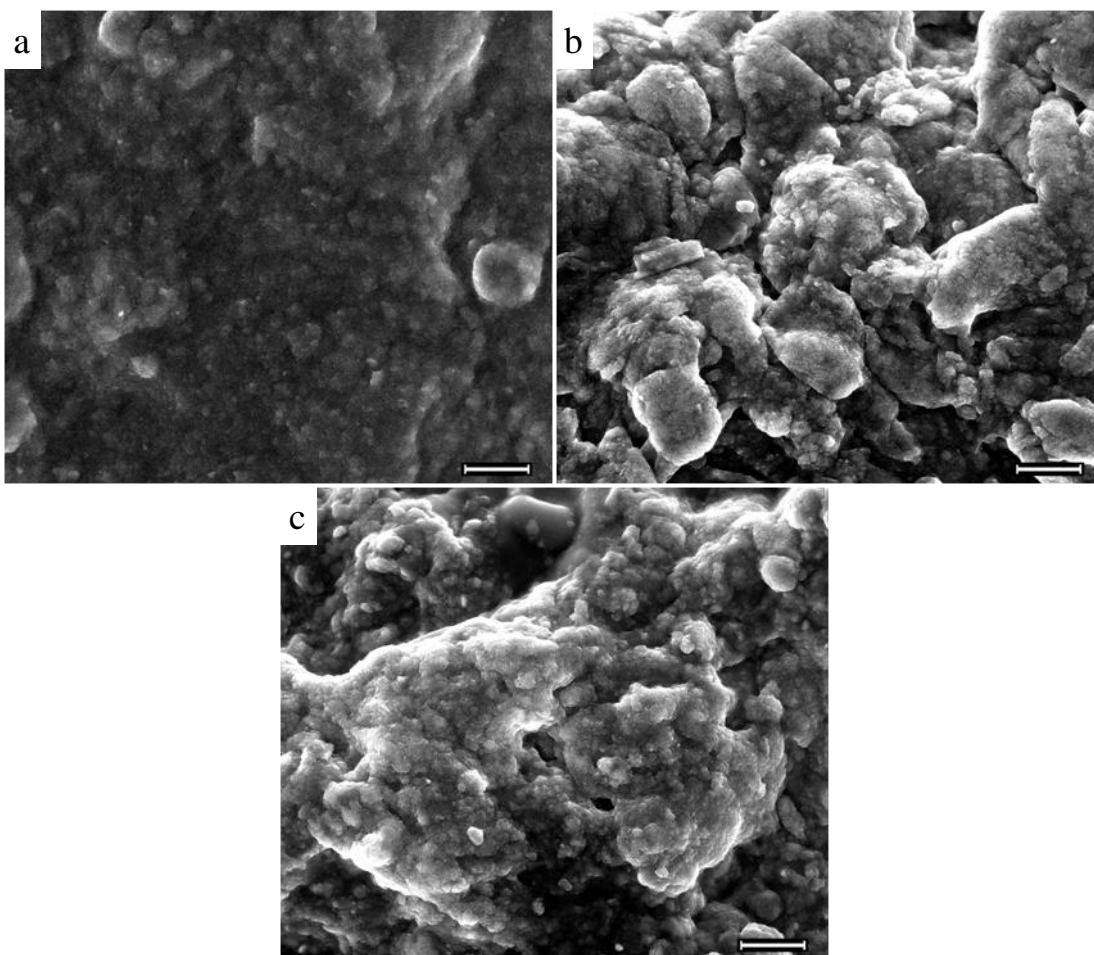


**Figure 3.5: ESEM images of kaolinite at the liquid limit for (a) DI water, (b) 1 wt.% xanthan gum, and (c) 2 wt.% guar gum. Scale bars represent 20  $\mu\text{m}$ . There is far less aggregation in (a) than in (b) and (c).**

### **3.3.3 Biopolymer Cross-linking**

Cross-linkers are compounds that form bonds between separate polymer strands. Molecular strands of xanthan gum strongly associate with calcium ions. This is due to ionic attraction between the anionic xanthan gum and the calcium cations and due to the geometry of the xanthan gum/calcium complex being favored over other divalent cations (Sutherland 1994). Since cross-links make polymer systems more rigid, the addition of  $\text{Ca}(\text{NO}_3)_2$  to the xanthan gum solutions resulted in an observable increase in viscosity.

To examine the influence of cross-linking on the behavior of the clay-biopolymer system, 0.1 M  $\text{Ca}(\text{NO}_3)_2$  solution was used instead of DI water to prepare the xanthan gum solutions that were added to the clay sample for liquid limit measurements. Figure 3.6 reflects this increase in viscosity. There is a dramatic increase in the liquid limit for xanthan gum concentrations of 2 wt.% and greater.

It is interesting to discuss the two points with xanthan concentrations of 0 and 1 wt.%. At 0 wt.% xanthan gum, the addition of  $\text{Ca}(\text{NO}_3)_2$  decreases the liquid limit compared with that of DI water. This is caused by the presence of divalent  $\text{Ca}^{2+}$  in the pore fluid, which increases the solution ionic strength and reduces the thickness of the electric double layer on kaolinite particle surfaces. At 1 wt.% xanthan concentration, the liquid limit for the  $\text{Ca}(\text{NO}_3)_2$  solution is still smaller than that for DI water. The reason is that while cross-linking of xanthan polymer strands

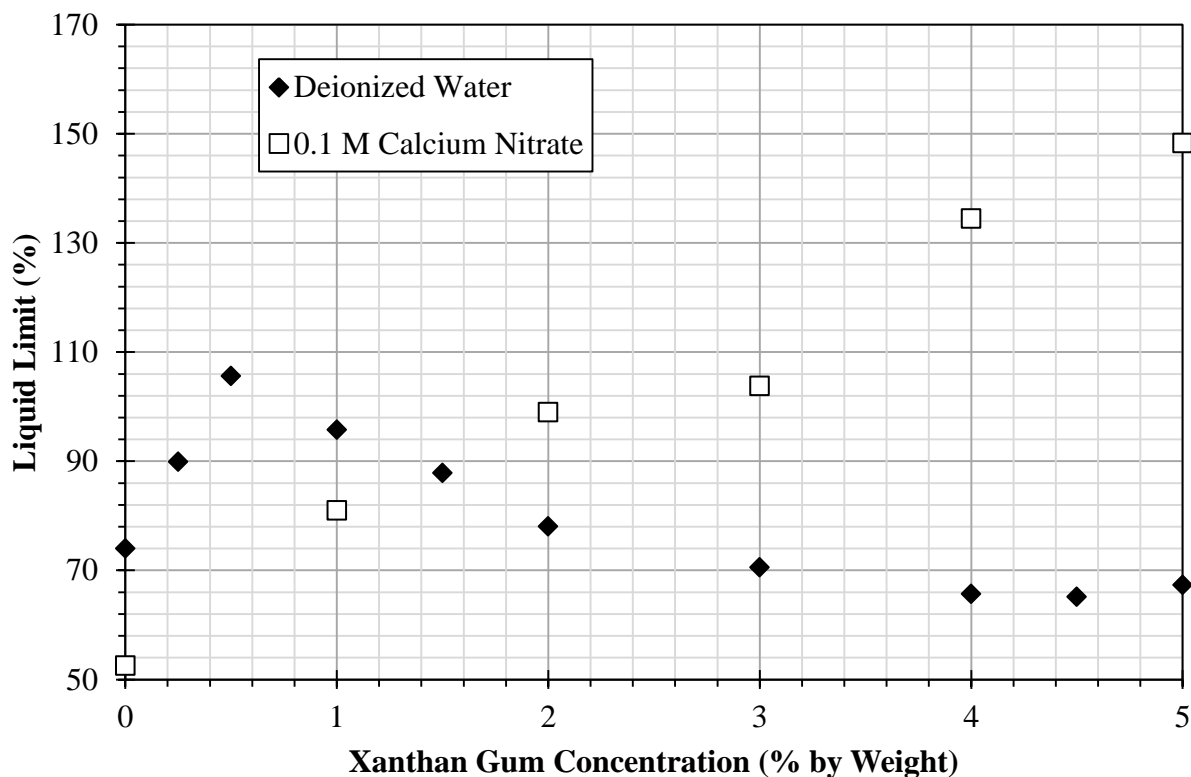


**Figure 3.6: Liquid limit of kaolinite as a function of xanthan gum concentration and background ion.**

occurs in the mixture, the degree of cross-linking is not significant enough to compensate for the reduction caused by the double layer thickness reduction.

Increases in the liquid limit produced through cross-linking suggests that clays containing natural EPS or that have an artificially added biopolymer can be further strengthened through the use of common chemicals, like calcium. The addition of inorganic compounds can modify the behavior of the clay-biopolymer system. This demonstrates how these interactions can change the engineering behavior of the system.

### **3.3.4 Biopolymer Adsorption on Kaolinite**

Inorganic compounds can also change how much biopolymer clay particles can adsorb via ionic or hydrogen bonds. Guar gum attaches itself to the surface of kaolinite particles by forming hydrogen bonds with the surface of the kaolinite (Ma and Pawlik 2007). When sodium cations in the background solution fill cation exchange sites on the surface of kaolinite, the sodium cations form a thick, stable interfacial water layer around the kaolinite particles because the sodium cations are well hydrated. This interfacial water layer then prevents the approach of molecular strands of guar gum, and that inhibits the ability of guar gum to form hydrogen bonds with kaolinite.

Potassium cations, however, are poorly hydrated. The presence of potassium on the surface of kaolinite disrupts the interfacial water layer around kaolinite particles. This enhances the ability of guar gum to approach and bond to the kaolinite particles. Ma and Pawlik (2007) demonstrated that a background 0.01 M NaCl solution results in about the same amount of guar gum adsorbed on kaolinite as deionized water, while a background 0.01 M KCl solution approximately doubles the amount of guar gum adsorbed on kaolinite.

Figure 3.7 illustrates how changes in guar gum adsorption affect the liquid limit. Although the data is less clear for guar gum concentrations less than 1.5 wt.%, the 1.5 wt.% and 2 wt.% concentrations show that the addition of potassium results in a greater reduction in the liquid limit than sodium.

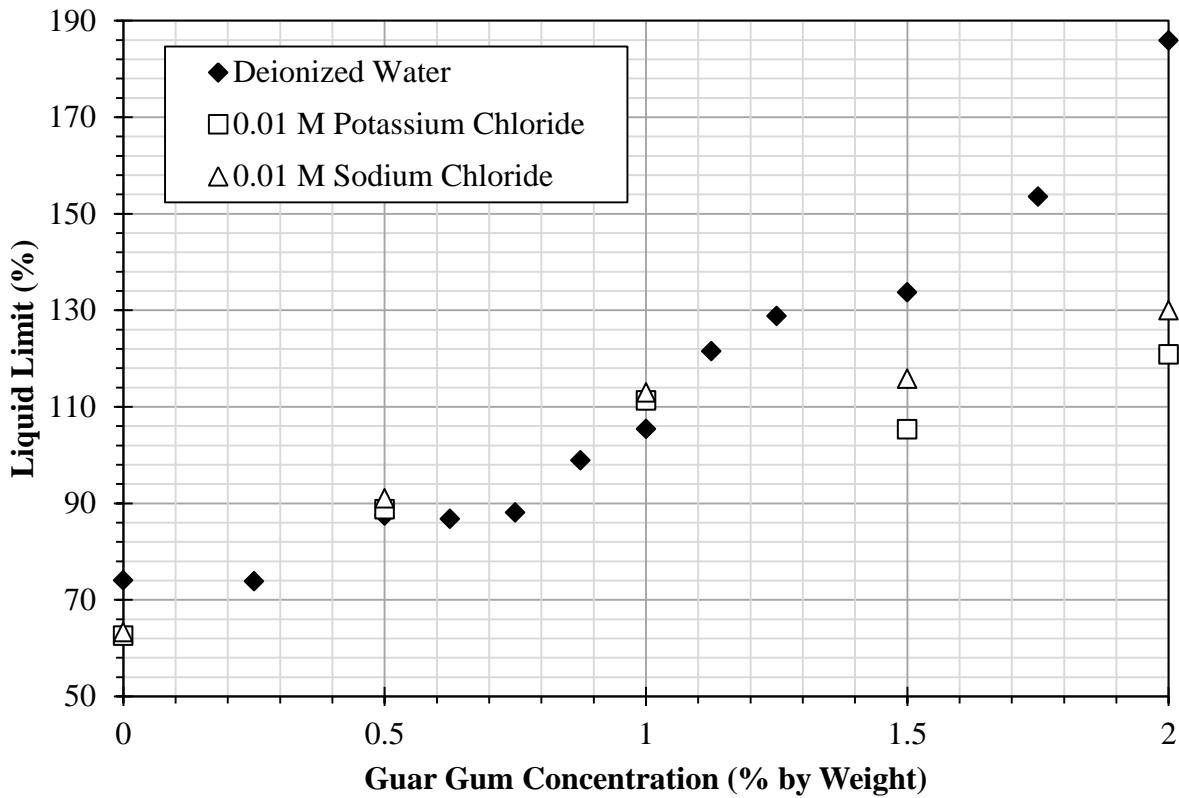


**Figure 3.7: Liquid limit of kaolinite as a function of guar gum concentration and background ion.**

Both sodium and potassium at 0.01 M concentration will reduce the liquid limit by the same amount when there is no biopolymer. This is because the equal ionic strength of the two solutions will equally compress the electric double layer of the kaolinite, as demonstrated by the liquid limits of 62.6% and 63.3% for the 0.01 M KCl and 0.01 M NaCl solutions, respectively. However, at the 2 wt.% guar gum concentration, the solution with potassium as the background cation resulted in a liquid limit of 120.8%, while the solution with sodium as the background cation possessed a liquid limit of 130.0%. The difference in liquid limit for the two separate



cations is caused by potassium increasing the amount of guar gum adsorbed to the surface of the kaolinite. This increase in adsorption then causes more aggregation, as demonstrated by the reduction in the liquid limit.

Figure 3.8 shows ESEM images. These images are of the soil fabric for kaolinite at the liquid limit for 2 wt.% guar gum made with DI water, 2 wt.% guar gum with 0.01 M KCl, and 2 wt.% guar gum with 0.01 M NaCl.

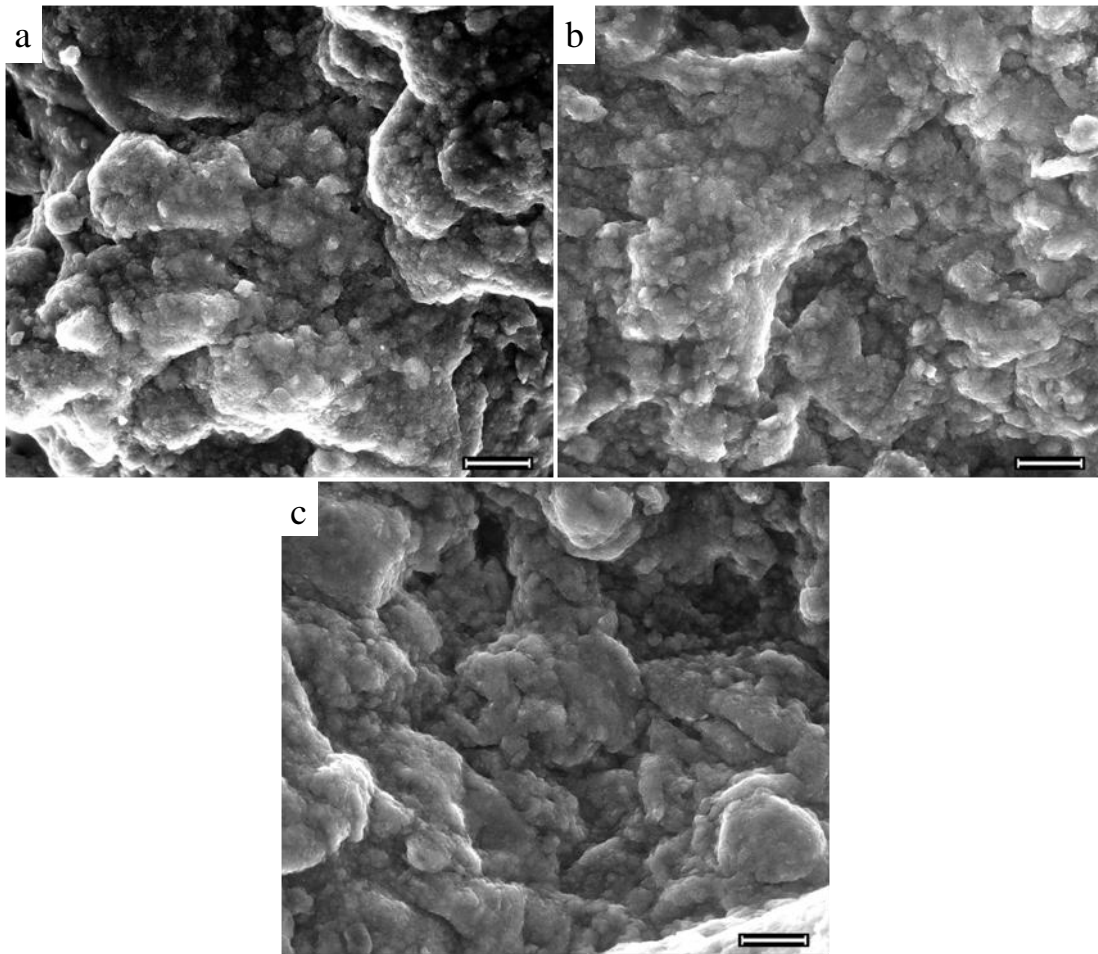


**Figure 3.8: ESEM images of kaolinite at the liquid limit for 2 wt.% guar gum solution made with (a) DI water, (b) 0.01 M KCl, and (c) 0.01 M NaCl. Scale bars represent 20  $\mu\text{m}$ . Aggregation is evident in all three images.**

Dontsova and Bigham (2005) revealed that the addition of  $\text{Ca}(\text{NO}_3)_2$  to xanthan gum and kaolinite mixtures increases the amount of xanthan adsorbed on the surface of kaolinite.

Divalent calcium cations act as ionic bridges, bonding anionic xanthan gum to anionic kaolinite particles. Figure 3.6 does not show the corresponding reduction in liquid limit due to increased xanthan gum adsorption. This is because the increase in the liquid limit resulting from cross-linking overcomes the effects of increased adsorption and aggregation.

### **3.3.5 Engineering Implications**

Liquid limit is a simple but important index property for cohesive soils. It reflects the particle-level interactions and soil microstructure (Zhang et al. 2004). The undrained shear strength of most soils at the liquid limit is 1.7-2.0 kPa (Sharma and Bora 2003), and the undrained shear strength is a function of water content (Zentar et al. 2009). At a given water content, a soil with higher liquid limit should have a higher shear strength than a soil with a lower liquid limit. This suggests that the presence of biopolymers in a cohesive soil can increase the undrained shear strength. Therefore, biopolymers, if properly introduced into cohesive soils or coastal sediments, can possibly increase the undrained shear strength and erosional resistance.

In most natural environments, soil pore fluid contains dissolved salts. The type and concentration of these background salts can also actively interact with biopolymer molecules and clay particles. There are five types of active nanoscale interactions within the clay particle, biopolymer, and cation system: (1) biopolymer-induced aggregation of clay particles; (2) polymer cross-linking caused by divalent cations; (3) the formation of a clay-polymer interconnected network via cation bridging and hydrogen bonds; (4) variation of double layer thickness on clay surfaces caused by the types and concentrations of cations; and (5) the competing adsorption of cations and biopolymer molecules onto clay surfaces. Interactions two and three can increase the undrained shear strength, while the others decrease it.

The macroscopic properties of the clay-biopolymer-cation system are the combined overall consequence of all the above described nanoscale interactions competing with each other. Understanding these interactions can help optimize the complex system to achieve desired changes in the engineering properties. Furthermore, a deeper understanding can be exploited to develop biological technologies to engineer soils. For instance, different bacteria can be introduced to a soil sequentially followed by adding a cross-linking agent to enhance soil strength.

### **3.4 Conclusions**

Laboratory experiments were conducted to measure liquid limits of kaolinite clay with varying biopolymer concentrations and background ions in the pore fluid to study influences of biopolymers on the behavior and engineering properties of cohesive soils in natural environments. Xanthan gum, an anionic bacterial extracellular polysaccharide, and guar gum, a neutrally charged plant polysaccharide, were two biopolymers used as EPS analogs. Three types of background cations in the pore fluid, including  $\text{Ca}^{2+}$ ,  $\text{Na}^+$ , and  $\text{K}^+$ , were also used to examine how background cations interfere with clay-biopolymer interactions.

From the experimental results, the following conclusions can be drawn:

- The liquid limit of kaolinite generally increases with the pore fluid biopolymer concentration due to increased viscosity, especially at higher concentrations.
- Biopolymer-induced aggregation at lower concentrations (e.g., xanthan gum) may overcome the influence of viscosity and hence slightly decrease the liquid limit.
- At the same pore fluid viscosity, increases in liquid limits caused by guar gum are much greater than that by xanthan gum because of more extensive interaction between guar gum and

clay particles, which results in extensive hydrogen bonding networks between guar gum and clay particles.

- Addition of cross-linking agents to a biopolymer solution in the pore fluid can greatly increase the liquid limit, since cross-linking can significantly increase the viscosity of pore fluids.
- Monovalent cations (e.g.,  $K^+$  and  $Na^+$ ) have preferred adsorption over biopolymers onto the clay particle surface, resulting in slight decreases in liquid limits.
- Presence of biopolymers in a cohesive soil can increase the undrained shear strength, at least for higher water content conditions, such as soft coastal or marine sediments at the water-sediment interface.

## **CHAPTER 4. THE EFFECT OF EXOPOLYMERS, VOID RATIO, AND CATIONS ON THE EROSIONAL RESISTANCE OF KAOLINITE\***

### **4.1 Introduction**

Currents or flows gradually remove soil particles on sediment surfaces. This erosion causes much infrastructure and natural habitat damage, especially along the United States coastline. Louisiana is severely afflicted by this problem, losing one acre of land every 24 minutes because of weak wetland sediment (Fischetti 2001) and subsidence. Of bridge failures between 1989 and 2000, 15.51% were caused by scouring of bridge foundations (Wardhana and Hadipriono 2003), and both external and internal erosion can cause failures of river banks, levees, and dams (Parker and Jenne 1967; Sherard et al. 1972).

One common method for rapidly rebuilding wetlands lost through erosion or subsidence is hydraulic pumping of dredged sediment to recreate the wetlands. However, the high water content muddy fill deposited by hydraulic pumping has low shear strength. This poor stability makes freshly deposited fill susceptible to erosion, especially until plants become established.

Care must also be used in amending the soil to improve shear strength because of the toxic or caustic nature of many soil stabilizers. Specifically, ASTM standard D 6276 (ASTM 2006) states that calcium hydroxide or calcium oxide must be added to a soil at a concentration that raises soil pH to 12.4, and this pH is far too alkaline for a healthy marsh ecosystem. Many grouts, such as polyacrylamide, are also toxic, and human exposure must be minimized. Given the large scale and environmentally sensitive nature of wetland restoration projects, traditional amendments are too risky to use.

---

\*Material reprinted from Nugent et al. (2010) with permission from the ASCE and Nugent et al. (2011a) posted ahead of print with permission from the ASCE.

Further, any compound used for improving slurry stability must not inhibit or slow vegetation growth, since plants are also important for increasing sediment stability. Tengbeh (1993) demonstrated that grass roots can provide a five-fold increase in shear strength over a wide range of water contents, and de Baets et al. (2007) showed that plant roots can increase surface erosion resistance. In addition, the World Health Organization (1975; 1987) has found that guar gum and xanthan gum are safe for mammals, while Sandford et al. (1984) and Wallace (1986) suggest that these biopolymers make an acceptable agricultural fertilizer ingredient and soil conditioner for promoting plant growth. This information provides a strong argument for the use of exopolymers to temporarily improve sediment stability because they may not put the environment at risk like other typical soil stabilizers while plants become established.

Soil environments have large populations of microorganisms, and an important product formed by micro-communities of bacteria is exopolymers, or extracellular polymeric substances (EPS) (Sutherland 2001). Microorganisms produce exopolymers to regulate the microenvironment and to protect themselves against predation and drying (Maier et al. 2000). Numerous studies have been performed demonstrating the usefulness of exopolymers in the environment.

Typically, exopolymers serve to increase the erosional resistance of sediments when present on sediment surfaces (Widdows et al. 2006; Yallop et al. 2000). In intertidal mudflats, a newly-placed sediment's stability was directly correspondent to that sediment's production and quantity of EPS (Widdows et al. 2006). In sand, *Alteromonas atlantica* built a biofilm that immensely increased the critical shear velocity necessary for the start of sand erosion (Dade et al. 1990). Further, sediment EPS has been found to positively correlate with erosional resistance, while humic acids negatively correlate with erosional resistance (Gerbersdorf et al. 2007).

In addition, a few pilot studies have explored the application of exopolymers to soil treatment and improvement. For instance, artificially added EPS dramatically increased the tensile strength of air-dried strips of clay (Chenu and Guérif 1991). Also, the addition of xanthan gum significantly increased the shear strength of Leighton Buzzard sand (Çabalar and Çanakci 2005). Another preliminary study by Nugent et al. (2009) demonstrated how two EPS analogues, guar gum and xanthan gum, changed the kaolinite's liquid limit.

Louisiana State University (LSU) is studying bioengineered sediment stabilization through the use of exopolymer amendments. This effort seeks a solution for wetland erosion that will have minimal environmental impact. Because the Lower Mississippi River Basin and the Northern Gulf Coast mostly have cohesive sediments, this is the type of sediment used.

This chapter describes how the erosional resistance of a pure kaolinite clay is enhanced using two exopolymer analogues, guar gum, a neutral polysaccharide derived from plants, and xanthan gum, a microbially produced anionic polysaccharide. A cohesive strength meter (CSM) is used to measure the critical value of shear stress  $\tau_{oCr}$  of high water content muds, representative of newly placed hydraulically pumped dredge fill. The initial water content of the muds is varied to determine how void ratio influences erosional resistance. Changes in  $\tau_{oCr}$  are explained in terms of nanoscale chemical and physical interactions between exopolymer strands and clay particles. These chemical and physical interactions are further explored by adding cations to the pore fluid. Methods for practical application of exopolymers for erosion control are then discussed.

## **4.2 Materials and Methods**

A relatively pure, untreated, kaolinite clay sample purchased from Theile Kaolin Company was used for this study. Particles smaller than 2  $\mu\text{m}$  made up 98 wt.% of the sample.

The specific gravity is 2.63, while the average specific surface area measured 20-26 m<sup>2</sup>/g (Flick 1989). Kaolinite was chosen to minimize variance caused by the sediment. Although pure mineral kaolinite is not representative of the composition of Louisiana wetland sediment, it provides a good starting point for determining mechanisms of biopolymer and clay interaction. Specifically, pure mineral kaolinite eliminates interference from naturally occurring organic material, and the low cation exchange capacity of kaolinite reduces variance from cations that can significantly change biopolymer and clay interaction (Nugent et al. 2009). The interaction mechanisms developed, however, will not be exclusive to kaolinite, which will allow extrapolation to other cohesive soils. Three inorganic salts were added as background ions to probe these interactions: calcium nitrate (Ca(NO<sub>3</sub>)<sub>2</sub>, ACS Grade) was purchased from EMD Chemicals Inc., and both sodium chloride (NaCl, ACS Grade) and potassium chloride (KCl, ACS Grade) were purchased from Mallinckrodt Chemicals.

Additionally, two EPS analogs were purchased. Laboratory Grade guar gum was purchased from Fisher Scientific. NF Grade xanthan gum was purchased from Spectrum Chemical Manufacturing Corporation. The EPS analogs are described below.

#### **4.2.1 Guar Gum**

This neutral polysaccharide comes from *Cyamopsis tetragonoloba* seeds (Risica et al. 2005). Its polymer backbone consists of mannose linked with  $\beta$ -1,4 bonds, and a single galactose is bonded to every second mannose (Whistler and Smart 1953). Guar gum is capable of hydrogen bonding because it possesses many hydroxyl (-OH) groups. Also, it has a neutral charge because it lacks readily ionizable functional groups, such as carboxylic acid (-COOH) groups.



Guar gum can produce viscous, pseudoplastic aqueous solutions representative of neutral microbial EPS, even though it is derived from plants. Guar gum has a commercial significance because it is readily available and inexpensive. It also has the ability to increase the viscosity of aqueous systems (Whitcomb et al. 1980).

#### **4.2.2 Xanthan Gum**

Xanthan gum is an anionic polysaccharide produced by the bacteria *Xanthomonas campestris* (Sutherland 1994). Its polymer backbone consists of glucose linked with  $\beta$ -1,4 bonds, and every second glucose possesses a mannose-glucuronic acid-mannose side chain (Hassler and Doherty 1990). The two mannoses are typically modified with an *O*-acetyl group added to the mannose closest to the glucose backbone, while the mannose furthest from the backbone contains a pyruvate ketal. However, the exact proportion of mannose modified depends on the bacterial strain and the physiological environment in which the bacteria grow (Sutherland 1994).

The anionic charge of xanthan gum comes from hydrogen atoms dissociating from carboxylic acid (-COOH) groups to form carboxylate (-COO<sup>-</sup>) anions (Bruice 2004). Xanthan gum's hydroxyl (-OH) groups also allow for hydrogen bonding. Xanthan gum is used commercially because just a small amount of it will greatly increase the viscosity of an aqueous system (Hassler and Doherty 1990). An increased shear rate, however, decreases its viscosity because it is pseudoplastic (Milas et al. 1985).

#### **4.2.3 Preparation of Biopolymer and Clay Mixtures**

Erosional resistance was measured using a CSM apparatus. This apparatus uses air pressure to force water through a brass jet contained inside of a sensor head, and the sensor head is shown in Figure 4.1. Before starting the test, the sensor head is pressed into the sediment

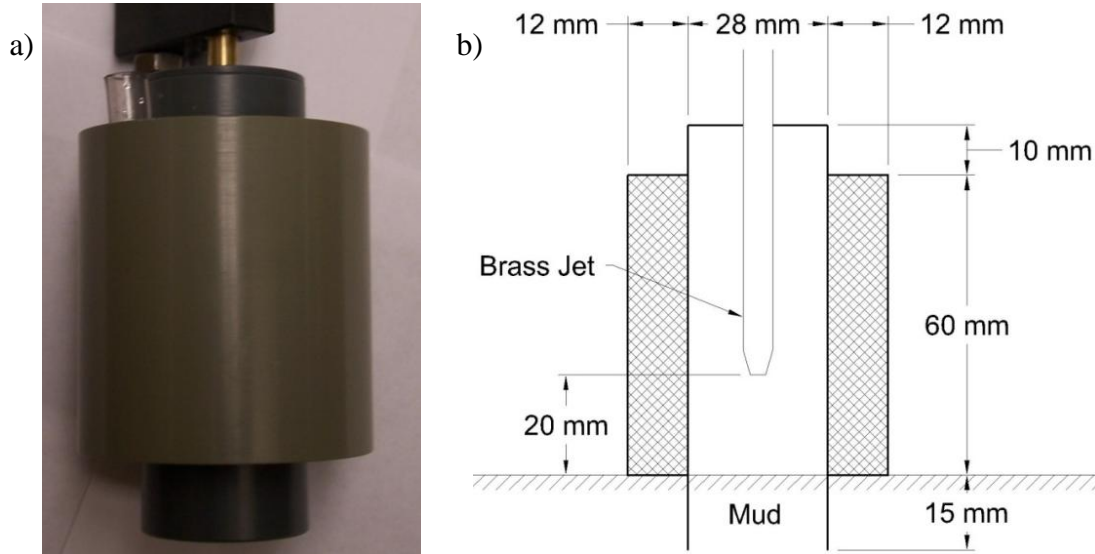


**Figure 4.1: (a) Picture of CSM sensor head and (b) schematic of CSM sensor head cross section inserted into a sediment surface.**

surface and filled with water. As the test progresses, the water jet is fired at the sediment surface, with increasing air pressure driving the water jet. Inside the sensor head is also an infrared emitter and detector. The amount of infrared light detected is reduced as sediment is eroded and suspended in the sensor head, and the apparatus electronically records these data.

Since the sensor head was designed to be pressed into sediment surfaces, the biopolymer and clay muds prepared for the CSM tests had to be prepared in a fashion that provides a consistent, accessible surface for the 63.5 mm (2.5 in.) wide sensor head. Glass beakers (400 ml) filled with 125 ml of mud provided a surface with enough clearance and sufficient sediment depth to prevent the water jet from eroding enough mud to reach the bottom of the beaker. Starting water contents  $w$  of 180%, 200%, and 220% were used because this amount of water, when mixed with the kaolinite chosen for this test, produces a fluid mud representative of high water content wetland mud.

It is not useful to describe biopolymer concentration in terms of its pore solution concentration because a saturated clay's water content decreases during consolidation and varies

in nature. Therefore, the biopolymer mass ratio, or  $R_{bm}$ , is used to measure concentration, which is the ratio of dry biopolymer mass to the sediment dry mass. To produce the specimens used for the CSM tests, a 1.5 wt.% guar gum solution and a 1.5 wt.% xanthan gum solution were first made.

Although there are other means of making homogenous biopolymer solutions that involve the addition of chemicals, such as glycol and alcohol (Phillips and Williams 2000), it seems that direct physical means of mixing the solutions would be preferred for large scale application in the field. This is because it would save on costs, since additional chemicals would not have to be purchased. Therefore, these tests used physical mixing.

Dry biopolymer powder was slowly added into either deionized (DI) water, 0.1 M  $\text{Ca}(\text{NO}_3)_2$ , 0.2 M NaCl, 0.01 M NaCl, or 0.01 M KCl that was stirred by a stir bar over several minutes to reduce clumping. An immersion blender was then used to break down biopolymer powder clumps in the solutions to completely homogenize the solutions. Next, predetermined masses of biopolymer solution, dry kaolinite powder, and either DI water or salt solution were mixed to produce 125 ml specimens with 180%, 200%, and 220% water contents, the desired background cations, and appropriate  $R_{bm}$  values.

Thirty-nine specimens were made, which included kaolinite without biopolymer, guar gum and kaolinite mixtures with concentrations of 0.005, 0.010, 0.015, and 0.020  $R_{bm}$ , and xanthan gum and kaolinite mixtures with concentrations of 0.005, 0.010, 0.015, and 0.020  $R_{bm}$ . After adding the materials for each specimen, the materials were lightly stirred with a spatula to prevent driving kaolinite powder into the air and to partially mix the mud. Again, the immersion blender was used to make sure the mud was homogenized.

With the specimens fully mixed, each mud was loaded into a beaker by using a spatula to place portions of mud into the center of the beaker, while being careful not to trap any bubbles of air. As the muds were relatively fluid, they flowed outward and formed a reasonably smooth upper surface. Since dredging is normally done during calm weather and wave conditions, freshly deposited slurry will typically have a few days before being exposed to significant erosional events. Thus, the beakers of mud were placed in a refrigerator at 4 °C for 72 hours to let the mud briefly consolidate under its own weight while minimizing the effect of biological degradation.

After 72 hours, those refrigerated muds were allowed to warm to room temperature. Any water present on the slurry surface was carefully removed with a paper towel. Then, the CSM sensor head was inserted into the slurry surface and was used to measure  $\tau_{oCr}$ , as described in the next section.

#### **4.2.4 Cohesive Strength Meter Methodology and Data Analysis**

The apparatus employed was a MKIV 60psi CSM acquired from Partrac Ltd., and it was used based on the guidelines proposed by Tolhurst et al. (1999), as CSM tests do not have an ASTM standard defining their use. With the CSM sensor head in the sediment surface, the sensor head was carefully filled with DI water, and test program MUD 3 was activated. This test program involves activating the water jet for 0.3 seconds, and then measuring the infrared transmissivity of the water in the sensor head for 30 seconds before activating the jet again. As more sediment is eroded, the transmissivity of the suspension decreases because suspended sediment blocks part of the infrared light beam.

The jet was initially fired using a driving air pressure of 3.45 kPa (0.5 psi) with the pressure increased by 3.45 kPa (0.5 psi) until a pressure of 34.47 kPa (5 psi) was reached.

Afterwards, the pressure was incremented by 6.89 kPa (1 psi) until either a pressure of 413.69 kPa (60 psi) was reached or the operator ended the test early due to the transmissivity approaching 0%. Once the program was complete, some mud around the outside of the sensor head was removed to measure  $w$  according to ASTM standard D 2216 (ASTM 2006). The sensor head was then removed and cleaned.

Since the biopolymers are high molecular weight polysaccharides, they do not volatilize at  $110 \pm 5$  °C in the drying oven. As an example of how high molecular weight polysaccharides resist volatilization, wood that largely consists of high molecular weight polysaccharides (Sjötröm 1993) does not appreciably volatilize until the temperature is above 300 °C (U.S. 2007). Because of the biopolymers' lack of volatilization, they contribute to the weight of the solids when determining water content or void ratios.

Critical values of shear stress  $\tau_{oCr}$  for each specimen were determined from the raw CSM data by plotting the transmissivity against time, as shown in Figure 4.2. Transmissivity was plotted as a percentage, with 100% being the amount of infrared light passing through clear water in the sensor head and 0% being all infrared light blocked. Two lines were drawn, with the first line going through the linear points before the sediment significantly eroded, and the second line was drawn through the linear points where the sediment is appreciably eroded by the water jet. These are the two thin, straight lines in Figure 4.2. The intercept is the time where  $\tau_{oCr}$  is applied to the sediment. As this time is often between jet firings with discrete driving pressures, linear interpolation was used to calculate the intercept jet driving pressure. This driving pressure was then substituted into the equation developed by Tolhurst et al. (1999), which was used to plot the shear stress curve in Figure 4.2. Two arrows in Figure 4.2 illustrate substituting the interpolated pressure into the shear stress equation to get  $\tau_{oCr}$ .

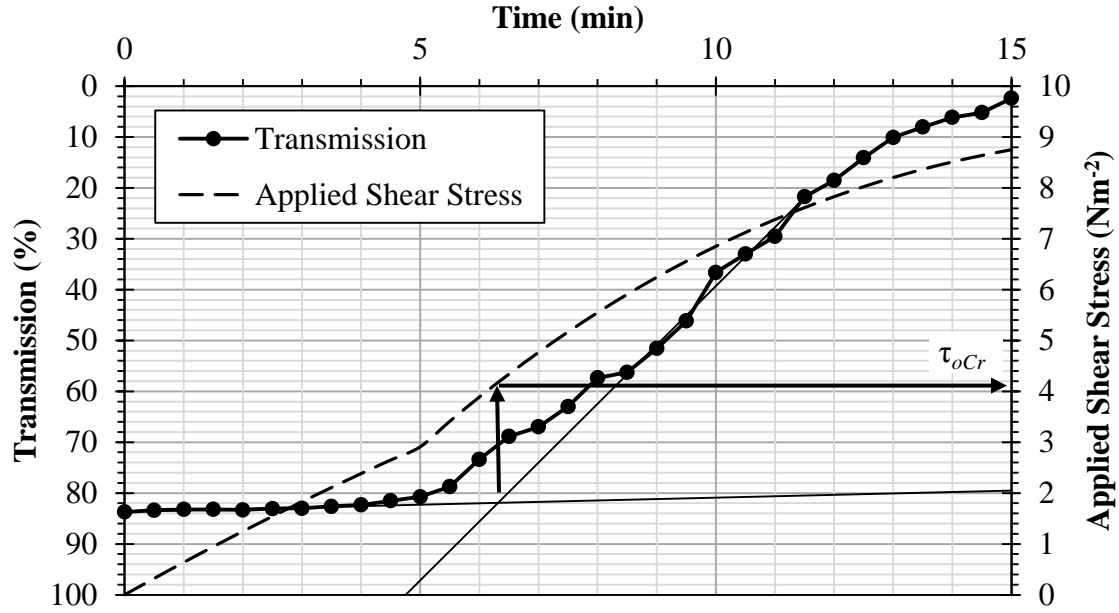


**Figure 4.2: Representative raw CSM data and data analysis.**

### 4.3 Results and Discussion

The results of the guar gum and kaolinite mixtures with DI water, as well as the results of the xanthan gum and kaolinite mixtures with DI water are provided in Figure 4.3. For this figure, the initial water contents for all specimens were 180%, and the liquid limit values are adapted from Nugent et al. (2009). Except for the 0.015 and 0.020  $R_{bm}$  xanthan gum mixtures, the specimens were able to support the weight of the water filled sensor head needed to successfully complete the CSM tests. The two high concentration xanthan gum mixtures were too fluid to support the water filled sensor head, so valid  $\tau_{oCr}$  or water content data could not be collected.

Results for guar gum and kaolinite mixtures with varying void ratios are provided in Figure 4.4, and xanthan gum and kaolinite mixtures with background cations results are illustrated in Figure 4.5. Figure 4.6 contains the results for guar gum and kaolinite mixtures with background cations. For the xanthan gum and guar gum specimens with background cations, initial water contents of 180% were used. In addition to the 0.015 and 0.020  $R_{bm}$  xanthan gum

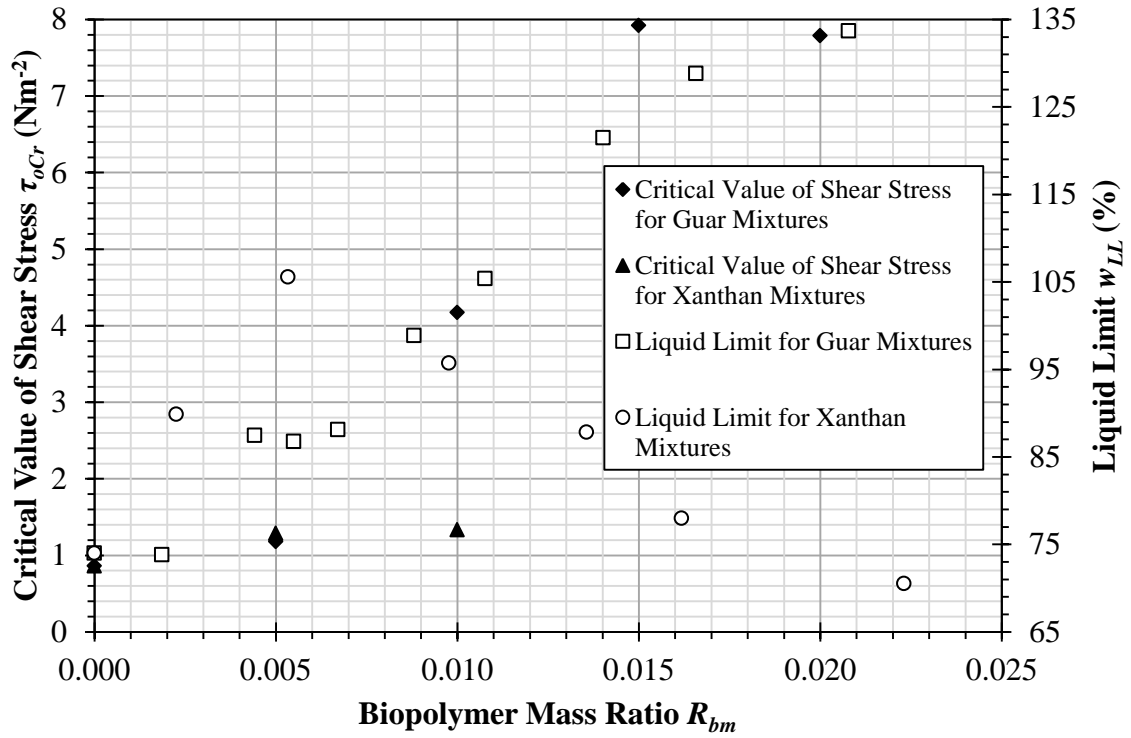


**Figure 4.3: Erosional resistance as a function of biopolymer concentration. Liquid limit values are adapted from Nugent et al. (2009).**

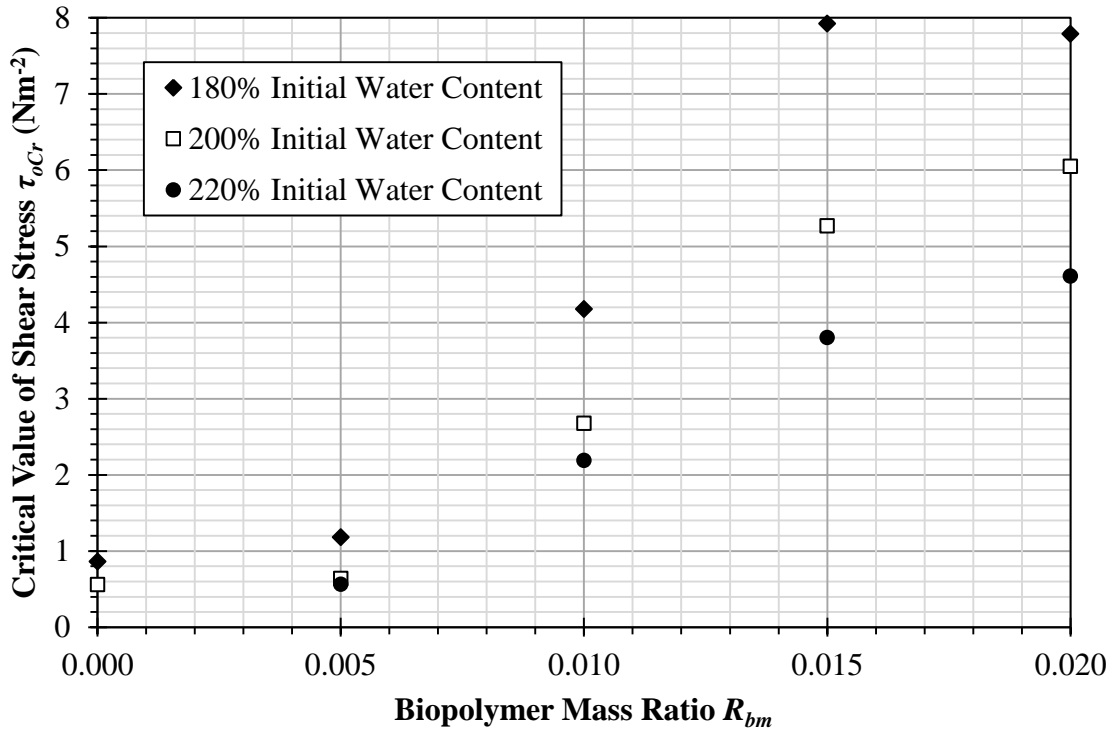


**Figure 4.4: Erosional resistance as a function of guar gum concentration and initial  $w$ .**

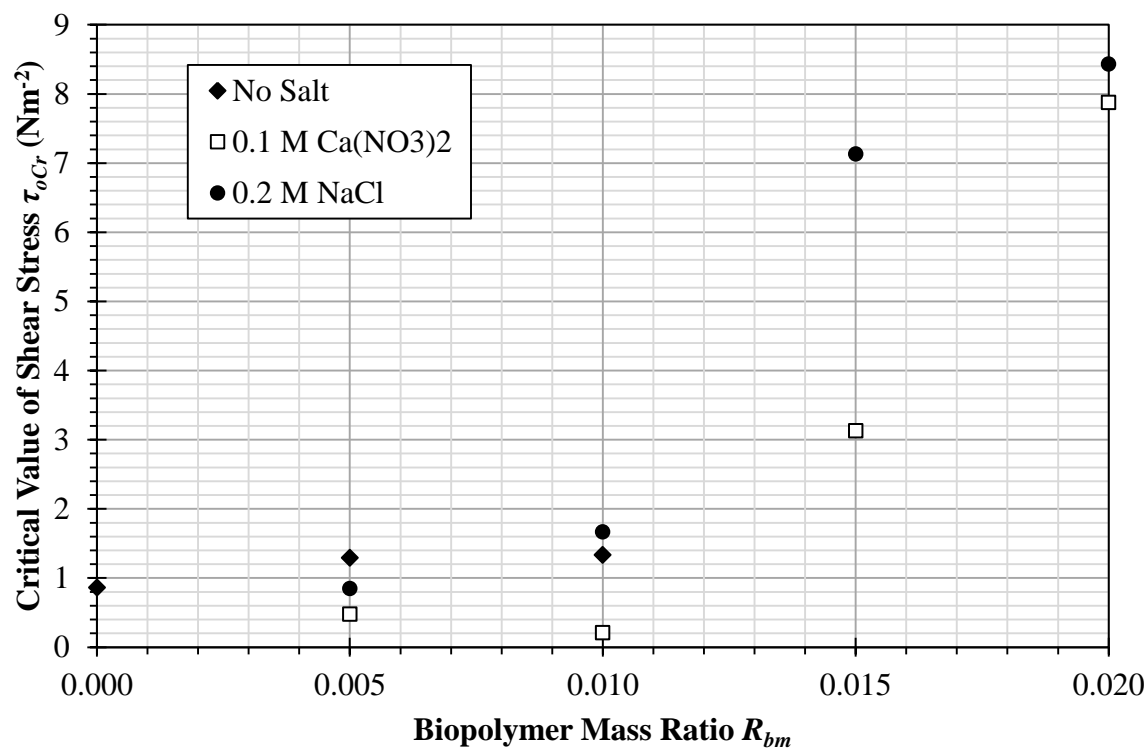


**Figure 4.5: Erosional resistance as a function of xanthan gum concentration and background cation.**

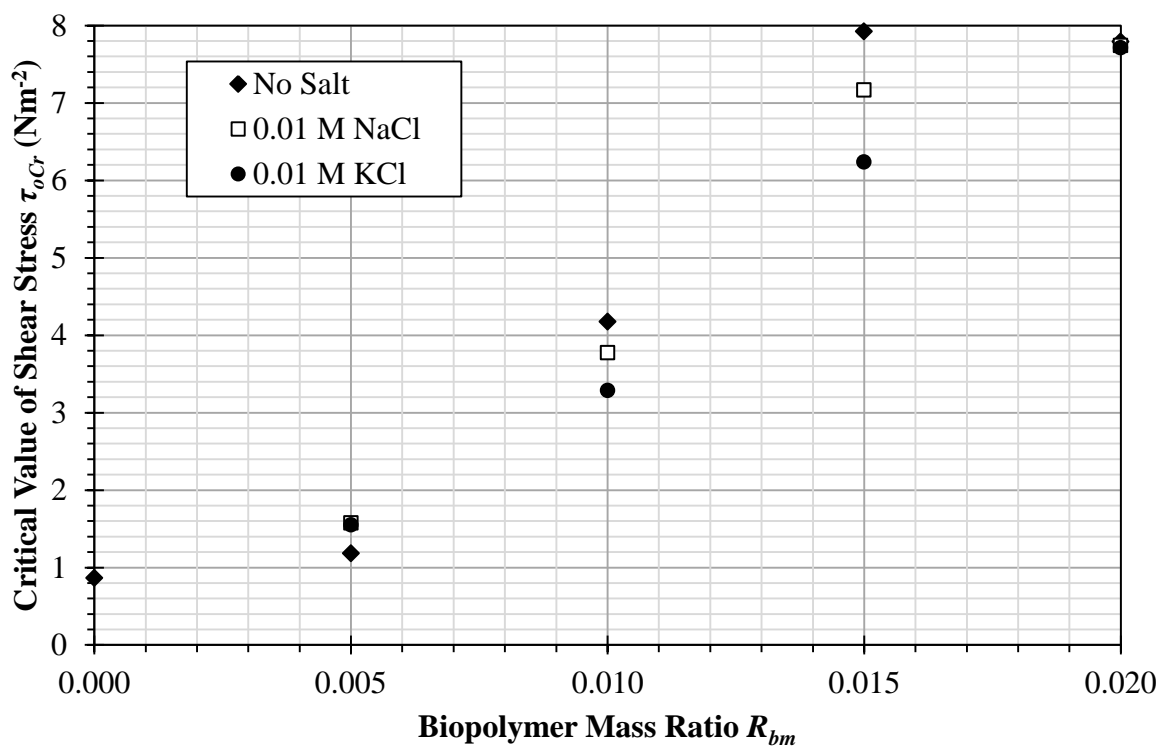


**Figure 4.6: Erosional resistance as a function of guar gum concentration and background cation.**



mixtures mentioned above, the plain kaolinite with 0.1 M  $\text{Ca}(\text{NO}_3)_2$ , 0.2 M NaCl, 0.01 M NaCl, 0.01 M KCl, and 220% initial  $w$  specimens were unable to support the weight of the water filled sensor head, so valid  $\tau_{oCr}$  and  $w$  data could not be collected. However, all the other specimens were successfully tested.

#### 4.3.1 Biopolymer Mixtures with DI Water and 180% Initial Water Content

As shown in Figure 4.3, erosional resistance for 0.015 and 0.020  $R_{bm}$  guar gum mixtures is increased by a factor of nine over kaolinite on its own, while 0.005 and 0.010  $R_{bm}$  xanthan gum mixtures increase erosional resistance by 1.5 times. Water contents for all the specimens illustrated in Figure 4.3 fell within  $178\% \pm 4\%$ . This reveals that little consolidation occurred and that these specimens all have approximately the same void ratio.

Figure 4.3 shows a clear relationship between  $\tau_{oCr}$  and the liquid limit for guar gum. Nugent et al. (2009) demonstrated that the liquid limit of a guar gum and clay mixture increases as the biopolymer concentration increases because the guar gum boosts the pore fluid viscosity. Since viscosity is a measure of the shear resistance of a fluid, increased pore fluid viscosity leads to greater shear resistance of the overall mixture. In addition, most soils have an undrained shear strength of 1.7-2.0 kPa at the liquid limit (Sharma and Bora 2003), and undrained shear strength is a function of water content (Zentar et al. 2009). Thus, a sediment with a higher liquid limit will generally have a higher undrained shear strength for a given water content. Watts et al. (2003) illustrated a positive correlation between fall cone measured sediment shear strength and  $\tau_{oCr}$ . As a result, the relationship between  $\tau_{oCr}$  and the liquid limit is the result of both Casagrande cup and CSM tests indirectly measuring sediment shear strength.

Also shown in Figure 4.3 is a correlation between  $\tau_{oCr}$  and the liquid limit for the 0.005 and 0.010  $R_{bm}$  xanthan gum mixtures, although this correlation is muted compared to the guar

gum mixtures. Xanthan gum was also demonstrated by Nugent et al. (2009) to increase the liquid limit by increasing the pore fluid viscosity. However, Nugent et al. (2009) revealed that aggregation caused by xanthan gum at intermediate concentrations reduces the liquid limit to below that of the clay with no biopolymer added. For these intermediate concentrations, the aggregation effect overpowers the pore fluid viscosity effect, while viscosity effects overpower aggregation effects at low and high concentrations.

Further, Garrels (1951) demonstrated that the water velocity needed to remove particles from sediment surfaces dramatically decreases as particle size increases for particles smaller than 0.5 mm. The fact that the 0.015 and 0.020  $R_{bm}$  xanthan gum mixtures were too fluid and weak to measure their erosional resistance, along with the sediment shear strength and  $\tau_{oCr}$  correlation provided by Watts et al. (2003), show that these higher concentration xanthan gum mixtures have a significantly reduced erosional resistance. Altogether, this suggests that biopolymer induced aggregation negatively affects erosional resistance in xanthan gum mixtures with concentrations greater than 0.010  $R_{bm}$ .

Nugent et al. (2009) also noted that nanoscale interaction between biopolymer strands and clay particles serves to change the liquid limit. Specifically, they found that at biopolymer concentrations with similar pore fluid viscosities, guar gum raises the liquid limit much higher than xanthan gum. This was explained as a result of the guar gum and kaolinite forming an extensive hydrogen bonding network. Xanthan gum and kaolinite interacted little since xanthan gum's negative charge and the overall negative charge kaolinite particles possess at solution pH greater than 2.35 (Alkan et al. 2005) caused electrostatic repulsion that minimized any bonding. A similar effect is demonstrated by the CSM results. Both the 0.020  $R_{bm}$  guar gum mixture and the 0.005  $R_{bm}$  xanthan gum mixture have zero shear rate pore fluid viscosities of about 30 Pa·s

(Whitcomb et al. 1980; Milas et al. 1985). However, the 0.020  $R_{bm}$  guar gum mixture has a  $\tau_{oCr}$  six times greater than the 0.005  $R_{bm}$  xanthan gum mixture. This disparity is the result of the guar gum and kaolinite forming a hydrogen bonding network, while the xanthan gum and kaolinite electrostatically repel each other.

#### **4.3.2 Guar Gum Mixtures with DI Water and Varying Initial Water Content**

As noted above, post consolidation  $w$  for the 180% initial  $w$  series in Figure 4.4 fell within  $178\% \pm 4\%$ , which reveals that little consolidation occurred and that these specimens have approximately the same void ratio. The 200% initial  $w$  series had final water contents of  $200\% \pm 5\%$  when excluding the 0.005  $R_{bm}$  mixture that had a 187%  $w$ . Final  $w$  for the 220% series were  $215\% \pm 5\%$  when excluding the 0.005  $R_{bm}$  mixture 186%  $w$ . Overall, the mixtures cover a range of void ratios from 4.58 to 5.79.

The previous section demonstrated that guar gum increases  $\tau_{oCr}$  by increasing pore fluid viscosities and by forming an extensive hydrogen bonding network between guar gum molecular strands and kaolinite platelets. Figure 4.4 shows that these effects serve to improve erosional resistance across a variety of  $w$  and void ratios. There is notable separation between the points for 0.010, 0.015, and 0.020  $R_{bm}$ , with void ratio increases of 9% producing approximately 25% decreases in  $\tau_{oCr}$ . Mixtures with 0.005  $R_{bm}$  concentration show less separation because self-weight consolidation of these mixtures brought their final void ratios closer together. Reddi and Bonala (1997) suggested that part of a clay's ability to resist erosion is due to particle interlocking. Higher void ratio clays would have less particle interlocking than lower void ratio clays, which leads to the reduced erosional resistance shown across biopolymer concentrations in Figure 4.4.

### 4.3.3 Xanthan Gum Mixtures with Calcium and Sodium Background Cations

Figure 4.5 demonstrates the effects of background cations on xanthan gum and kaolinite mixtures. As discussed previously, high concentration xanthan gum mixtures with no background cations have reduced erosional resistance due to biopolymer induced aggregation. Also, even when controlling for pore fluid viscosity, xanthan gum produces much less improvement in erosional resistance. This disparity is the result of the guar gum and kaolinite forming a hydrogen bonding network, while the xanthan gum and kaolinite electrostatically repel each other.

However, Nugent et al. (2009) found that adding calcium cations to the pore fluid allows the formation of ionic cross-links between anionic xanthan gum strands and kaolinite platelets. For the CSM tests, 0.1 M  $\text{Ca}(\text{NO}_3)_2$  was used to produce cross-links, and 0.2 M NaCl was used to balance negative charges without producing cross-links. Initial  $w$  for all mixtures shown in Figure 4.5 was 180%. The 0.1 M  $\text{Ca}(\text{NO}_3)_2$  series had final water contents of  $166\% \pm 8\%$ , and the 0.2 M NaCl series had final water contents of  $172\% \pm 8\%$ .

The relationship between clay liquid limits and  $\tau_{oCr}$  are also demonstrated by the results in Figure 4.5. This effect is seen with the kaolinite that has no biopolymer since the two muds with salts were too weak to be measured, while the mud without a background salt could be measured. Salts serve to reduce the liquid limit by reducing the size of the electric double layer, and the reduction in the liquid limit is reflected in the reduction in the erosional resistance. Xanthan mixtures with 0.015 and 0.020  $R_{bm}$  and with background cations have significantly higher  $\tau_{oCr}$  than the mixtures without background cations.

Xanthan gum possesses hydroxyl groups that can form a hydrogen bonding network similar to that produced by guar gum if the negative electrostatic charge of the xanthan gum

strands are overcome. This hydrogen bonding network brings the  $\tau_{oCr}$  of the high concentration xanthan gum mixtures closer to the  $\tau_{oCr}$  of the high concentration guar gum mixtures. Additionally, both the sodium and calcium salt solutions produced visible dispersion of the xanthan gum and kaolinite mixtures compared to mixtures made with DI water.

Goldberg and Glaubig (1987) showed that lowering the pH of a dispersed clay suspension can cause the clay to aggregate since a lower pH makes the clay more sensitive to the presence of salts. However, the fact that added salts caused dispersion demonstrates that the aggregation caused by xanthan gum is not likely the result of xanthan gum reducing mixture pH. Further, the cross-links produced by calcium cations visibly increase the number of aggregates in the muds relative to the muds made with sodium cations. As aggregation reduces  $\tau_{oCr}$ , the 0.1 M  $\text{Ca}(\text{NO}_3)_2$  series had smaller  $\tau_{oCr}$  values than the 0.2 M NaCl series, even though the 0.2 M NaCl series generally had a higher final water content than the 0.1 M  $\text{Ca}(\text{NO}_3)_2$  series.

#### **4.3.4 Guar Gum Mixtures with Sodium and Potassium Background Cations**

Effects of background cations on guar gum and kaolinite mixtures are demonstrated by the results in Figure 4.6. Nugent et al. (2009) revealed that potassium cations in the pore fluid of guar gum and kaolinite mixtures increase the adsorption of guar gum on kaolinite platelet surfaces. This adsorption reduces the liquid limit through increased aggregation. To correct for electric double layer effects, they compared the mixtures with potassium cations to mixtures with the same concentration of sodium cations, since sodium cations would induce the same electric double layer effects as potassium without the increase in adsorption.

For the CSM tests, 0.01 M KCl was used to increase guar gum adsorption on kaolinite particle surfaces, and 0.01 M NaCl was used to induce the same changes in electric double layer effects without modifying adsorption. Initial  $w$  for all mixtures shown in Figure 4.6 was 180%.

The 0.01 M KCl series had final water contents of  $180\% \pm 4\%$  when excluding the 0.005  $R_{bm}$  mixture that had a 165%  $w$ . The 0.01 M NaCl series had final water contents of  $181\% \pm 3\%$  when excluding the 0.005  $R_{bm}$  mixture that had a 172%  $w$ .

Again, the data in Figure 4.6 show that erosional resistance is reduced by increasing aggregation and by reducing the size of the electric double layer around kaolinite particles. Except for the 0.005  $R_{bm}$  mixtures, the mixtures with background cations had a lower  $\tau_{oCr}$  than the mixtures with just DI water. The 0.005  $R_{bm}$  mixtures with background cations had lower water contents than the 0.005  $R_{bm}$  mixture with just DI water due to self-weight consolidation, which helped increase the erosional resistance of the mixtures with background cations. For the 0.005, 0.010, 0.015, and 0.020  $R_{bm}$  mixtures, the mixture at a given  $R_{bm}$  with potassium cations had a lower  $\tau_{oCr}$  than the mixture with sodium cations because of increased aggregation as a result of increased biopolymer adsorption.

#### **4.4 Practical Applications**

Guar gum and xanthan gum that are added to hydraulically pumped dredged sediment can potentially improve resistance to erosion in wetlands, while likely minimizing environmental damage. Their non-toxicity should also allow plant growth that greatly stabilizes the soil. The biopolymer can easily be added to the sediment through a hydraulic dredge's slurry pump, where it can be completely mixed with the sediment by the slurry output pipe's turbulence.

Although xanthan gum shows poor results in mixtures with no background cations added, natural sediments are unlikely to be so ion poor. Thus, the xanthan gum mixtures with background cations added are more representative of the improvements that can be expected in practice. This study demonstrates that the addition of guar gum or xanthan gum to newly placed

slurry could substantially reduce wetland erosion. This is because both can raise erosional resistance by almost one order of magnitude.

Also note that the pore fluid viscosity, aggregation, hydrogen bonding, electrostatic repulsion, cross-linking, and adsorption mechanisms described are not interactions exclusive to kaolinite. For example, Ma and Pawlik (2007) found that guar gum forms hydrogen bonds with many minerals, including kaolinite. Therefore, it is possible to extrapolate the results for kaolinite to other clays. However, more study is needed to fully characterize these interactions across a broad range of biopolymers and sediments.

#### **4.5 Conclusions**

This study involved performing CSM tests on a kaolinite clay with differing biopolymer concentrations, void ratios, and background cations to see how the interaction of these materials would affect its resistance to erosion. Two polysaccharides, similar to natural soil EPS, were used. The polysaccharides included the neutral, plant derived guar gum and the anionic bacterial exopolymer xanthan gum. The following conclusions can be made from the results of the tests:

- As Casagrande cup and CSM tests both indirectly measure shear strength, the results of both tests are linked.
- Increasing biopolymer concentration increases the pore fluid viscosity, and this leads to increased erosional resistance.
- Biopolymer induced aggregation negatively effects erosional resistance.
- For a given pore fluid viscosity, guar gum produces substantially more erosional resistance than xanthan gum in DI water since guar gum establishes a hydrogen bonding network between guar gum strands and kaolinite particles.

- Increasing biopolymer concentration increases erosional resistance across void ratios over the range of 4.58 to 5.79.
- Void ratios greater than the minimum tested value of 4.58 lead to reduced erosional resistance due to reduced particle interlocking.
- Cations in the pore fluid will balance the negative charge of xanthan gum strands and allow xanthan gum to establish a hydrogen bonding network between xanthan gum strands and kaolinite particles. This significantly improves the erosional resistance of xanthan gum mixtures.
- Cations that cause biopolymer cross-linking increase aggregation, and this marginally reduces the erosional resistance of the mud.
- Cations that cause increased biopolymer adsorption on kaolinite particles increases aggregation, and this also marginally reduces the erosional resistance of the mud.



## **CHAPTER 5. THE EFFECT OF EXOPOLYMERS ON THE COMPRESSIBILITY OF KAOLINITE\***

### **5.1 Introduction**

Subsidence, the reduction in land height due to soil consolidation, and erosion, the removal of sediment by currents or flows, threaten many estuaries and bays in the US. Coastal wetlands and cities in Louisiana are especially vulnerable, with subsidence reducing land height by 5-10 mm per year (Tornqvist et al. 2008) and with erosion destroying one acre of land every 24 minutes (Fischetti 2001). One common method for rapidly rebuilding lost wetlands is hydraulic dredging and placing the material on subsiding marshes or creating new marshes in open water. However, the high water content slurry deposited by hydraulic dredging is very compressible with low shear strength, and this poor stability makes freshly deposited slurry susceptible to subsidence and erosion.

Although there are many soil amendments that can reduce compressibility and improve shear strength, such as lime and Portland cement, these soil stabilizers are often caustic or toxic. The large scale and environmentally sensitive nature of wetland restoration projects makes these traditional amendments too risky to use. Additionally, Tengbeh (1993) demonstrated that grass roots can provide a five-fold increase in shear strength over a wide range of water contents, and de Baets et al. (2007) showed that plant roots can increase surface erosion resistance. Therefore, any compound used for improving slurry stability must not inhibit or slow plant growth, since plants are also important for increasing sediment stability.

A possible solution to this problem is the use of exopolymers as a soil amendment. Exopolymers are an important component of biofilms formed by bacterial micro-communities in soil (Sutherland 2001). These exopolymers are manufactured and secreted by bacteria to protect

---

\*Material reprinted from Nugent et al. (2011b) posted ahead of print with permission from the ASCE.

themselves from predators and to make the environment more hospitable (Maier et al. 2000). Most of these exopolymers are high molecular weight polysaccharides. They affect soil behavior and engineering properties because they contain chemically active, electrically charged groups that especially interact with high surface area and electrically charged clay minerals (Sutherland 2001). General interest in improving soils through other biological processes, such as biocementation and bioclogging, has also been increasing (Ivanov and Chu 2008; Mitchell and Santamarina 2005).

Recent studies have successfully demonstrated that exopolymers on sediment surfaces greatly increase sediment erosional resistance (Widdows et al. 2006; Yallop et al. 2000). Along with the Widdows et al. (2006) field study on intertidal mudflats that showed a strong correlation between the sediment's production and quantity of EPS to the newly placed sediment's stability, Dade et al. (1990) proved that *Alteromonas atlantica* builds a biofilm that increases critical shear velocity necessary for sand erosion. Additionally, Çabalar and Çanakci (2005) discovered that the addition of xanthan gum to Leighton Buzzard sand greatly increased the sand's shear strength. Chenu and Guérif (1991) found that air-dried strips of kaolinite and montmorillonite clay minerals developed significantly increased tensile strength after being combined with EPS, and Martin et al. (1996) showed an increase in strength of low plasticity clayey silt when it was combined with xanthan gum. Also, Nugent et al. (2009) produced a preliminary study on how the nanoscale interactions between kaolinite and two EPS analogues, guar gum and xanthan gum, change the kaolinite's liquid limit, and they showed that increases in the liquid limit imply increases in the undrained shear strength under high water content conditions.

Therefore, to combat the problem of wetland subsidence and erosion, Louisiana State University (LSU) is studying methods for bioengineered sediment stabilization with low

environmental impact. Cohesive sediments are the primary focus of this investigation since the Lower Mississippi River Basin and the Northern Gulf Coast primarily consist of cohesive, fine-grained sediments. Attention is directed towards soil improvement by amending the sediment with exopolymers. Specific exopolymers being tested are guar gum and xanthan gum.

The World Health Organization (1975; 1987) performed toxicity studies for guar gum and xanthan gum and found that they do not represent a hazard to health and that there was no need to establish an acceptable daily intake of the substances. Further, Sandford et al. (1984) established that both guar gum and xanthan gum are used in agricultural fertilizers and feed supplements with no harm to the environment. With this in mind, these two exopolymer analogs show little evidence in causing environmental harm should they be used for sediment stability. However, it must be proved that application of these two exopolymer analogs at the concentrations recommended in this dissertation will be environmentally benign.

This chapter provides the results of a battery of 1D consolidation tests performed on a kaolinite clay. Guar gum, an electrostatically neutral plant polysaccharide, and xanthan gum, an anionic bacterial extracellular polysaccharide, were used as exopolymer analogues. These two biopolymers were added to the kaolinite to produce mixtures of biopolymer and kaolinite with varying concentrations. Qualitative changes in the overall consolidation properties of the mixtures were related to the nanoscale interactions between kaolinite particles and molecular biopolymer strands. Potential applications were then discussed.

## **5.2 Materials and Methods**

This study used a relatively pure, untreated, kaolinite clay sample, which was purchased from Theile Kaolin Company. Ninety-eight percent by weight (wt.%) of the sample was made up of particles smaller than 2  $\mu\text{m}$ . The average specific surface area measured 20-26  $\text{m}^2/\text{g}$ . The

specific gravity was 2.63 (Flick 1989). Kaolinite particles possess an overall negative charge at solution pH greater than 2.35 (Alkan et al. 2005).

Two EPS analogs were also used. The guar gum (Laboratory Grade) was purchased from Fisher Scientific. The xanthan gum (NF Grade) was purchased from Spectrum Chemical Manufacturing Corporation. These EPS analogs are more thoroughly described below.

### **5.2.1 Guar Gum**

This neutral polysaccharide comes from *Cyamopsis tetragonoloba* seeds. It has a high molecular weight, measuring up to  $2 \times 10^6$  Da (Risica et al. 2005). Mannose molecules linked with  $\beta$ -1,4 bonds form its polymer backbone, with a single galactose bonding to every second mannose (Whistler and Smart 1953). Guar gum can form hydrogen bonds through its many hydroxyl (-OH) groups. The neutral charge of guar gum is due to its lack of ionizable carboxylic acid (-COOH) groups. It is possible for the hydrogen in hydroxyl groups to dissociate, but this process requires a surrounding solution with very high pH (Bruice 2004).

Although guar gum is not microbially produced, it can produce viscous, pseudoplastic aqueous solutions like a neutrally charged microbial EPS. This ability is the result of its high molecular weight and extensive, hydrogen bonding promoted chain hyperentanglements (Goycoolea et al. 1995; Cheng et al. 2002). Hyperentanglements are a type of intermolecular association (Rao 2007). Guar gum's availability, inexpensiveness, and ability to increase aqueous systems' viscosity give it commercial significance (Whitcomb et al. 1980).

### **5.2.2 Xanthan Gum**

This anionic polysaccharide is produced by the bacteria *Xanthomonas campestris* (Sutherland 1994). Its molecular weight generally ranges from 0.9 to  $1.6 \times 10^6$  Da, with the exact weight determined by the bacterial strain and the physiological environment surrounding

the bacteria during production (Sutherland 1994). Glucose molecules linked with  $\beta$ -1,4 bonds make up the xanthan gum polymer backbone, with a mannose-glucuronic acid-mannose side chain attached to every second glucose (Hassler and Doherty 1990). The mannoses are typically modified by adding an *O*-acetyl group to the mannose closest to the backbone of the glucose and by adding a pyruvate ketal to the mannose furthest from the glucose backbone in a proportion that also depends on the strain of the bacteria and the physiological environment (Sutherland 1994).

Hydrogen atoms of xanthan gum easily dissociate from carboxylic acid (-COOH) groups to form carboxylate (-COO<sup>-</sup>) anions (Bruice 2004). Hydrogen dissociation from carboxylic acid groups on the glucuronic acid and pyruvate give xanthan gum its anionic charge. Xanthan gum can also form hydrogen bonds with its numerous hydroxyl (-OH) groups. Small amounts of xanthan gum significantly increase an aqueous system's viscosity, which makes it a commonly used commercial substance (Hassler and Doherty 1990). However, since the xanthan gum solution is pseudoplastic, its viscosity decreases with an increased shear rate (Milas et al. 1985).

### **5.2.3 Preparation of Biopolymer and Clay Mixtures**

Because the water content of saturated clay decreases during consolidation, and because clay water content will vary in nature for many reasons, biopolymer concentration cannot usefully be described in terms of pore solution concentration. Instead, the concentration is described in terms of the ratio of dry biopolymer mass to the sediment dry mass. This concentration is called the biopolymer mass ratio, or  $R_{bm}$ .

To create homogeneous biopolymer and kaolinite mixtures with a desired biopolymer concentration, the amount of dry kaolinite needed for the test was estimated, and then the required dry mass of biopolymer was calculated by multiplying the dry kaolinite mass by the

wanted  $R_{bm}$ . The dry biopolymer powder was next dissolved into a small amount of distilled/deionized (DDI) water through a physical mixing procedure, rather than using a chemical means, since physical mixing would be preferred for large-scale field applications. Clumping was prevented in low concentration solutions by slowly adding, over several minutes, biopolymer powder to liquid that was stirred by a stir bar. Remaining biopolymer powder clumps in higher concentration solutions were broken down by an immersion blender to homogenize the solution.

After making the homogenized biopolymer solution, the previously set mass of dry kaolinite was added to the solution and gently stirred by hand with a spatula to moisten the kaolinite powder. Additional DDI water was mixed into the biopolymer and kaolinite mixture until the mixture was a fluid slurry. The immersion blender was then used to ensure that the slurry was homogenized. This slurry was used immediately or stored in a 4 °C refrigerator to minimize biological degradation. Refrigerated slurries were tested after they warmed to room temperature (approximately 22 °C).

For the consolidation tests, kaolinite without biopolymer, guar gum and kaolinite mixtures with concentrations of 0.005, 0.010, 0.015, and 0.020  $R_{bm}$ , and xanthan gum and kaolinite mixtures with concentrations of 0.005, 0.010, 0.015, and 0.020  $R_{bm}$  were used. After each test, the water contents were measured according to ASTM standard D 2216 (ASTM 2006). Since the biopolymers are high molecular weight polysaccharides, they do not volatilize at  $110 \pm 5$  °C in the drying oven. As an example of how high molecular weight polysaccharides resist volatilization, wood that largely consists of high molecular weight polysaccharides (Sjötröm 1993) does not appreciably volatilize until the temperature is above 300 °C (U.S. 2007). This results in the biopolymer adding to the solid fraction of the water contents and void ratios.

### 5.2.4 Test Apparatus and Methods

The 1D consolidation tests were performed in accordance with ASTM D 2435 (ASTM 2006) using a GeoJac ICON automated load frame manufactured by Geotechnical Test Acquisition and Control. As seen in Figure 5.1, clay and biopolymer mixtures required considerable time to finish primary consolidation when a 25.4 mm (1 in.) specimen ring was used. In order to accelerate the tests, a 12.7 mm (1/2 in.) tall and 63.5 mm (2.5 in.) diameter specimen ring was used, instead.

Since the materials tested were slurries, they were loaded into the machine by first placing a porous stone with a filter paper into the consolidation cell. Then the specimen ring was aligned on top of the porous stone. A spatula was next used to place portions of slurry into the center of the ring, while being careful not to trap any bubbles of air. Once the ring was full, the top surface of the slurry was flattened using a straightedge.

The load schedule started at a vertical effective stress  $\sigma_{vo}'$  of 23.94 kPa (500 psf) and increased to 766.08 kPa (16000 psf) for a total of six steps with a load increment factor of one, except for the third step. The third step used a 100 kPa (2088.54 psf) load instead of 95.76 kPa (2000 psf). A 100 kPa load allows the results to be compared against the intrinsic compression line (ICL) developed by Burland (1990). The ICL is relevant since it was created to describe the behavior of reconstituted soils made from a slurry.

For each test, the first load increment was held for 500 minutes, and every load after the first was held for 400 minutes. Data for each load increment was analyzed using the log-time method. The void ratio  $e$  at the end of primary consolidation, coefficient of consolidation  $c_v$ , hydraulic conductivity  $k$ , and coefficient of secondary compression  $C_{\alpha\epsilon}$  were computed for each

load, while the normal compression index  $C_c$  and hydraulic conductivity change index  $C_k$  was determined for the mixture.

### 5.3 Results and Discussion

The results of 1D consolidation tests for kaolinite with no biopolymer and for guar gum and kaolinite mixtures are illustrated in Figure 5.2, Figure 5.3, Figure 5.4, Figure 5.5, Figure 5.6, and Figure 5.7. Figure 5.2 illustrates the  $e$  versus  $\sigma_{vo}'$  deformation curves, and Figure 5.3 has the associated  $e$  versus  $c_v$  data. Figure 5.4 shows  $C_{ae}$  versus  $R_{bm}$  for representative vertical loads, and Figure 5.5 has example  $\varepsilon$  versus  $t$  curves to show how creep changes over different vertical loads. Figure 5.6 depicts the calculated  $e$  versus  $k$ , and Figure 5.7 compares the consolidation results to the ICL. Note that a point for the 23.94 kPa load of 0.020  $R_{bm}$  guar gum mixture is missing in each figure because the slurry did not reach the end of primary consolidation by the end of the load increment.

The 1D consolidation test results for kaolinite with no biopolymer and for xanthan gum and kaolinite mixtures are illustrated in Figure 5.8, Figure 5.9, Figure 5.10, Figure 5.11, Figure 5.12, and Figure 5.13. These figures exhibit the  $e$  versus  $\sigma_{vo}'$  deformation curves,  $e$  versus  $c_v$ ,  $C_{ae}$  versus  $R_{bm}$  for representative loads, example  $\varepsilon$  versus  $t$  curves, calculated  $e$  versus  $k$ , and comparison against the ICL, respectively. Table 5.1 provides  $C_c$  and  $C_k$  for guar gum and kaolinite mixtures as well as xanthan gum and kaolinite mixtures.

**Table 5.1: Fitted line data for guar gum and kaolinite mixtures and xanthan gum and kaolinite mixtures.**

$R_{bm}$	Guar Gum Mixtures		Xanthan Gum Mixtures	
	$C_c$	$C_k$	$C_c$	$C_k$
0.000	0.617	1.059	0.617	1.059
0.005	0.422	0.637	0.644	0.573
0.010	0.548	0.520	0.638	1.887
0.015	0.662	0.732	1.058	2.178
0.020	0.638	1.116	1.029	2.564



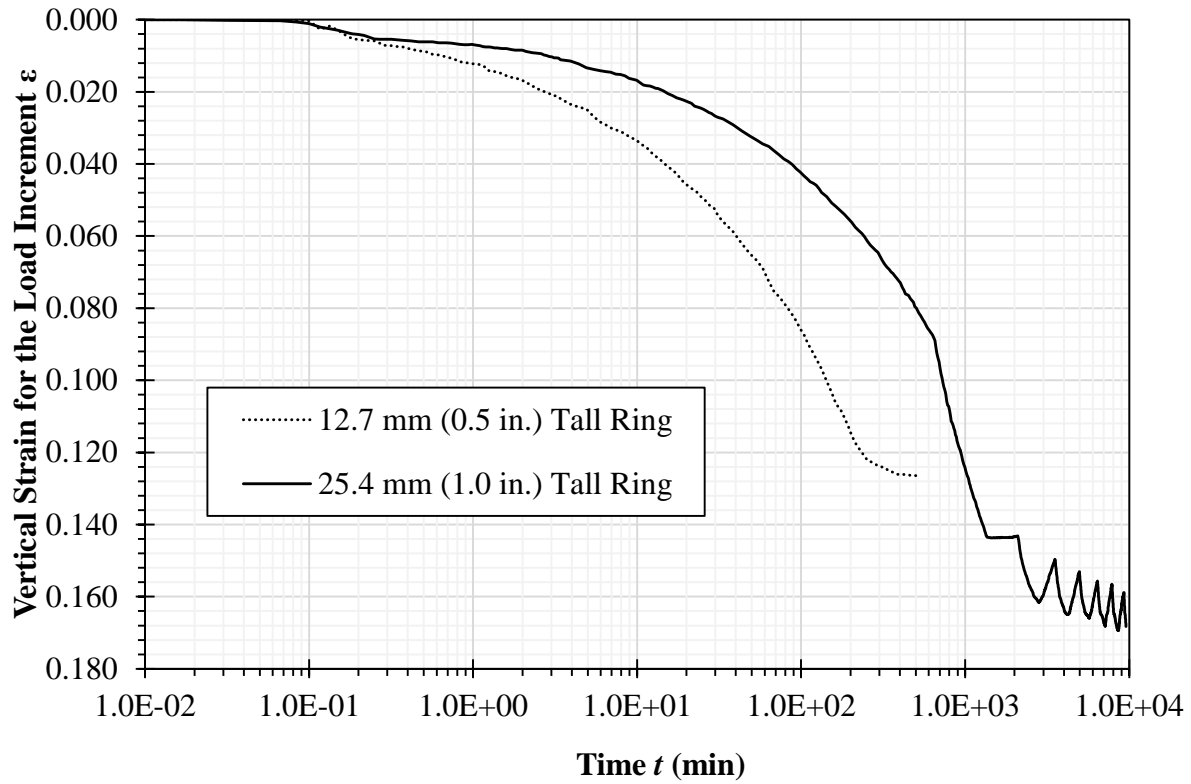


Figure 5.1: Strain vs. time for a 0.020  $R_{bm}$  xanthan gum mixture under 23.94 kPa (500 psf) vertical load by ring height.

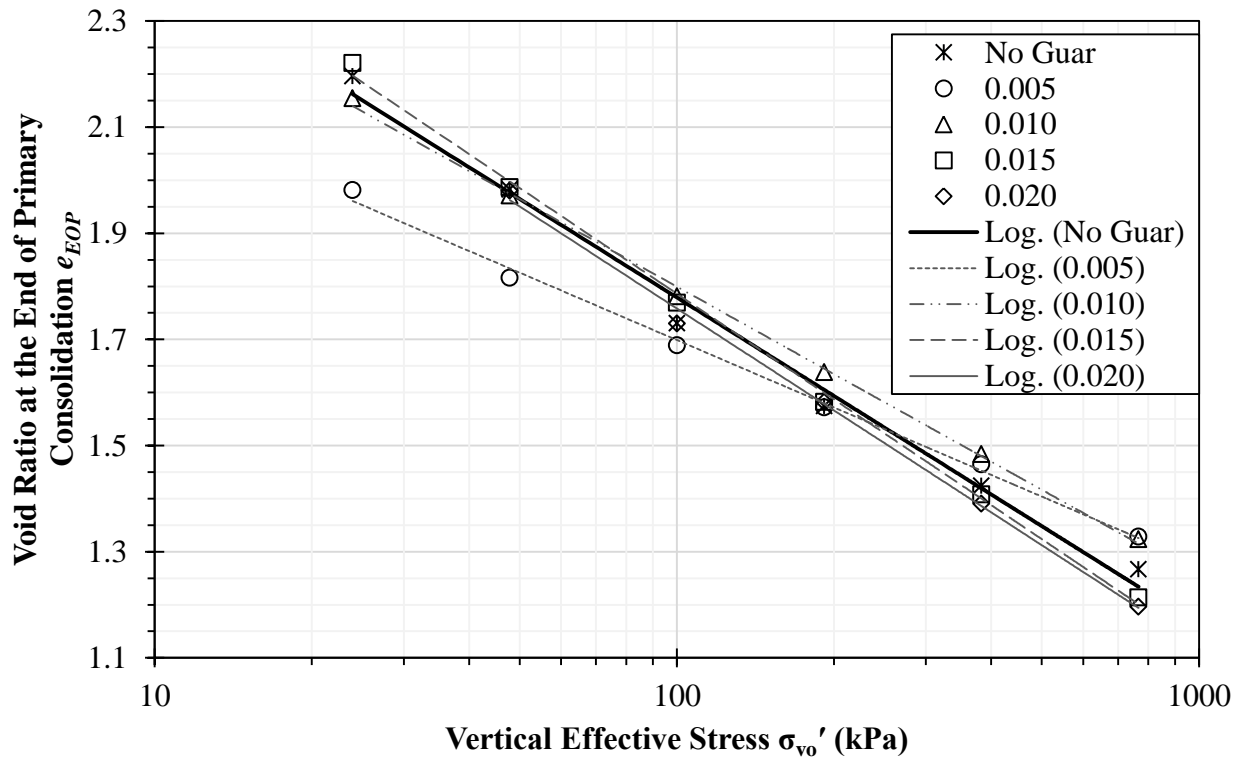


Figure 5.2: Void ratio vs. vertical effective stress for guar gum and kaolinite mixtures.

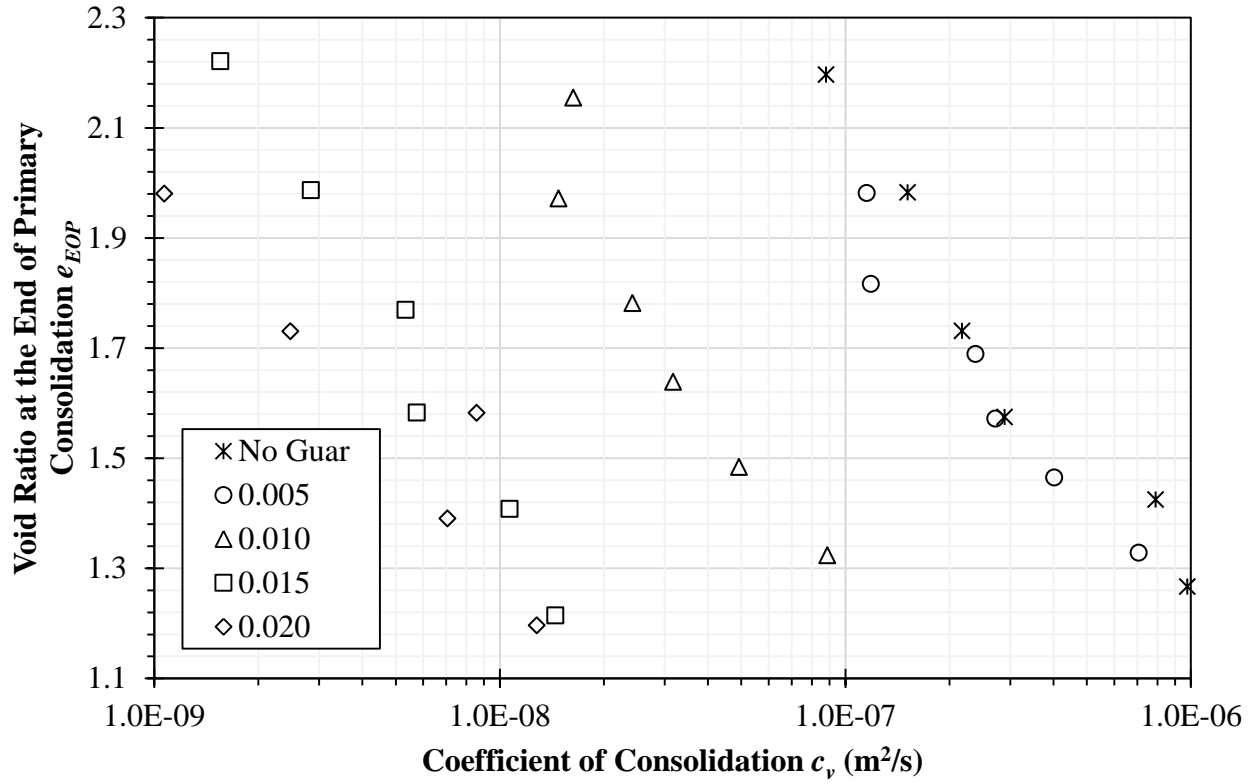


Figure 5.3: Void ratio vs. coefficient of consolidation for guar gum and kaolinite mixtures.

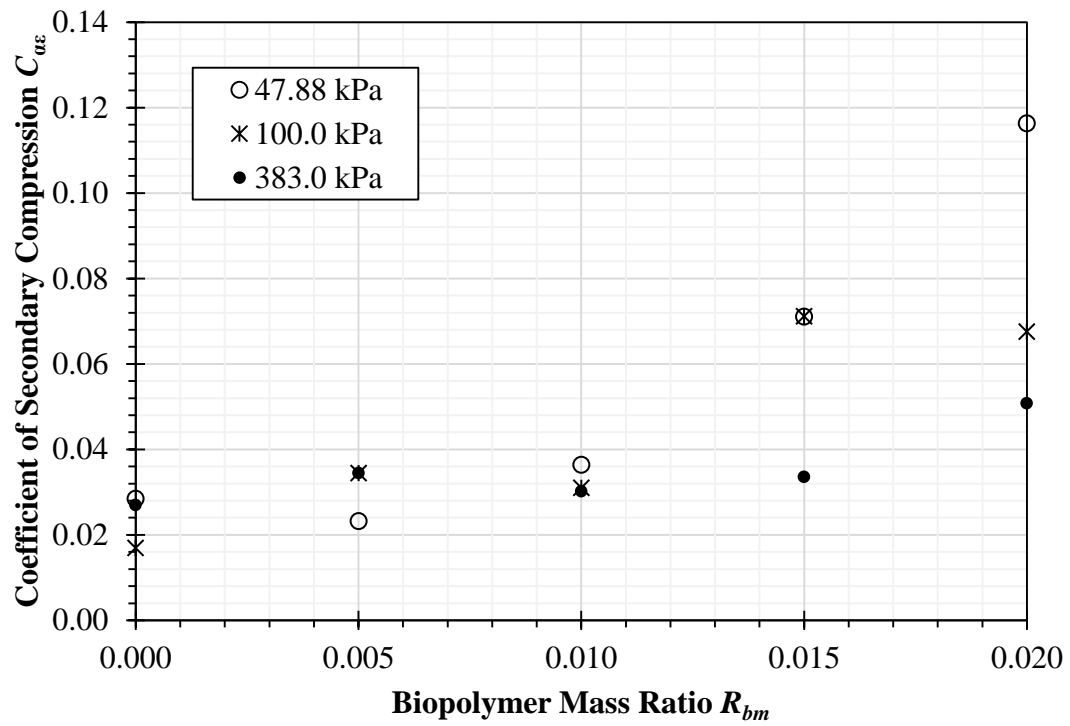


Figure 5.4: Coefficient of secondary compression vs. biopolymer mass ratio for guar gum and kaolinite mixtures.

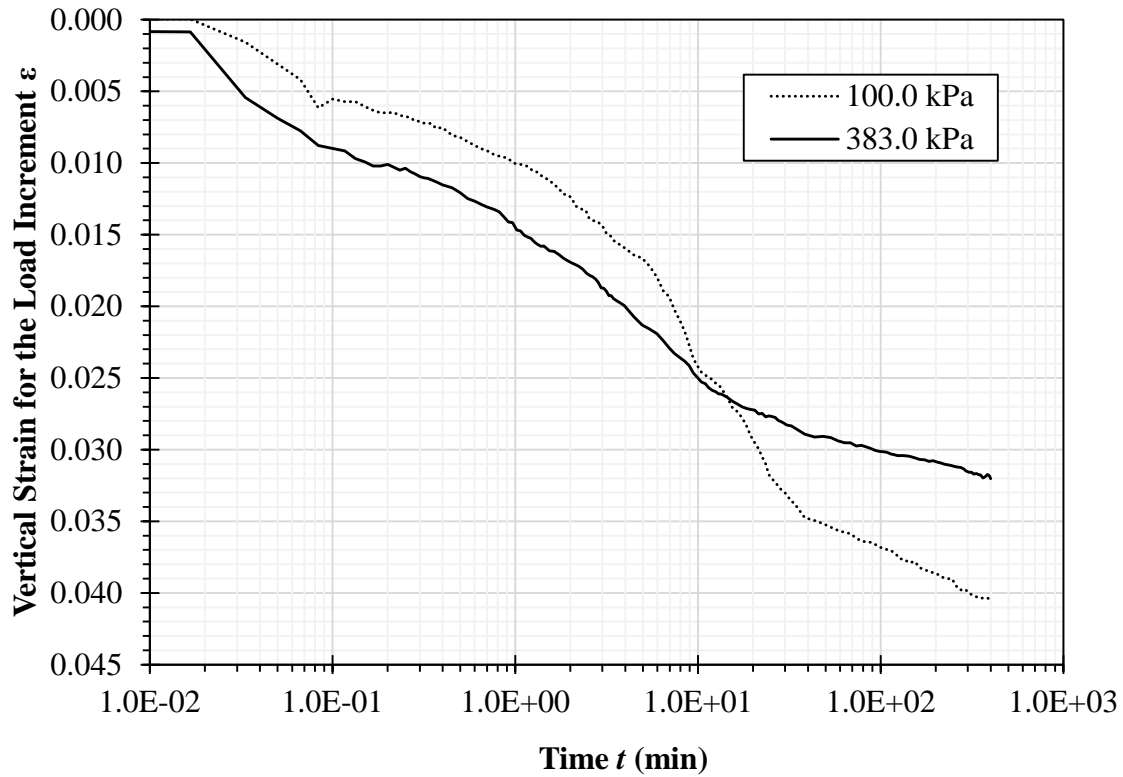


Figure 5.5: Strain vs. time for two load increments of a 0.015  $R_{bm}$  guar gum mixture.

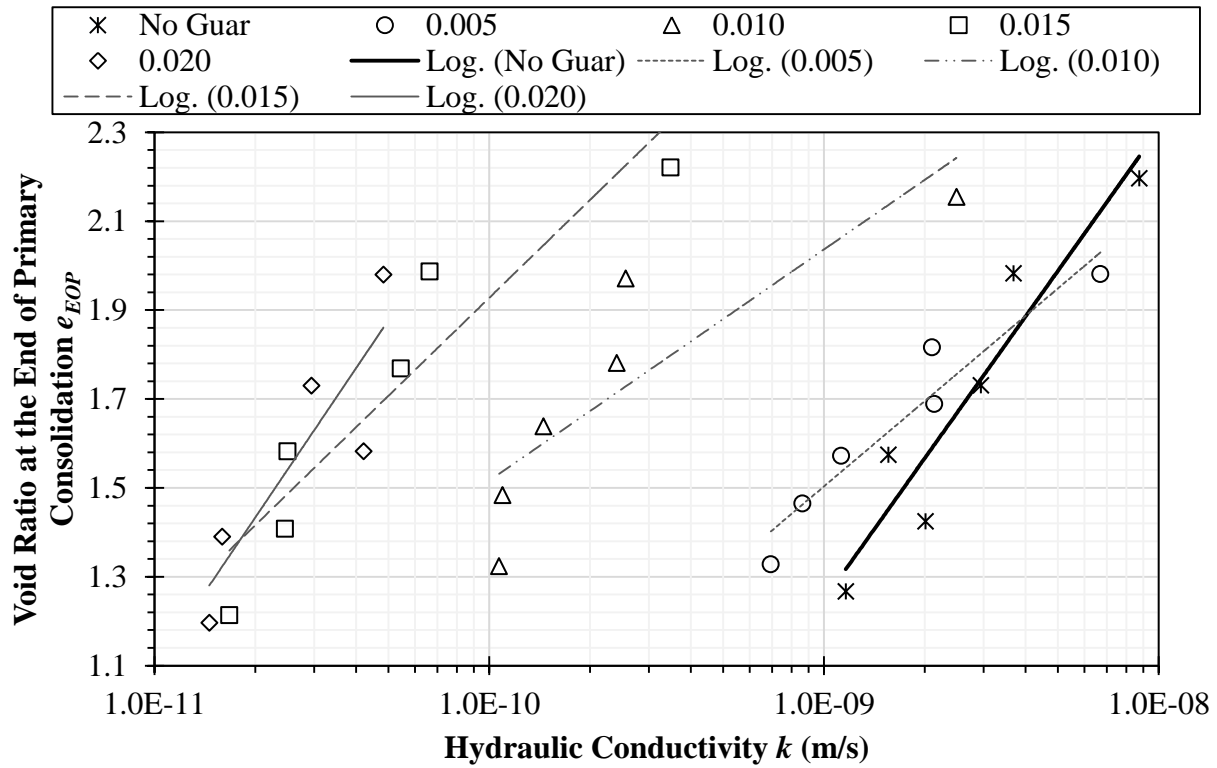


Figure 5.6: Void ratio vs. hydraulic conductivity for guar gum and kaolinite mixtures.

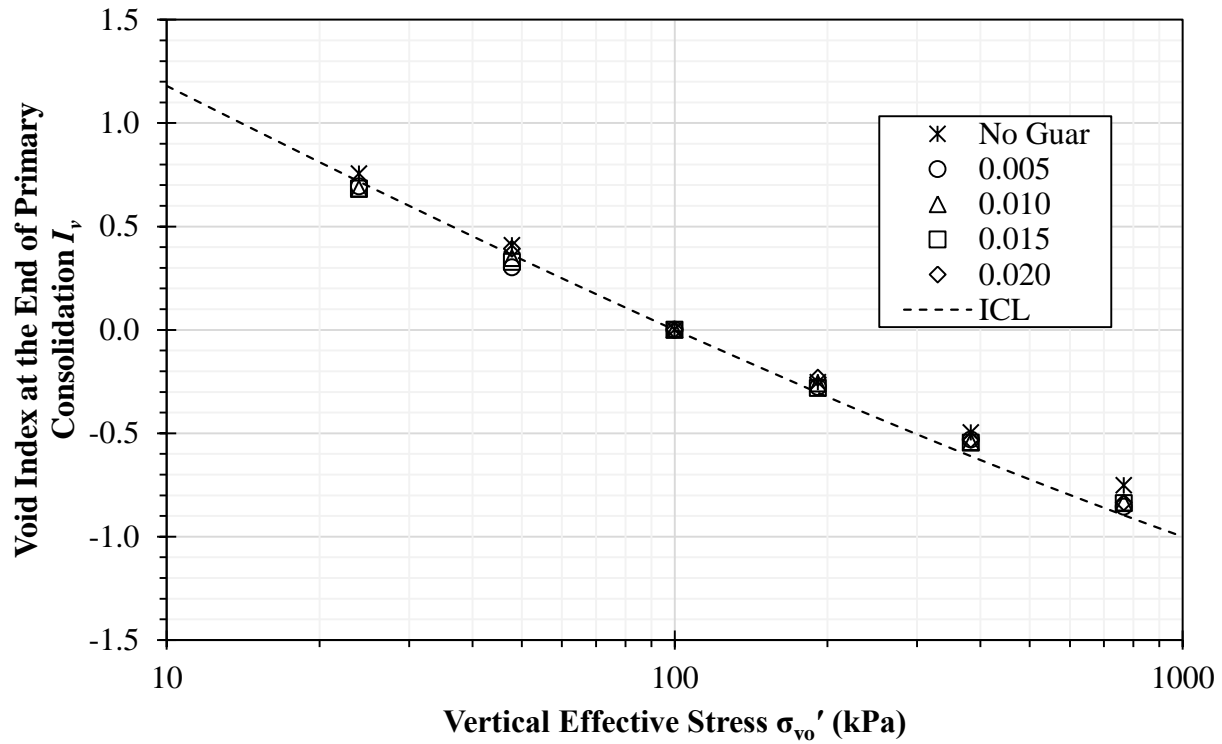


Figure 5.7: Void index vs. vertical effective stress for guar gum and kaolinite mixtures. ICL is from Burland (1990).

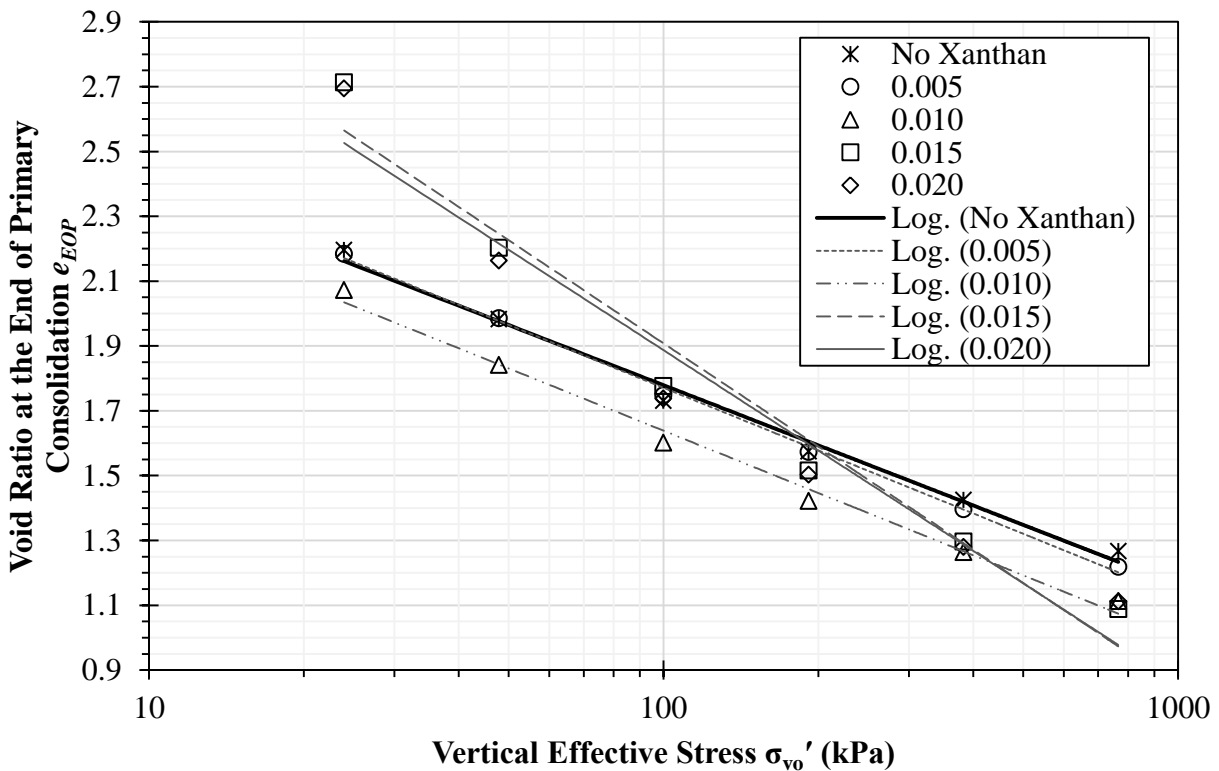
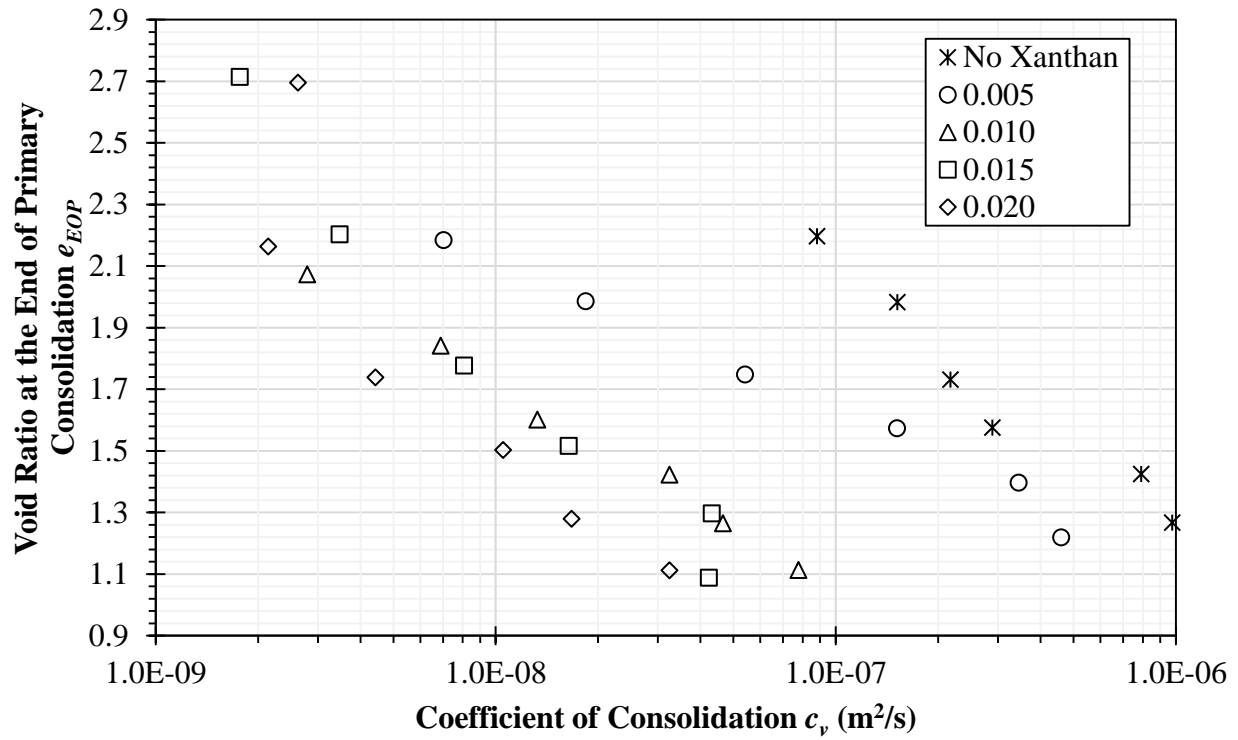
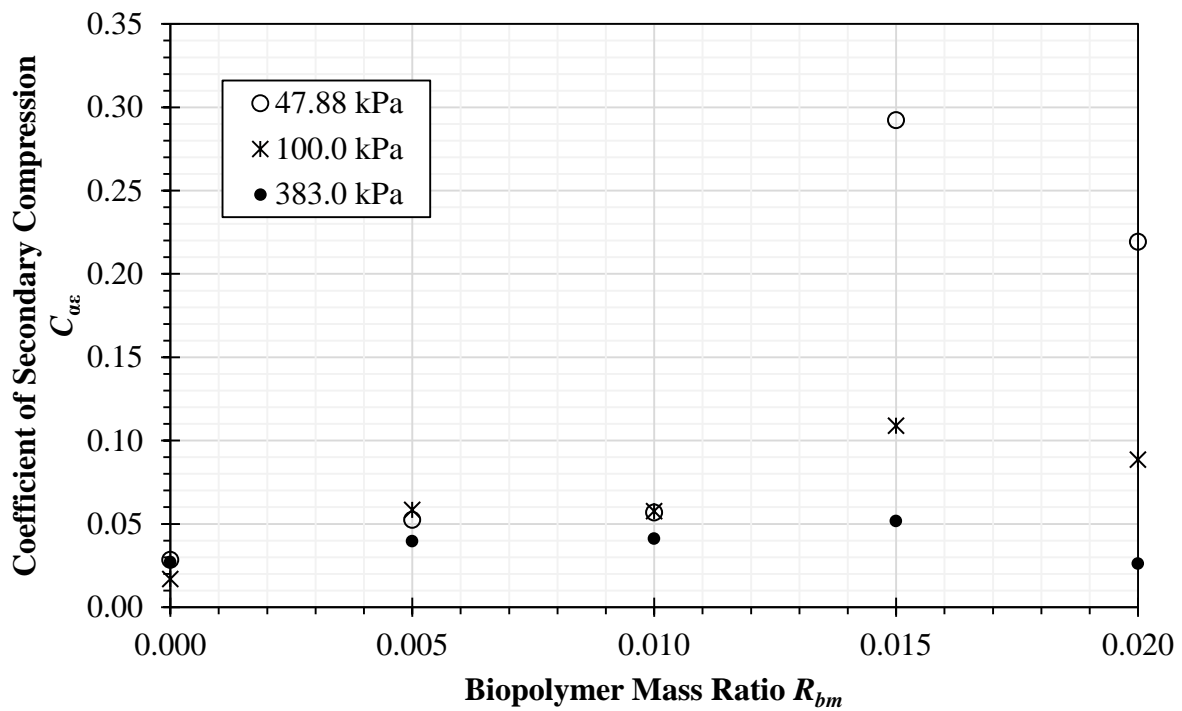


Figure 5.8: Void ratio vs. vertical effective stress for xanthan gum and kaolinite mixtures.



**Figure 5.9: Void ratio vs. coefficient of consolidation for xanthan gum and kaolinite mixtures.**



**Figure 5.10: Coefficient of secondary compression vs. biopolymer mass ratio for xanthan gum and kaolinite mixtures.**

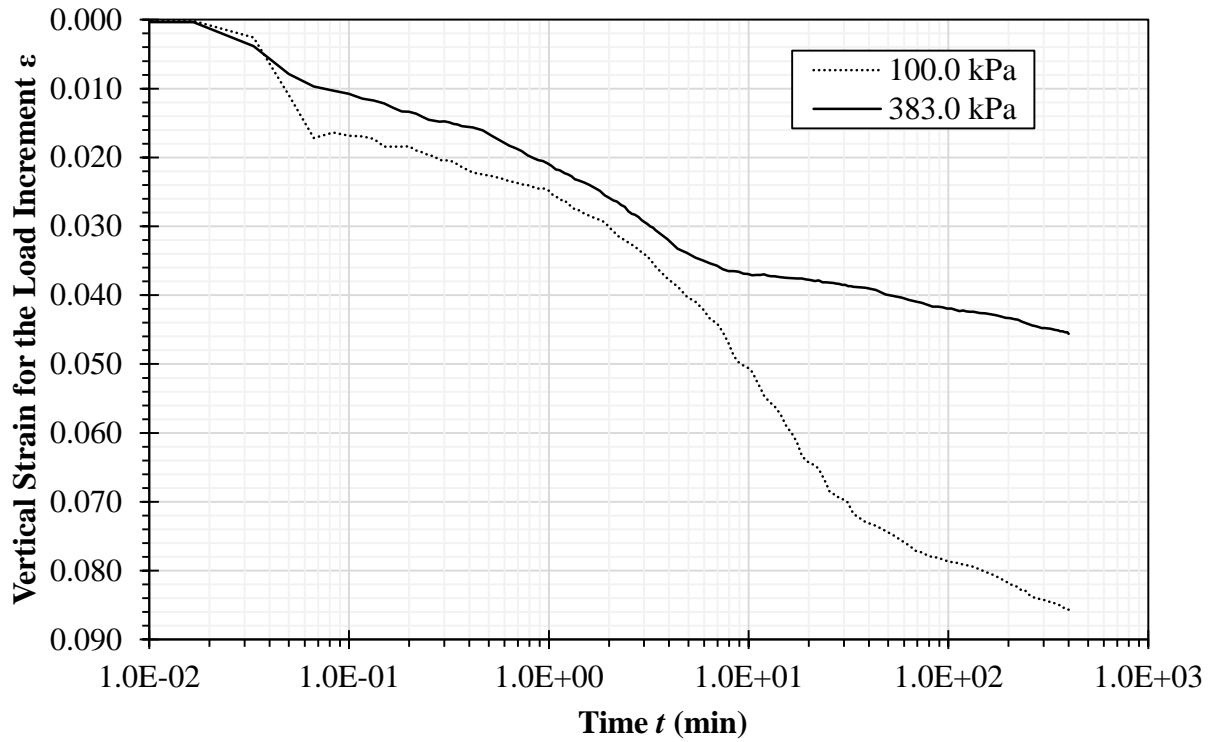


Figure 5.11: Strain vs. time for two load increments of a 0.015  $R_{bm}$  xanthan gum and kaolinite mixture.

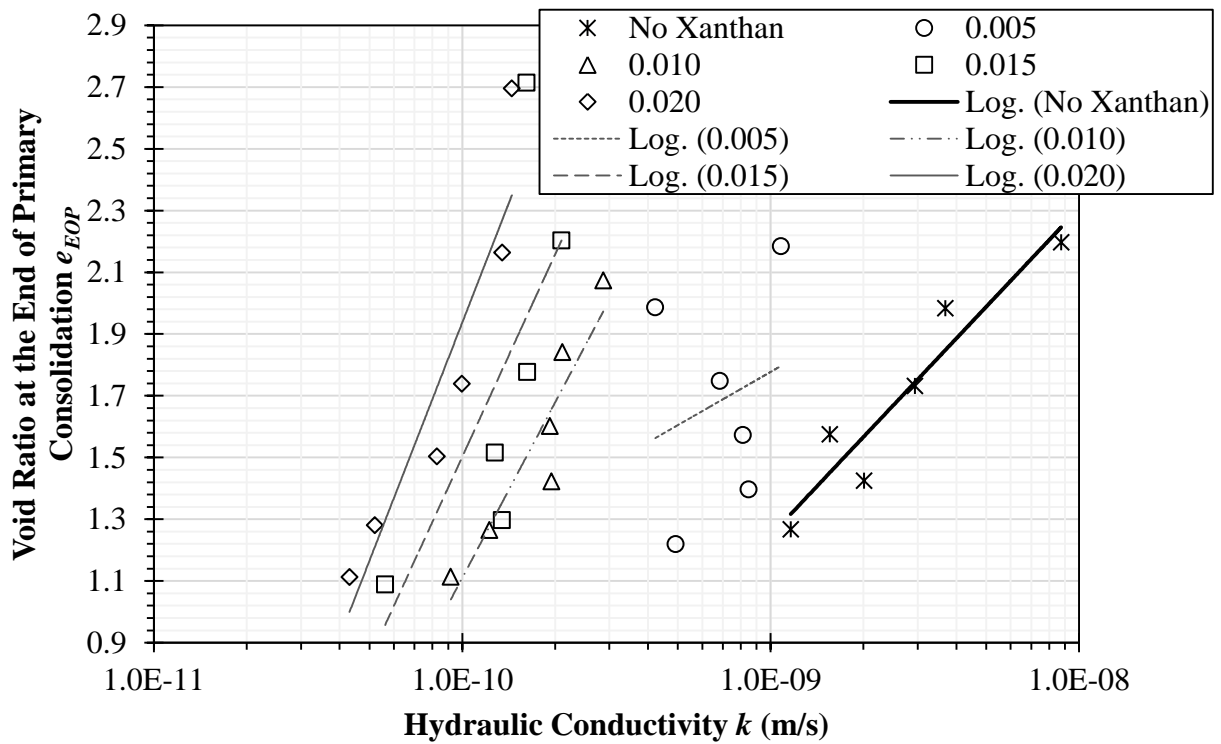
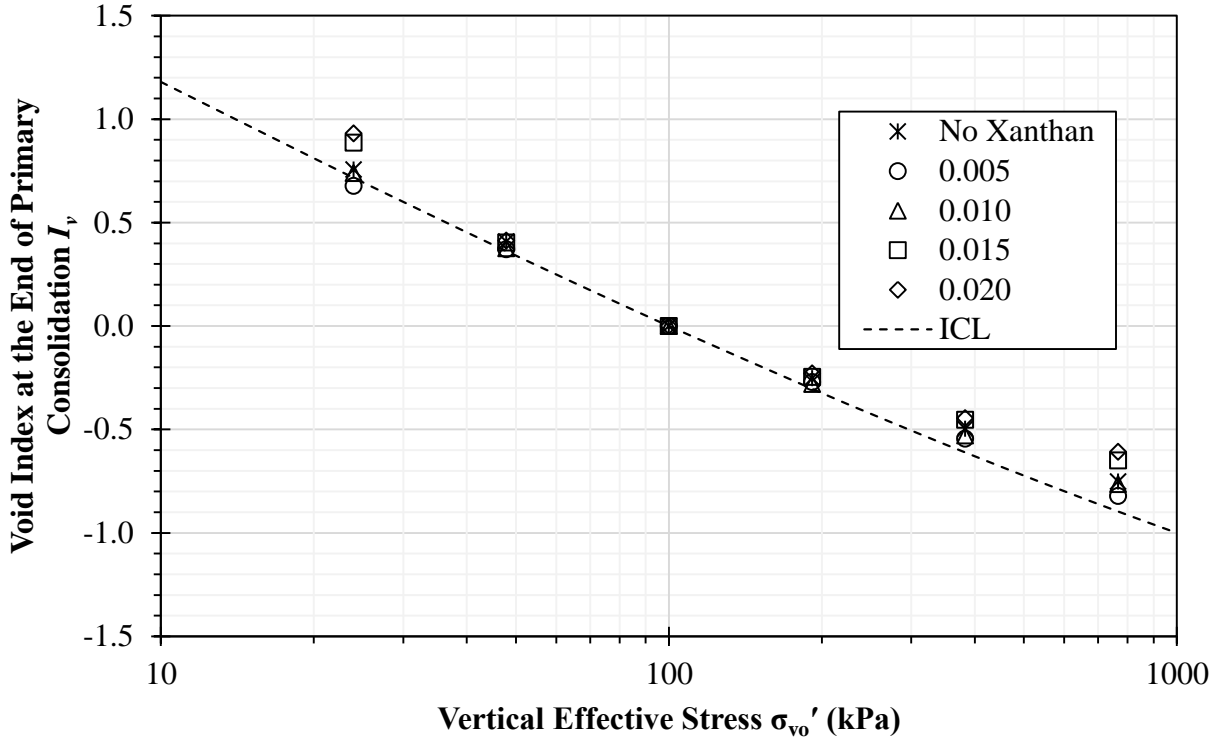


Figure 5.12: Void ratio vs. hydraulic conductivity for xanthan gum and kaolinite mixtures.



**Figure 5.13: Void index vs. vertical effective stress for xanthan gum and kaolinite mixtures. ICL is from Burland (1990).**

### 5.3.1 Guar Gum and Kaolinite Mixtures

Figure 5.2 and Table 5.1 demonstrate that a 0.005  $R_{bm}$  guar gum and kaolinite mixture has a lower compressibility than just kaolinite. The compressibility increases with greater guar gum concentrations up to 0.015  $R_{bm}$ , where additional guar gum results in little further change.

Ma and Pawlik (2007) explained that guar gum forms hydrogen bonds directly with kaolinite surfaces. Additionally, Podsiadlo et al. (2007) showed that hydrogen bonding between organic polymers and clay particles can result in a highly linked clay-polymer network. At 0.005  $R_{bm}$ , the guar gum appears to attach to kaolinite particles and form a highly linked network that increases the stiffness of the overall system by 31.6% over kaolinite on its own. At 0.005 and 0.010  $R_{bm}$ , guar gum also serves to lower the end of primary consolidation  $e$  at small vertical effective stresses.

At low loads, small quantities of guar gum can fill voids in the kaolinite fabric and lower the void ratio relative to raw kaolinite, while the increased stiffness allows for a more porous structure relative to raw kaolinite at high stresses. However, as  $R_{bm}$  increases, guar gum displaces more particles of kaolinite, and the negative effects of this displacement take hold. Although guar gum contributes to the solid volume used to calculate  $e$ , it does not contribute to the rigidity of soil pores in the same fashion as additional clay particles. This causes an increase in  $C_c$  for 0.010, 0.015, and 0.020  $R_{bm}$  mixtures relative to the 0.005  $R_{bm}$  mixture.

Increases in compressibility are also demonstrated in increases in  $C_{\alpha\epsilon}$ . This is illustrated in Figure 5.4. Figure 5.4 shows that  $C_{\alpha\epsilon}$  is significantly increased in 0.015 and 0.020  $R_{bm}$  mixtures at low vertical effective stress. Kaolinite with no biopolymer, however, displays the expected behavior of a reasonably constant and small  $C_{\alpha\epsilon}$ , and low concentration mixtures show only negligible change in creep.

Wang and Xu (2007) demonstrated that secondary compression is a continuation of the soil skeleton deformation that occurs during primary consolidation.  $C_c$  is relatively high for 0.015 and 0.020  $R_{bm}$  mixtures due to the reduced rigidity of guar gum. Therefore, it follows that the increase in secondary compression in high  $R_{bm}$  mixtures is the result of the continued strain of molecular guar gum strands.

Figure 5.5 demonstrates how  $C_{\alpha\epsilon}$  is reduced for high vertical effective stresses in high concentration guar gum mixtures. This suggests that large vertical stresses accelerate soil skeleton deformation in high  $R_{bm}$  mixtures. Thus, most of the increase in strain due to guar gum will occur during primary consolidation at high loads, and this leaves the secondary compression behavior more similar to just kaolinite. Small changes in creep for low concentration mixtures



can also be explained with this mechanism. Low guar gum concentrations mean that the guar gum may rapidly finish deforming, even under low loads.

Figure 5.6 provides the change in  $k$  for different void ratios and  $R_{bm}$ . Table 5.1 shows  $C_k$  values. The hydraulic conductivity generally decreases with increasing vertical effective stress for just kaolinite and all of the guar gum and kaolinite mixtures. This behavior is because  $k$  generally decreases as  $e$  decreases.

Figure 5.6 also shows that  $k$  is only slightly changed with a guar gum concentration of  $0.005 R_{bm}$ , but  $k$  is reduced for guar gum concentrations of  $0.010 R_{bm}$  and greater. However, this reduction does not become greater with concentrations over  $0.015 R_{bm}$ . Because small increases in guar gum solution concentrations induce order of magnitude increases in the zero shear rate dynamic viscosities of the solutions (Whitcomb et al. 1980), the pore fluid viscosity of the  $0.005 R_{bm}$  guar gum and kaolinite mixture would be significantly higher than kaolinite with no biopolymer. There would be a similar increase in pore fluid viscosity as  $R_{bm}$  increases from  $0.015$  to  $0.020$ . For both of these cases, the change in  $k$  is minimal. The reduction in  $k$  is, therefore, probably not a result of increasing the pore fluid viscosity but caused by guar gum physically blocking or constricting pore spaces. At a concentration of  $0.005 R_{bm}$ , the guar gum has not blocked enough pore spaces to significantly impact hydraulic conductivity. At  $0.015 R_{bm}$ ,  $k$  has been reduced by two orders of magnitude, and all pore spaces available for guar gum to block have been filled.

This reduction in hydraulic conductivity also means that the rate of consolidation has been dramatically reduced. Figure 5.3 shows order of magnitude reductions in  $c_v$  that correspond to reductions in  $k$ . Note that  $c_v$  increases as the void ratio decreases for a given mixture for all mixtures tested. The coefficient of compressibility for each mixture decreases much faster than

the decrease in hydraulic conductivity for each mixture. Since this behavior is observed in the kaolinite on its own, it is an underlying property of the clay tested and not a result of the added biopolymer.

Figure 5.7 provides a comparison between the compressibility results and Burland's (1990) ICL. Kaolinite and guar gum mixtures of all concentrations very closely follow the ICL with almost no deviation. Since the ICL was developed using consolidation data from reconstituted clay slurries, Figure 5.7 shows that the normalized consolidation behavior of kaolinite and guar gum mixtures does not deviate from the normalized consolidation behavior of other clays.

### **5.3.2 Xanthan Gum and Kaolinite Mixtures**

Figure 5.8 and Table 5.1 show the results of consolidation tests on xanthan gum and kaolinite mixtures, and they illustrate that the values of  $C_c$  for all xanthan gum and kaolinite mixtures are greater than the value of  $C_c$  for just kaolinite. Since xanthan gum is anionic, strands of xanthan gum repel each other. Xanthan gum strands also repel particles of kaolinite because kaolinite has a slight overall negative charge. Even though xanthan gum can be adsorbed by kaolinite (Dontsova & Bigham 2005) and has the functional groups needed to form hydrogen bonds, electrostatic repulsion prevents xanthan gum and kaolinite mixtures from showing the same improvements in stiffness demonstrated with guar gum. For the 0.005  $R_{bm}$  mixture, the xanthan gum is probably at a low enough concentration to avoid interaction with particles of kaolinite by occupying voids in the kaolinite fabric. The result is just a slight change in the properties of the mixture.

Xanthan gum and kaolinite mixtures with a  $R_{bm}$  of 0.010 and above form noticeable curves in Figure 5.8, instead of the expected straight normal compression line. The mixtures

with 0.015 and 0.020  $R_{bm}$  have much higher void ratios at the end of primary consolidation than just kaolinite at low loads. This is likely because the electrostatic repulsion between strands of xanthan gum and kaolinite particles allows the mixture to resist low vertical loads, even when void spaces are large. Thus, the electrostatic repulsion acts to reduce the effective stress that is applied to the soil skeleton. At high vertical loads, the electrostatic repulsion is overcome.

The normal compression lines for the mixtures begin to straighten and demonstrate higher compressibility than kaolinite without biopolymer, due to compressible xanthan gum replacing stiff kaolinite particles. Although the 0.010  $R_{bm}$  mixture does not have a higher  $e$  than kaolinite with no biopolymer under the loads tested, extrapolating the curve at low loads suggests the curve would move above the just kaolinite normal compression line. The lower quantity of xanthan gum in the 0.010  $R_{bm}$  mixture means that the electrostatic repulsion is overcome at very low stresses.

Figure 5.10 illustrates the changes in creep caused by different concentrations of xanthan gum. The mechanisms for this are similar to the mechanisms for guar gum mixtures with the addition of electrostatic repulsion. At low loads and xanthan gum concentrations of 0.015 and 0.020  $R_{bm}$ ,  $C_{ae}$  is much greater than for low concentration xanthan gum mixtures.

Figure 5.11 shows how  $C_{ae}$  is reduced for high  $R_{bm}$  xanthan gum mixtures at high vertical load. Although electrostatic repulsion helps high  $R_{bm}$  xanthan gum mixtures to resist strain during primary consolidation, it appears to leave large voids in the soil skeleton that can close over time. For 0.005 and 0.010  $R_{bm}$  xanthan gum mixtures,  $C_{ae}$  for most loads is slightly greater than the values for just kaolinite, but these increases are small compared to the amount of scatter.

Changes in xanthan gum and kaolinite mixture hydraulic conductivity are shown in Figure 5.12 with  $C_k$  values in Table 5.1. Xanthan gum at a concentration of 0.010  $R_{bm}$  reduces  $k$

by about one order of magnitude, but higher concentrations produce diminishing further reductions in hydraulic conductivity. Like guar gum, small quantities of xanthan gum can increase the pore fluid viscosity by orders of magnitude (Milas et al. 1985). This suggests that xanthan gum also lowers  $k$  by blocking and constricting voids in the kaolinite fabric, instead of by increasing pore fluid viscosity. As with guar gum, reductions in the hydraulic conductivity increase the time required for consolidation with reductions in  $c_v$  seen in Figure 5.9. Again, the increase in  $c_v$  with smaller void ratios is a property of the kaolinite used and not the result of adding xanthan gum.

Figure 5.13 provides a comparison between the compressibility results and Burland's (1990) ICL. Kaolinite and xanthan gum mixtures do not follow the ICL as well as kaolinite and guar gum mixtures. This is because of the unusual curvature in the normal compression lines of kaolinite and xanthan gum mixtures. Since the ICL was developed using consolidation data from reconstituted clay slurries, Figure 5.13 shows that the normalized consolidation behavior of kaolinite and xanthan gum mixtures does deviate from the normalized consolidation behavior of other clays.

### **5.3.3 Comparison between Guar Gum and Xanthan Gum Results**

Differences in the nanoscale mechanisms of interaction between biopolymer and clay likely induce significant changes in the macroscale consolidation behavior of the mixture. Guar gum interactions with kaolinite are dominated by hydrogen bonding between molecular guar gum strands and kaolinite particles. Xanthan gum interactions, however, are controlled by electrostatic repulsion between molecular xanthan gum strands and kaolinite particles. The resulting contrasts in compression behaviors are illustrated in Figure 5.14.

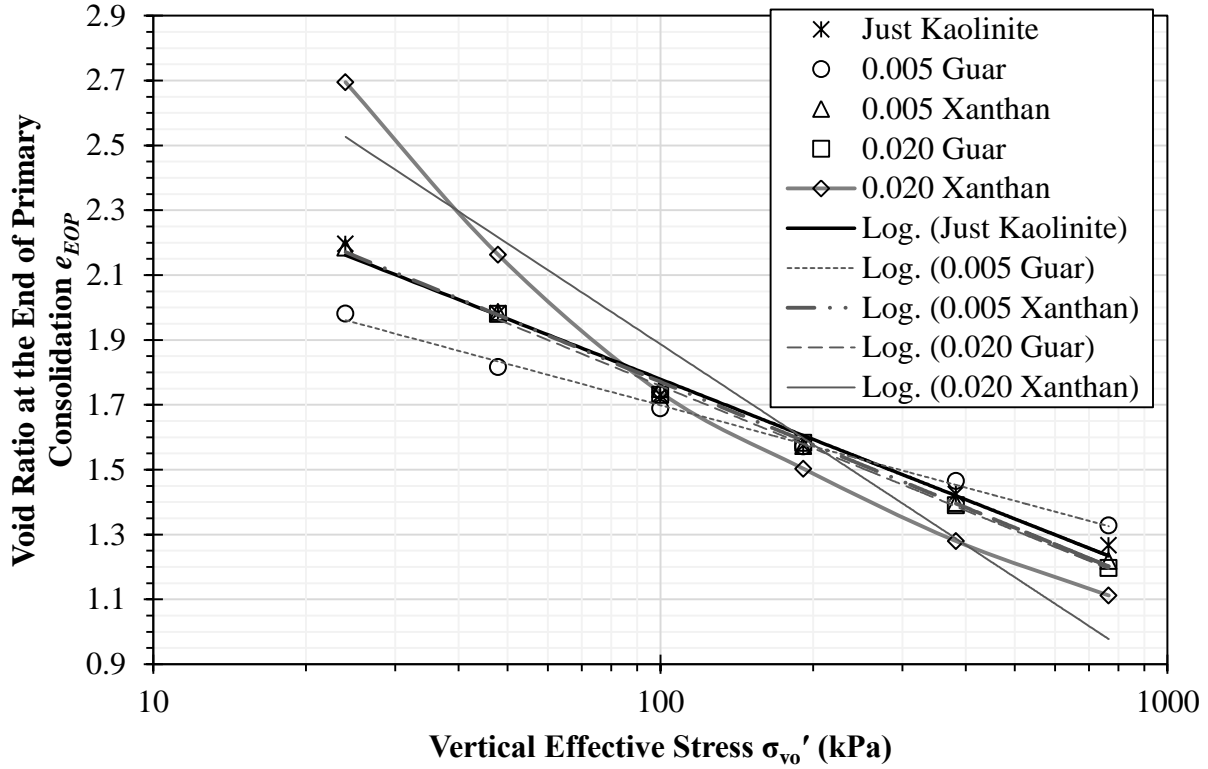


**Figure 5.14: Void ratio vs. vertical effective stress for biopolymer and kaolinite mixtures.**

Even at the same concentration of 0.005  $R_{bm}$ , the hydrogen bonding network established by guar gum reduces compressibility, but the electrostatic repulsion of anionic xanthan gum prevents interaction and negligibly changes compressibility. At 0.020  $R_{bm}$ , biopolymer displacement of clay particles increases compressibility for both guar gum and xanthan gum mixtures. However, guar gum mixtures simply lose the gains provided by hydrogen bonding, while the electrostatic repulsion produced by xanthan gum dramatically increases compressibility above the amount for just kaolinite. Figure 5.14 also highlights the curvature in the compression line that is the result of electrostatic repulsion reducing the effective stress on the soil skeleton.

A comparison of creep behavior between the two biopolymers is provided in Figure 5.15. For a given low load and biopolymer concentrations of 0.015 and 0.020  $R_{bm}$ ,  $C_{\alpha\epsilon}$  is much greater for xanthan gum mixtures than it is for guar gum mixtures at the same concentration. Electrostatic repulsion seems to help high  $R_{bm}$  xanthan gum mixtures to defer strain from primary

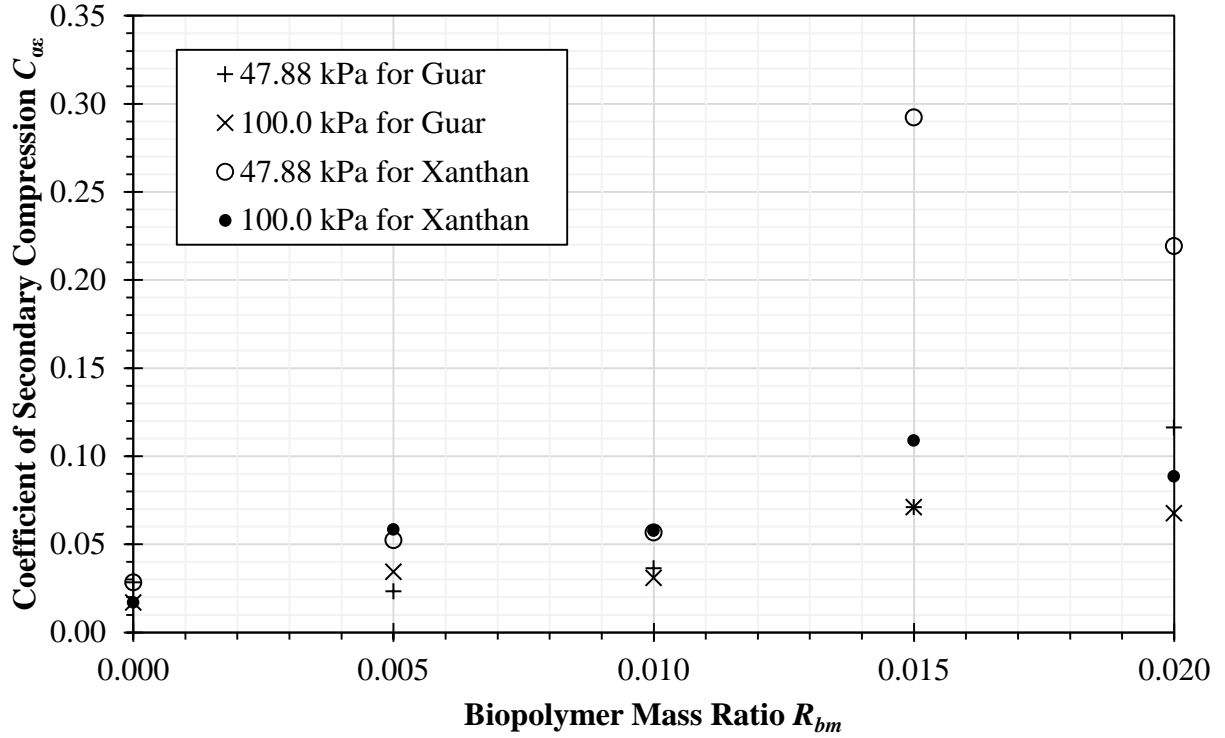


**Figure 5.15: Coefficient of secondary compression vs. biopolymer mass ratio by vertical load and biopolymer.**

consolidation to secondary compression. Both biopolymers only show slight differences in creep compared to just kaolinite at low concentrations, but xanthan gum mixtures show a slightly greater elevation in  $C_{\alpha\epsilon}$ .

Figure 5.16 illustrates the hydraulic conductivity of guar gum and xanthan gum mixtures at similar concentrations. Both guar gum and xanthan gum produce a similar reduction in hydraulic conductivity at  $0.010 R_{bm}$ . Electrostatic charge probably does not cause xanthan gum mixture  $k$  to diverge from guar gum mixture values until higher concentrations. Xanthan gum's repulsive electric field prevents it from fitting into smaller pores in the kaolinite fabric, but the lack of a repulsive electric field would let guar gum fit into and clog those pores. The  $0.020 R_{bm}$  guar gum mixture would then have a smaller effective pore size distribution and  $k$  than the  $0.020 R_{bm}$  xanthan gum mixture.

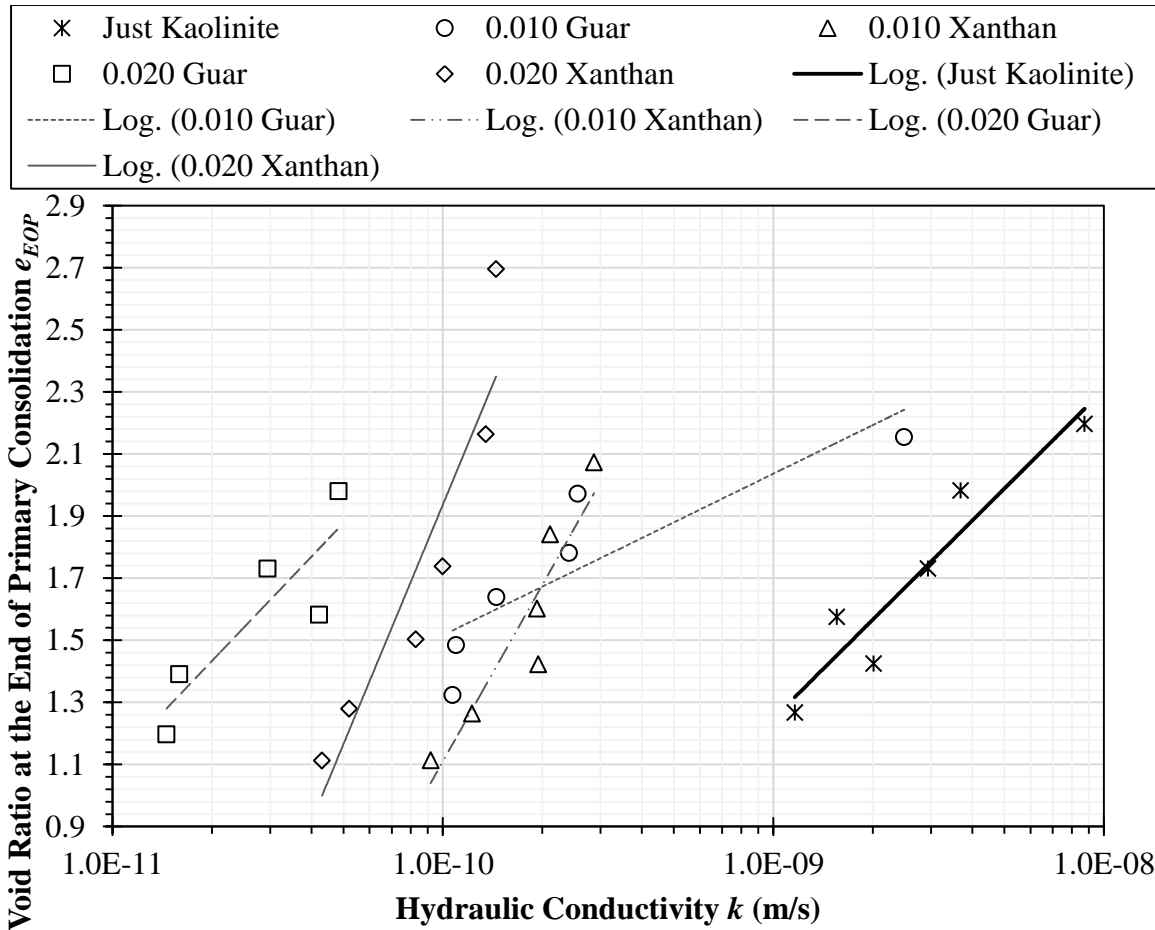


**Figure 5.16: Void ratio vs. hydraulic conductivity by biopolymer.**

## 5.4 Practical Applications

Changes induced in the consolidation properties of biopolymer and clay mixtures in this study show that there are potential uses and limitations for biopolymer amendment of clay. The high viscosities of low concentration biopolymer solutions make biopolymer grouting unfeasible, especially for low permeability clay. Instead, biopolymer would have to be directly mixed into the soil to be improved. In addition, other soil amendments, such as lime, can produce greater reductions in compressibility than those demonstrated here with biopolymer amendment.

However, both guar gum and xanthan gum are non-toxic polysaccharides, so they have the potential to stabilize hydraulically dredged fill used to restore wetlands without environmental damage. This initial reinforcement will give plants the time to grow and provide

additional improvement. The slurry pump in a hydraulic dredge provides a convenient spot to add biopolymer to the sediment, and turbulence in the slurry output pipe can serve to thoroughly mix the biopolymer with the sediment. As seen in the results of this study, a lean guar gum concentration of 0.005  $R_{bm}$  can reduce compressibility with a negligible change in creep and almost no decrease in hydraulic conductivity or the rate of consolidation. This suggests less wetland will be lost due to settlement of newly placed slurry.

Although the electrostatic repulsion of xanthan gum makes it appear to be a poor candidate for soil improvement, the results seen in this study are a special case. Kaolinite has a relatively low cation exchange capacity, and DDI water is effectively cation free. As a result, there are virtually no cations to balance xanthan gum's negative charge. Natural sediments will contain monovalent cations that will balance the negative charges and allow xanthan gum to form hydrogen bonds and divalent cations that can form ionic bridges. Continued study is needed to completely characterize the interactions between xanthan gum and kaolinite.

The reductions in hydraulic conductivity suggest there are uses for biopolymers in clay liners. Biopolymer may be mixed with on-site fine-grained sediments to produce an impermeable layer that mimics the effects of bioclogging. This local sediment layer could augment traditional bentonite barriers, but the reduction in hydraulic conductivity could be temporary since microorganisms can degrade biopolymers over time. Reductions in hydraulic conductivity also come at the price of increased compressibility and creep, as high concentrations of biopolymer are needed to minimize the hydraulic conductivity.

## 5.5 Conclusions

Consolidation tests were performed on a kaolinite clay with different concentrations of biopolymer added to determine how biopolymer and clay interactions can influence the



consolidation properties of the mixture. Guar gum, an electrostatically neutral plant polysaccharide, and xanthan gum, an anionic bacterial extracellular polysaccharide, were used in this study since they are similar to EPS found naturally in soil. Based on the results of the tests, the following conclusions for guar gum and kaolinite mixtures can be made:

- At low concentrations, guar gum and kaolinite form a hydrogen bonding network that decreases mixture compressibility by up to 31.6%.
- At high concentrations, solid kaolinite particles are displaced by strands of guar gum. Since guar gum is more compressible than kaolinite, compressibility increases. This increase in compressibility will be greater than the reduction in compressibility due to hydrogen bonding at high enough concentrations.
- Increases in compressibility will also be reflected in increases in  $C_{ae}$ , not just  $C_c$ .
- Guar gum reduces hydraulic conductivity by clogging pores. Since guar gum cannot fit in pores of all sizes, this reduction has a limit.
- Reductions in hydraulic conductivity additionally induce reductions in the rate of consolidation.

The test results also allow the following conclusions to be made for xanthan gum and kaolinite mixtures:

- A hydrogen bonding network with kaolinite cannot be formed by xanthan gum because of electrostatic repulsion.
- Xanthan gum, at very low concentrations, does not interact with kaolinite because it hides in pore spaces.
- Effective stress on the kaolinite skeleton is reduced by electrostatic repulsion when the kaolinite and xanthan gum mixtures have a high concentration and low total vertical

stresses. This significantly increases  $e$  at the end of primary consolidation and increases the rate of creep.

- For high concentrations and high vertical stresses, xanthan gum and kaolinite mixtures show higher compressibility than kaolinite without biopolymer because of biopolymer displacement of clay particles.
- Xanthan gum also reduces hydraulic conductivity by clogging pores. Since xanthan gum strands have an electric field, they are effectively larger than guar gum strands. This prevents xanthan gum from reducing hydraulic conductivity as much as guar gum at high concentrations.
- Reductions in hydraulic conductivity also produce reductions in the rate of consolidation.

## **CHAPTER 6. DIRECT SHEAR MEASUREMENT OF THE EFFECT OF EXOPOLYMERS ON THE SHEAR STRENGTH OF KAOLINITE**

### **6.1 Introduction**

Direct shear tests and triaxial tests are two common means of measuring the shear strength of soils. However, the predefined shear plane and incomplete control over specimen drainage, inherent to direct shear tests, makes undrained shear strength results for clays nonconservative. Consolidation results from Chapter 5 reveal that a complete set of triaxial tests would be extremely time consuming, so direct shear tests were performed to rapidly survey the effect of exopolymers on the undrained shear strength of kaolinite. As the specific exopolymer and exopolymer concentrations that produce the most shear strength improvement are of greatest interest to practicing engineers, the results of a series of direct shear tests would make it possible to target fewer triaxial tests on the most important exopolymer and exopolymer concentration.

For these direct shear tests, guar gum, an electrostatically neutral plant polysaccharide, and xanthan gum, an anionic bacterial extracellular polysaccharide, were used as exopolymer analogues. These two biopolymers were added to kaolinite to produce mixtures of biopolymer and kaolinite with varying concentrations. Qualitative changes in shear strength were then related to nanoscale interactions between kaolinite particles and molecular biopolymer strands.

### **6.2 Materials and Methods**

The guar gum, xanthan gum, and kaolinite that were described in Sections 5.2, 5.2.1, and 5.2.2 were used for these direct shear tests. The procedures for performing the direct shear tests are described in the following section.

#### **6.2.1 Direct Shear Test Apparatus and Methods**

The direct shear tests were performed based on ASTM D 3080 (ASTM 2006) using an automated DigiShear device manufactured by Trautwein Soil Testing Equipment Company.

These tests also used biopolymer and clay slurries with a constant  $R_{bm}$ . The slurries were prepared as described in Section 5.2.3. A modified shear box was used to perform all of the tests on the mixtures.

A stainless steel spacer with holes was placed in the bottom half of the shear box so that there was a 3.175 mm (1/8 in.) distance from the specimen bottom to the shear plane. The top half of the box was 9.525 mm (3/8 in.) thick so that the initial specimen height was 12.7 mm (1/2 in.), and the specimen hole in the box was 63.5 mm (2.5 in.) in diameter. With the box assembled, slurry was loaded into the shear box in a similar fashion to how it was loaded for the consolidation tests described in Section 5.2.4. Since the slurry was highly compressible (50% strain is typical), placing the shear plane 3.175 mm above the specimen bottom resulted in the specimen getting sheared approximately in the middle.

For each test, the slurry was initially loaded to 15.80 kPa (330 psf) for 24 hours. This was to stiffen the slurry and reduce extrusion during the next load increment. The second load increment was either 47.88 kPa (1000 psf), 100 kPa (2088.54 psf), 191.52 kPa (4000 psf), or 287.28 kPa (6000 psf), and the load was held for 24 hours for the specimen to reach the end of primary consolidation. After consolidation, the specimen was sheared at a rate of 0.889 mm/min (0.035 in./min) over a distance of 12.192 mm (0.48 in.).

A 100 kPa load allows the results to be compared against the intrinsic strength line ( $IS_uL$ ) developed by Chandler (2000). The  $IS_uL$  is relevant since it was created to describe the behavior of reconstituted soils made from a slurry. Specifically, the  $IS_uL$  describes the shear strength of reconstituted soils that are  $K_0$  consolidated and then sheared in undrained triaxial compression.

Direct shear tests apply shear stress along a predefined shear plane and do not have complete control over specimen drainage. Therefore, this direct shear test method does not

provide the most conservative measurement of undrained shear strength. However, the vane shear test described in ASTM D 4648 (ASTM 2006) suffers from the same weaknesses, but it is still considered valid for measuring undrained shear strength. Since direct shear tests provide a convenient way to consolidate slurries before shear and allow control over the normal stress applied, direct shear was used instead of vane shear. For each test, the undrained shear strength  $s_u$  was calculated, and the end of shear  $e$  was measured. The SHANSEP model constant  $S$  was also calculated for each mixture by plotting  $s_u$  against the initial, pre-shear vertical stress  $\sigma_{vo}'$ .

### 6.3 Results and Discussion

Figure 6.1 and Figure 6.2 show the results of direct shear tests on guar gum and kaolinite mixtures, as well as kaolinite without biopolymer, with  $s_u$  vs.  $\sigma_{vo}'$  in Figure 6.1 and a comparison of the shear strength data against the IS<sub>u</sub>L in Figure 6.2. Table 6.1 gives the  $S$  and  $R^2$  calculated from the tests on guar gum and kaolinite mixtures. The direct shear test results for xanthan gum and kaolinite mixtures, as well as kaolinite without biopolymer, are illustrated in Figure 6.3 and Figure 6.4, with  $s_u$  vs.  $\sigma_{vo}'$  in Figure 6.3 and a comparison of the shear strength data against the IS<sub>u</sub>L in Figure 6.4. Table 6.1 also has  $S$  and  $R^2$  calculated from the tests on xanthan gum and kaolinite mixtures.

**Table 6.1: Fitted line data for guar gum and kaolinite mixtures and xanthan gum and kaolinite mixtures.**

$R_{bm}$	Guar Gum Mixture Results		Xanthan Gum Mixture Results	
	$S$	$R^2$ for $S$	$S$	$R^2$ for $S$
0.000	0.4687	0.9740	0.4687	0.9740
0.005	0.5276	0.9922	0.4318	0.9850
0.010	0.4867	0.9522	0.4945	0.9722
0.015	0.3870	0.9882	0.3334	0.9597
0.020	0.3442	0.9668	0.2880	0.8299

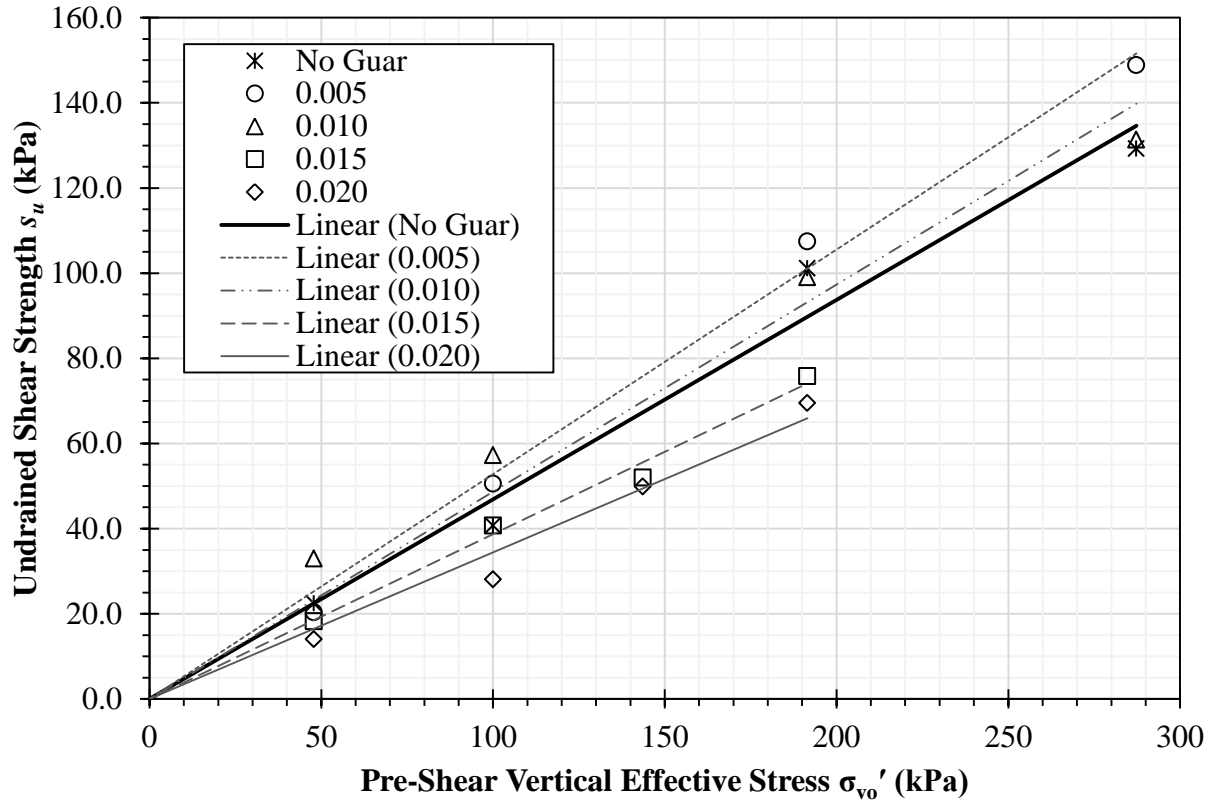


**Figure 6.1: Undrained shear strength vs. pre-shear vertical effective stress for guar gum and kaolinite mixtures.**

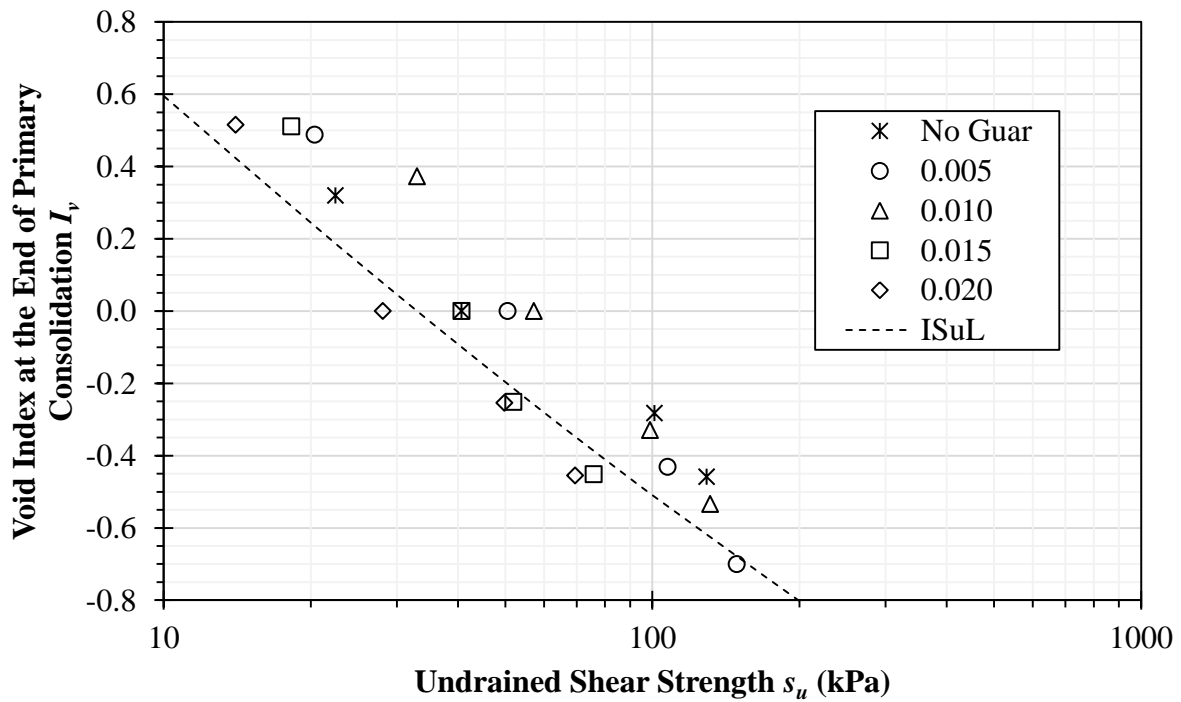


**Figure 6.2: Void index vs. undrained shear strength for guar gum and kaolinite mixtures. IS<sub>u</sub>L is from Chandler (2000).**

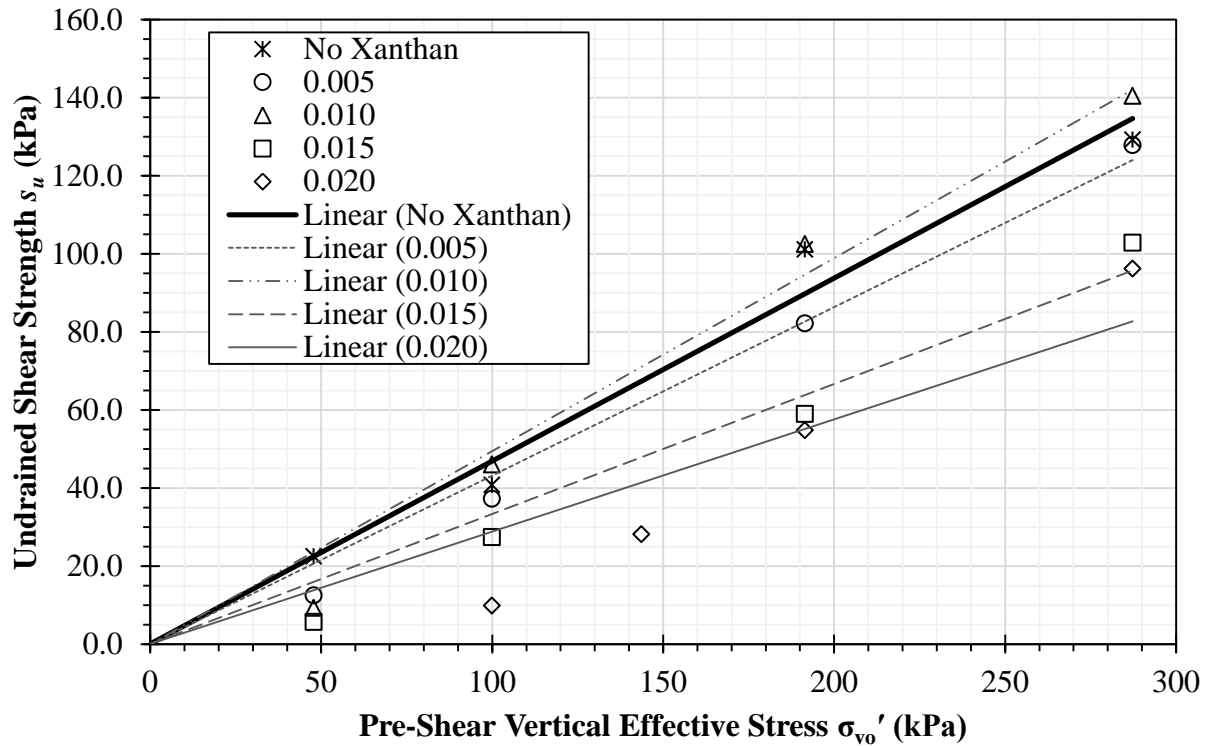


Figure 6.3: Undrained shear strength vs. pre-shear vertical effective stress for xanthan gum and kaolinite mixtures.

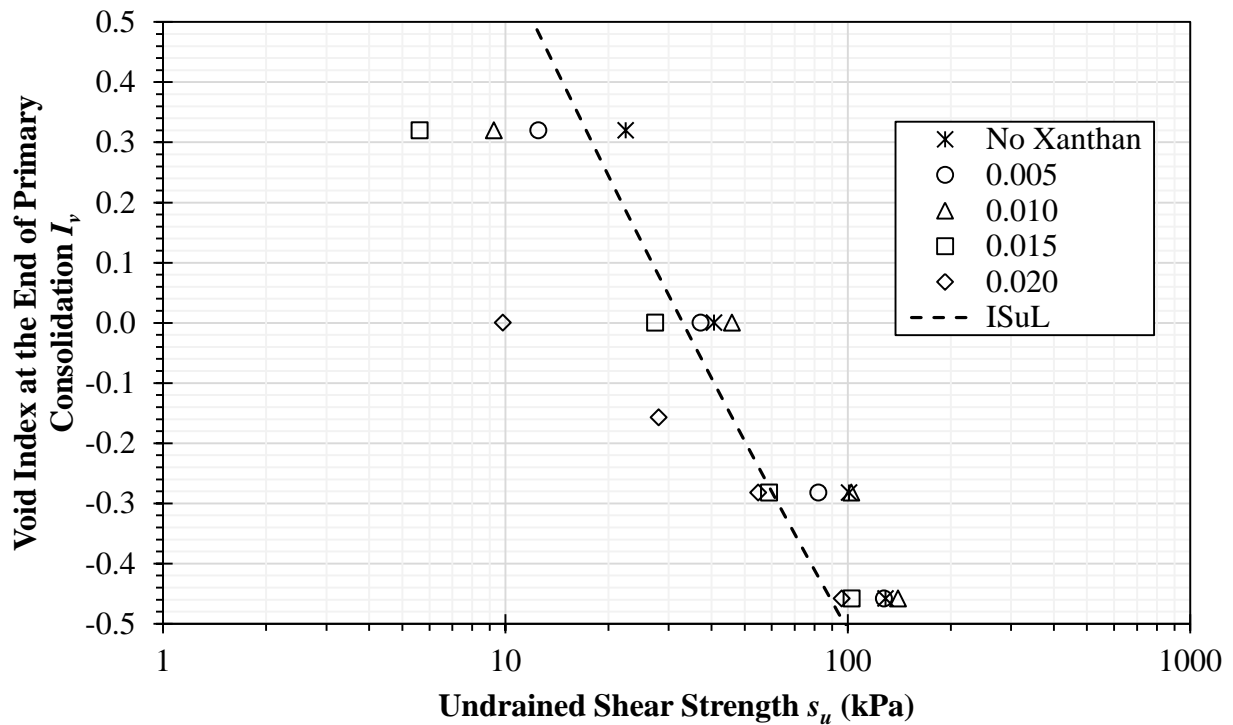


Figure 6.4: Void index vs. undrained shear strength for xanthan gum and kaolinite mixtures. IS<sub>u</sub>L is from Chandler (2000).

### 6.3.1 Guar Gum and Kaolinite Mixtures

The changes in the undrained shear strength of guar gum and kaolinite mixtures are demonstrated in Figure 6.1 and Table 6.1. Just as the highly linked clay-polymer network in 0.005 and 0.010  $R_{bm}$  guar gum mixtures increased their consolidation stiffness, the direct shear tests show that  $S$  is increased from 0.4687 for kaolinite alone to 0.5276 for 0.005  $R_{bm}$  guar gum mixtures and 0.4867 for 0.010  $R_{bm}$  guar gum mixtures. This results in a 12.6% increase in  $S$  for 0.005  $R_{bm}$  guar gum mixtures. The gains seen at 0.005 and 0.010  $R_{bm}$  are lost at concentrations of 0.015 and 0.020  $R_{bm}$ , which is also similar to the consolidation results.

At 0.005  $R_{bm}$ , the guar gum is probably able to establish bonds between kaolinite particles that would otherwise not interact, raising the shear resistance of the mixture by acting as a kind of cement. However, as the guar gum concentration increases, strands of guar gum likely block direct particle to particle contact. As the friction produced at contact points is what provides most of the critical state shear resistance of kaolinite, replacing these direct particle contacts with kaolinite platelet to guar gum strand contacts reduces the overall shear resistance. This is because there is comparatively less friction between strands of guar gum and kaolinite particles. The effect of this reduction in direct particle to particle contact is especially strong in the 0.020  $R_{bm}$  mixture, with an  $S$  reduction of 0.1245 compared to kaolinite without biopolymer.

Figure 6.2 shows how the shear response of the mixtures compares with the  $IS_uL$ . Although there is some scatter, the guar gum and kaolinite mixtures reasonably follow the  $IS_uL$ . Chandler (2000) developed the  $IS_uL$  using undrained triaxial compression data, so the fact that the direct shear data shows slightly higher shear strength at a given void index is not surprising, as direct shear tests are typically less conservative than triaxial tests. Since the  $IS_uL$  was developed using shear strength data from reconstituted clay slurries, Figure 6.2 shows that the



normalized shear behavior of kaolinite and guar gum mixtures does not deviate from the normalized shear behavior of other clays.

The liquid limit test data in Chapter 3 suggested that as the biopolymer concentration increases, the dynamic viscosity of the biopolymer solution in the clay pores increases, and the shear resistance of the mixture should increase as well. However, this assertion is contradicted by the direct shear results. Since the shear resistance of a viscous fluid is a function of the rate of strain, viscosity effects of the biopolymer solution become more important for rapidly applied loads. A Casagrande cup, which was used in Chapter 3 to measure liquid limits, applies rapid impact loads on fine-grained sediment, while the direct shear tests applied a much slower rate of strain. This slower shearing made viscosity effects negligible.

### **6.3.2 Xanthan Gum and Kaolinite Mixtures**

Figure 6.3 and Table 6.1 provide the shear response for the xanthan gum and kaolinite mixtures. Again, the interactions between xanthan gum and kaolinite appear to be similar to guar gum interactions with the addition of electrostatic repulsion.

At  $0.005 R_{bm}$ , the small quantity of xanthan gum is repelled from the kaolinite and is hidden in the voids in the clay fabric. This xanthan gum still exerts a repulsive force on the kaolinite skeleton, causing a slight reduction in the effective normal stress. Reduced normal forces at kaolinite particle contact points result in reduced frictional forces and creates a 7.9% reduction in  $S$ .

At  $0.010 R_{bm}$ , the xanthan gum concentration becomes high enough that there is probably no longer room for the xanthan gum strands to avoid interactions with the kaolinite in the clay voids. The normal stresses applied are sufficient to overcome these repulsive forces in a similar fashion to the way they are overcome during the consolidation tests in Chapter 5. Since kaolinite

particles typically have a small number of sites with localized positive charges along the particle edge, the xanthan gum could potentially form ionic bonds with kaolinite at these sites. Because ionic bonds are substantially stronger than hydrogen bonds, this limited bond network is able to overshadow the negative effects of electrostatic repulsion and reductions in direct particle to particle contact. This ionic bond network, instead, seems to increase  $S$  over the value for kaolinite alone.

However, continuing to increase the xanthan gum concentration brings electrostatic repulsion back as the dominant mechanism of interaction. Combined with reducing direct particle to particle contact, electrostatic repulsion drives  $S$  for 0.015  $R_{bm}$  xanthan gum mixture to less than the  $S$  for 0.020  $R_{bm}$  guar gum mixture.

The high concentration xanthan gum mixtures do not appear to form lines that cross the origin in Figure 6.2. Instead, the 0.015  $R_{bm}$  xanthan gum mixture wants to cross the horizontal axis at 35 kPa, and the 0.020  $R_{bm}$  xanthan gum mixture wants to cross the horizontal axis at 79 kPa. This suggests that at 0.015 and 0.020  $R_{bm}$  concentrations, electrostatic repulsion reduces the effective stress by 35 kPa and 79 kPa, respectively.

With these deviations in xanthan gum and kaolinite mixture behavior, relative to typical clay behavior, and the deviations in xanthan gum mixture consolidation behavior discussed in Section 5.3.2, it is no surprise that Figure 6.4 shows results that do not follow expected clay behavior. Figure 6.4 shows how the shear response of the mixtures compares with the  $IS_uL$ . In addition to some scatter, the xanthan gum and kaolinite mixtures deviate from the  $IS_uL$  at 0.015 and 0.020  $R_{bm}$ .

Because Chandler (2000) developed the  $IS_uL$  using undrained triaxial compression data, it is again not surprising that the direct shear data shows slightly higher shear strength at a given

void index for lower biopolymer concentrations, given the direct shear tests are generally less conservative than triaxial tests. Since the  $IS_uL$  was developed using shear strength data from reconstituted clay slurries, Figure 6.4 shows that the normalized shear behavior of kaolinite and xanthan gum mixtures does deviate from the normalized shear behavior of other clays.

## 6.4 Conclusions

To determine how biopolymer and clay interactions can influence the shear strength of a mixture, direct shear tests were performed on a kaolinite clay that had different concentrations of biopolymer added to it. In an effort to duplicate natural EPS found in the soil, two different polysaccharides, that were similar to the EPS, were used in this study. These polysaccharides were guar gum, which is an electrostatically neutral plant polysaccharide, and xanthan gum, which is an anionic bacterial extracellular polysaccharide. Results of the tests allow the following conclusions for guar gum and kaolinite mixtures to be made:

- The hydrogen bonding network formed by kaolinite and guar gum at low concentrations increases critical state shear resistance by up to 12.6%.
- Kaolinite particle displacement at high guar gum concentrations causes direct kaolinite to kaolinite contact points to be replaced with kaolinite to guar gum contact points. Since the coefficient of friction for kaolinite and guar gum contacts are smaller than for kaolinite particle to kaolinite particle contacts, critical state shear resistance is reduced. Reductions in shear resistance will be more significant than increases in shear resistance due to hydrogen bonding at sufficiently high concentrations.

From the test results, the following conclusions can also be made for xanthan gum and kaolinite mixtures:

- Electrostatic repulsion prevents xanthan gum from forming a hydrogen bonding network with kaolinite. However, if the electrostatic repulsion is overcome with a sufficiently high normal stress, an ionic bonding network can be developed with xanthan gum bonding to localized positive charge sites on kaolinite particles.
- At very low concentrations, xanthan gum is able to avoid interaction with kaolinite by hiding in pore spaces. Even at these low concentrations, there is still a 7.9% reduction in shear resistance.
- Moderate concentrations of xanthan gum can increase the shear resistance beyond the value for pure kaolinite due to the ionic bonding network.
- At high concentration and low total normal stresses, electrostatic repulsion reduces the effective stress on the kaolinite skeleton. This dramatically reduces shear resistance.
- For high concentrations and high normal stresses, xanthan gum and kaolinite mixtures show lower shear resistance than kaolinite without biopolymer for similar reasons as high concentration guar gum mixtures.

## CHAPTER 7. TRIAXIAL MEASUREMENT OF THE EFFECT OF EXOPOLYMERS ON THE SHEAR STRENGTH OF KAOLINITE

### 7.1 Introduction

Interest has been growing in biologically improving soil (Ivanov and Chu 2008; Mitchell and Santamarina 2005). One method receiving attention is the addition of exopolymers to sediments. Exopolymers, or extracellular polymeric substances (EPS), are an important component of bacterial biofilms. Many of these biofilm exopolymers are high molecular weight polysaccharides that possess chemically active, electrically charged functional groups (Sutherland 2001). These functional groups interact with sediment particles, especially clay minerals, because they have high specific surface areas and electrical charges.

Studies by Widdows et al. (2006) and Yallop et al. (2000) illustrated that the erosional resistance of sediment surfaces is improved by exopolymers. Nugent et al. (2010) also showed that guar gum added to kaolinite can increase the erosional resistance by almost one order of magnitude. Nugent et al. (2011b) further demonstrated that the stiffness of kaolinite can similarly be enhanced when guar gum at a relatively low concentration of 0.005 dry mass biopolymer to dry mass clay, or  $R_{bm}$ , is mixed with the kaolinite.

This chapter shows the results of CK<sub>0</sub>U triaxial tests on kaolinite and guar gum mixtures with concentrations of 0.0025, 0.0050, 0.0075, and 0.0100  $R_{bm}$ . As this range of mixtures best shows the potential improvement in stiffness out of the biopolymer and clay mixtures tested by Nugent et al. (2011b), the behavior of these mixtures would most interest any practicing engineer. Further, guar gum consistently produces improvements in stiffness and erosional resistance without needing cations in the pore fluid, and this makes guar gum a more robust choice for soil improvement. Shear strengths of the mixtures are compared, and qualitative

changes in the overall strengths of the mixtures are related to the nanoscale interactions between kaolinite particles and molecular guar gum strands. Potential applications are then discussed.

## **7.2 Materials and Methods**

This study involves the use of a kaolinite clay sample. The sample was obtained from Theile Kaolin Company. Average specific surface area of the kaolinite measured 20-26 m<sup>2</sup>/g, and the specific gravity was 2.63 (Flick 1989). Kaolinite particles possess an overall negative charge at solution pH greater than 2.35 (Alkan et al. 2005).

Guar gum (Laboratory Grade), purchased from Fisher Scientific, was also used. Guar gum is a neutral polysaccharide extracted from *Cyamopsis tetragonoloba* seeds. Guar gum molecules have weights of up to  $2 \times 10^6$  Da (Risica et al. 2005), and a major feature of these guar gum molecules are their many hydroxyl (-OH) groups. These functional groups allow guar gum molecules to form hydrogen bonds. Although guar gum is not microbially produced, it can produce viscous, pseudoplastic aqueous solutions like a neutral microbial EPS. Guar gum's availability, inexpensiveness, and ability to increase aqueous systems' viscosity give it commercial significance (Whitcomb et al. 1980).

### **7.2.1 Preparation of Triaxial Specimens**

The triaxial tests were performed based on ASTM D 4767 (ASTM 2006), using the automated TruePath system manufactured by Trautwein Soil Testing Equipment Company. To begin testing, a slurry was prepared using the procedures described in Nugent et al (2011b). In turn, nine slurries were made for testing. These consisted of plain kaolinite and kaolinite with  $R_{bm}$  of 0.0025, 0.0050, 0.0075, and 0.0100, each having a water content of approximately 190%. The raw slurry could not be directly tested because the triaxial cell requires solid material.

To prepare the slurry for use in a triaxial cell, a 76.2 mm (3 in.) diameter porous stone was placed into the center of a plastic two liter beaker. A second, 63.5 mm (2.5 in.) diameter porous stone with a filter paper was then placed on top of the 76.2 mm (3 in.) diameter porous stone. Next, a 152.4 mm (6 in.) tall consolidation ring was placed on the 76.2 mm (3 in.) diameter porous stone so that the 63.5 mm (2.5 in.) diameter porous stone sat inside the bottom of the ring. This porous stone, inside the bottom of the ring, prevents slurry from extruding out of the bottom of the ring.

Slurry was then loaded into the ring in a similar fashion to how it was loaded for the consolidation tests described in Nugent et al. (2011b). Once the ring was full, the top surface of the slurry was flattened using a straightedge. The slurry was first stiffened by applying a 23.94 kPa (500 psf) load for 24 hours, and then the stiffened slurry was loaded to 71.82 kPa (1500 psf) and consolidated until the specimen reached the end of primary consolidation. Figure 7.1 provides images of the setup specimen preparation apparatus.

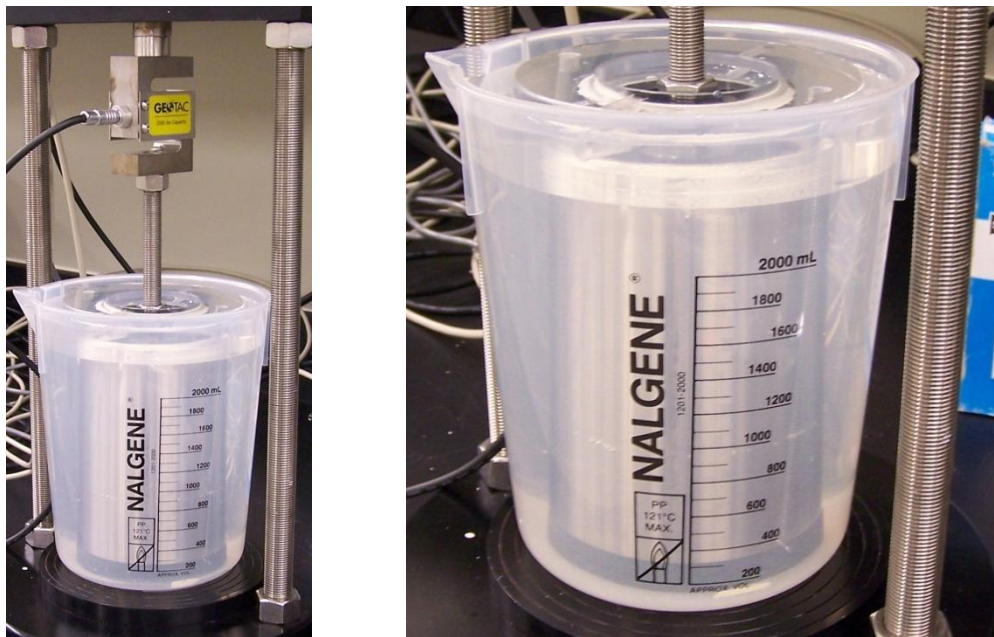


**Figure 7.1: Images of the triaxial specimen preparation apparatus.**

## 7.2.2 Triaxial Test Apparatus and Methods

After a specimen was prepared, it was extruded from the ring and trimmed into a 35.56 mm (1.4 in.) diameter and approximately 58.4 mm (2.3 in.) tall cylinder. Figure 7.2a shows a representative specimen after trimming. This resulted in a cylinder with a height to diameter ratio of about 1.64, which is slightly smaller than the ASTM recommended ratio of between 2 to 2.5. The reason the specimens were somewhat short is because a smaller consolidation load would result in specimens that were too soft to be handled, and a lower water content initial slurry would trap air bubbles. Next, this cylinder was loaded into a triaxial cell with four 6.35 mm (0.25 in.) wide filter paper strips along the perimeter of the specimen to accelerate consolidation and equalization of pore water pressures during shearing.

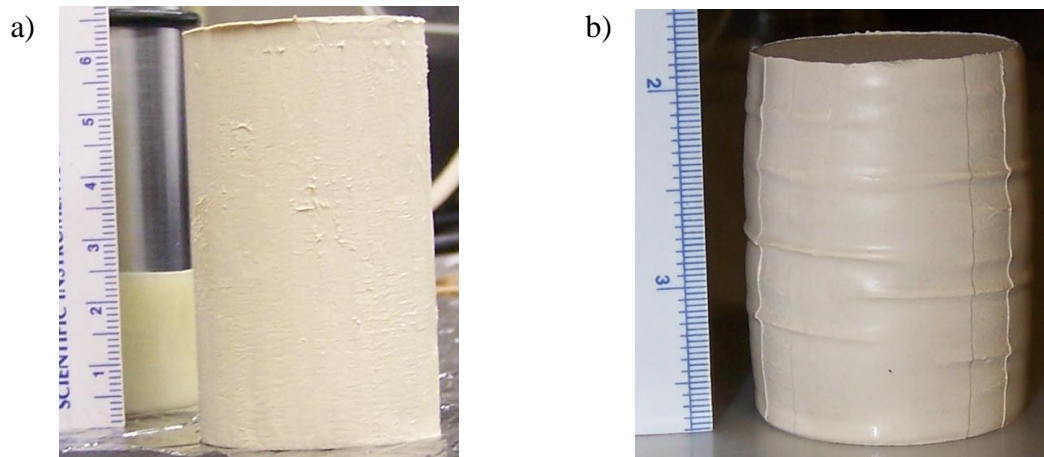


**Figure 7.2: Images of a representative triaxial specimen (a) after trimming (ruler scale in centimeters) and (b) after shearing (ruler scale in inches).**

Before the test was initiated, a 20.68 kPa (3 psi) membrane seating stress was applied. Also, a 344.74 kPa (50 psi) backpressure was administered to insure saturation. Backpressure was applied until the measured B-value was 0.98 or greater.

For all tests except for the 3.31 overconsolidation ratio (OCR) kaolinite only test,  $K_0$  consolidation was used to consolidate the specimen to an axial load of about 137 kPa, and either a 50 kPa or a 64 kPa axial load was used to unload the specimen depending on the OCR desired.



The 3.31 OCR kaolinite only test was consolidated to 89.8 kPa and unloaded to 27.1 kPa. Axial strain rates of 0.1%/hr. were used for the consolidation and unloading of all specimens. The low loads that were used produce conditions more similar to those found in Louisiana wetlands.

After both the loading and the unloading consolidation stages, the specimen was allowed to creep for at least 12 hours. Finally, the specimen was sheared using undrained compression with a constant cell pressure, increasing axial load, and an axial strain rate of 0.5%/hr to a maximum axial strain of 15%.

After the test, the data was analyzed according to ASTM D 4767 (ASTM 2006) with appropriate membrane and filter paper corrections applied. MIT stress paths were calculated using the following equations:

$$p' = \frac{\sigma'_1 + \sigma'_3}{2} \quad q = \frac{\sigma'_1 - \sigma'_3}{2} \quad (\text{Eqs. 7.1 and 7.2})$$

where  $\sigma'_1$  is the effective axial stress,  $\sigma'_3$  is the effective radial stress,  $p'$  is the MIT mean effective stress, and  $q$  is the MIT maximum shear stress. Note that the sign of  $q$  indicates how the specimen is sheared. A positive  $q$  means shearing through compression, while a negative  $q$  designates extension. The absolute value of  $q$  provides the maximum shear stress applied through the loading conditions.

Cam clay stress paths were calculated with the following equations:

$$p'_{cam} = \frac{\sigma'_1 + 2\sigma'_3}{3} \quad q_{cam} = \sigma'_1 - \sigma'_3 \quad (\text{Eqs. 7.3 and 7.4})$$

where  $p'_{cam}$  is the Cambridge effective mean stress and  $q_{cam}$  is the Cambridge deviator stress.

SHANSEP models (Ladd and Foott 1974) were fitted for kaolinite on its own and for 0.0050  $R_{bm}$  mixtures, and the kaolinite SHANSEP model was used to produce shear strength values for comparison against the other guar gum and clay tests. Specifically, the OCR of each

guar gum and kaolinite mixture was used in the kaolinite SHANSEP model to normalize the  $s_u/\sigma_{vo}'$  ratio of each test. The SHANSEP model uses the following relationship:

$$\frac{s_u}{\sigma_{vo}'} = S(OCR)^m \quad (\text{Eq. 7.5})$$

where  $s_u$  is the undrained shear strength,  $\sigma_{vo}'$  is the initial, pre-shear vertical stress,  $OCR$  is the overconsolidation ratio, and  $S$  and  $m$  are constants for the clay.

Modified Cam clay models (Roscoe and Burland 1968) were also used to try to describe the kaolinite only results. The modified Cam clay model uses an elliptical yield locus described by the following equation:

$$\frac{p'_{cam}}{p'_{cam,o}} = \frac{M^2}{M^2 + (q_{cam}/p'_{cam})^2} \quad (\text{Eq. 7.6})$$

where  $p'_{cam,o}$  is the reference mean stress for the yield locus and  $M$  is the shape factor for the Cam clay ellipse.  $M$  was calculated using the critical state friction angle  $\phi_{cs}'$  calculated from the normally consolidated kaolinite only test using the following equation:

$$M = \frac{6 \sin \phi_{cs}'}{3 - \sin \phi_{cs}'} \quad (\text{Eq. 7.7})$$

### 7.3 Results and Discussion

Table 7.1 provides the  $R_{bm}$ , initial specimen height  $h_o$ , initial specimen diameter  $d_o$ , initial specimen void ratio  $e_o$ , final specimen void ratio  $e_{final}$ , OCR,  $\sigma_{vo}'$ ,  $s_u$ ,  $s_u/\sigma_{vo}'$  ratio, axial strain at failure  $\epsilon_{a, fail}$ , compression index  $C_c$ , recompression index  $C_r$ , and total axial strain after consolidation  $\epsilon_{a, con}$  for every test performed. All of the tests ended with the specimen experiencing bulging failure. A representative failed specimen is pictured in Figure 7.2b.

Figures 7.3, 7.4, and 7.5 show the MIT stress path, stress vs. strain curves, and excess pore water pressure during shear for the kaolinite only tests, respectively. The normally consolidated kaolinite has a stress vs. strain curve with a peak strength similar to the normally

consolidated kaolinite with 4% Portland cement added, which was tested by Trhlíková et al. (2009). Trhlíková et al. (2009) used the cement to simulate the structure found in certain natural clays. Structure is the combined effects of fabric, composition, and interparticle forces (Mitchell and Soga 2005).

**Table 7.1: Summary of data for all triaxial tests performed. Dash indicates that the value was not measured.**

$R_{bm}$	$h_o$ (mm)	$d_o$ (mm)	$e_o$	$e_{final}$	OCR	$\sigma_{vo}'$ (kPa)	$s_u$ (kPa)	$s_u/\sigma_{vo}'$	$\varepsilon_{a, fail}$ (%)	$C_c$	$C_r$	$\varepsilon_{a, con}$ (%)
0.0000	59.7	35.6	1.793	1.470	1.00	135.3	31.2	0.2309	0.21	0.7345	-	11.56
0.0000	61.2	35.6	1.815	1.471	2.69	50.9	26.5	0.5213	1.11	0.7550	0.0207	12.23
0.0000	58.9	35.6	1.767	1.591	3.31	27.1	20.9	0.7717	0.71	0.6811	0.0162	6.38
0.0025	63.2	35.6	1.827	1.547	2.73	50.2	29.7	0.5920	1.77	0.6247	0.0239	9.88
0.0050	58.2	35.6	1.696	1.440	1.00	138.7	35.4	0.2552	0.44	0.5185	-	9.49
0.0050	62.0	35.6	1.709	1.470	2.18	63.9	32.1	0.5024	0.84	0.5305	0.0210	8.82
0.0050	61.2	35.6	1.763	1.515	2.76	49.2	30.8	0.6253	2.29	0.5789	0.0215	8.97
0.0075	59.2	35.6	1.672	1.438	2.73	50.5	28.8	0.5705	1.86	0.4828	0.0237	8.78
0.0100	59.7	35.6	1.703	1.445	2.74	50.8	26.7	0.5260	1.51	0.5707	0.0194	9.52

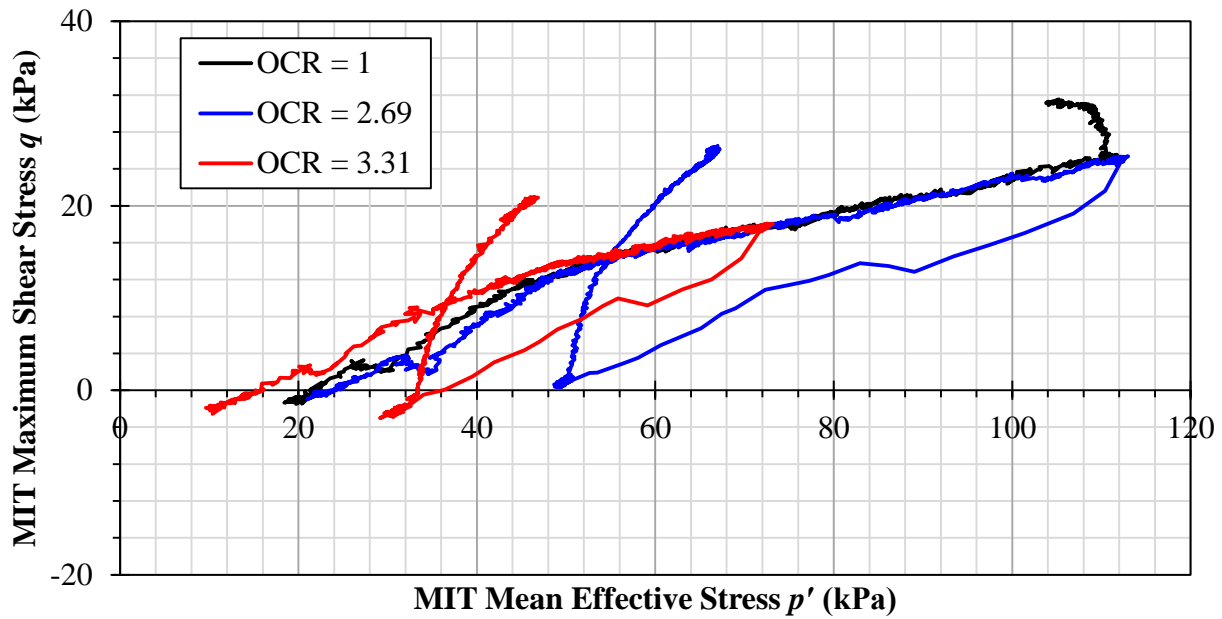


**Figure 7.3: MIT stress paths for tests performed on just kaolinite by OCR.**

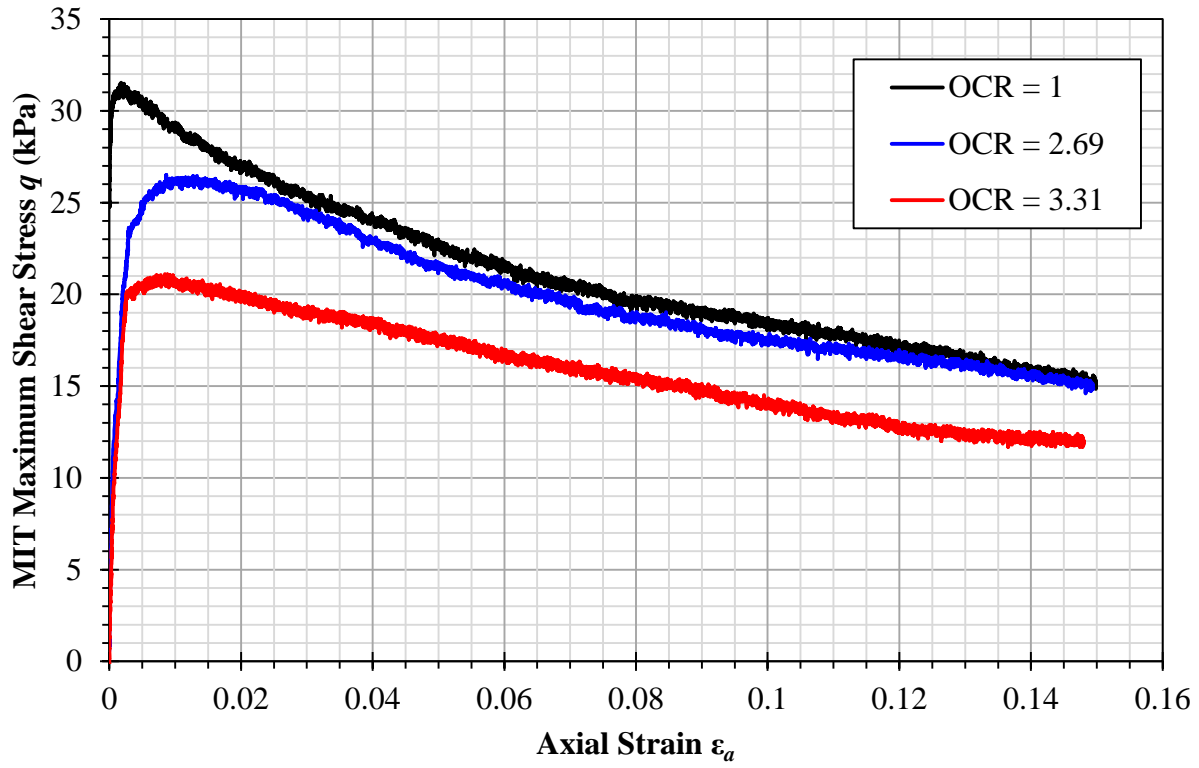


Figure 7.4: Stress vs. strain curves for tests performed on just kaolinite by OCR.

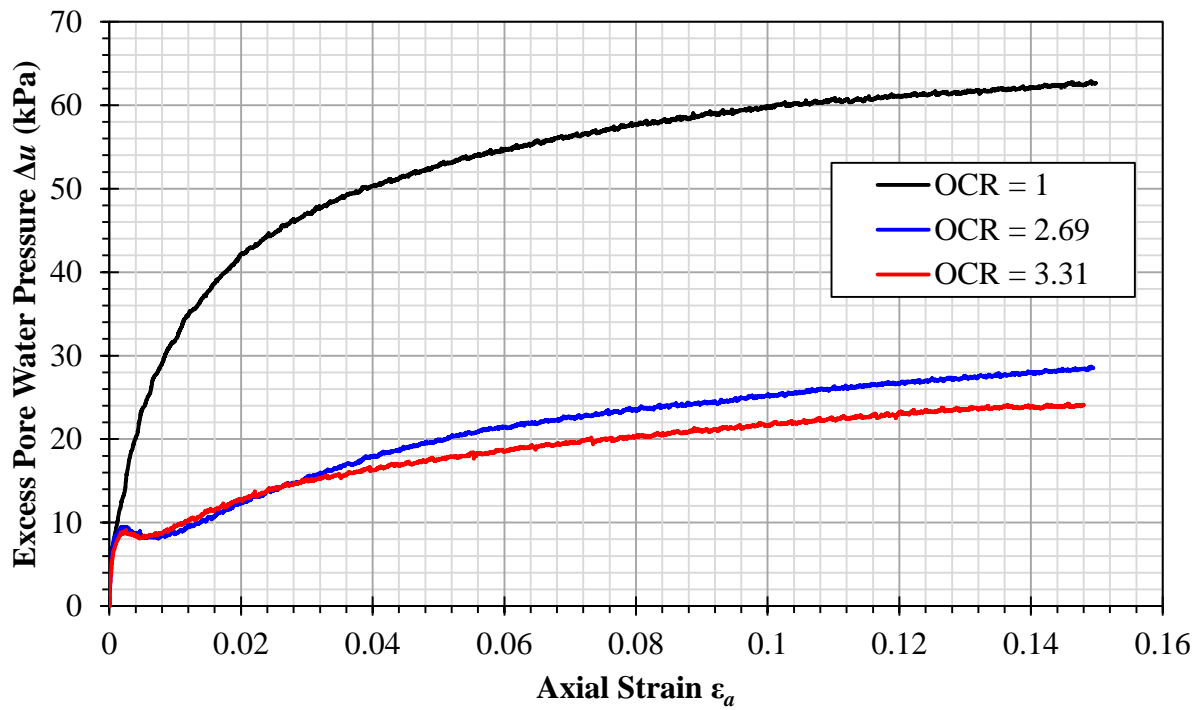


Figure 7.5: Excess pore water pressure during shear for tests performed on just kaolinite by OCR.

The normally consolidated kaolinite stress vs. strain curve also follows the shape predicted by Baudet and Stallebrass (2004) for a structured normally consolidated clay that rapidly destructures after reaching peak strength. This suggests that the kaolinite possesses a form of structure that is readily destroyed by shear, and this leads to the reduction in  $q$  seen in Figure 7.4. The stress vs. strain curves do not level off since the maximum strain tested was not large enough to let the kaolinite reach critical state.

Further, the overconsolidated tests show local excess pore water pressure peaks just before failure, which is behavior also found in the low confining stress triaxial tests performed by Guanghai (2010). Zhu and Yin (2000) performed CIUC triaxial tests on a marine clay using different strain rates during shear. At higher strain rates, the excess pore water pressure creates a similar shape that is absent at the slowest strain rate. Thus, the local peak is a strain rate effect that would likely not be present if a slower strain rate were used. Zhu and Yin (2000) also found that the marine clay did not exhibit any dilative behavior until an OCR of four. The kaolinite used in these tests displays equivalent behavior, which suggests that the kaolinite is still only lightly overconsolidated at an OCR of 3.31 or less.

Determination of the SHANSEP constants is shown in Figure 7.6 with values of 0.2267 for  $S$  and 0.9489 for  $m$  and a model  $R^2$  of 0.9740. Using the data from the normally consolidated test,  $\phi_{cs}'$  was calculated to be  $17.42^\circ$ , and the modified Cam clay  $M$  was 0.6653. However, the modified Cam clay model does not successfully predict the loose sand style behavior and local excess pore water pressure peaks previously described. Further, the Cambridge stress paths for the overconsolidated tests in Figure 7.7 move to the left after failure instead of the rightward movement towards the critical state line predicted by the model. Since the behavior of the

kaolinite is inadequately described by the modified Cam clay model, it was not used for modeling the other tests involving guar gum and kaolinite mixtures.

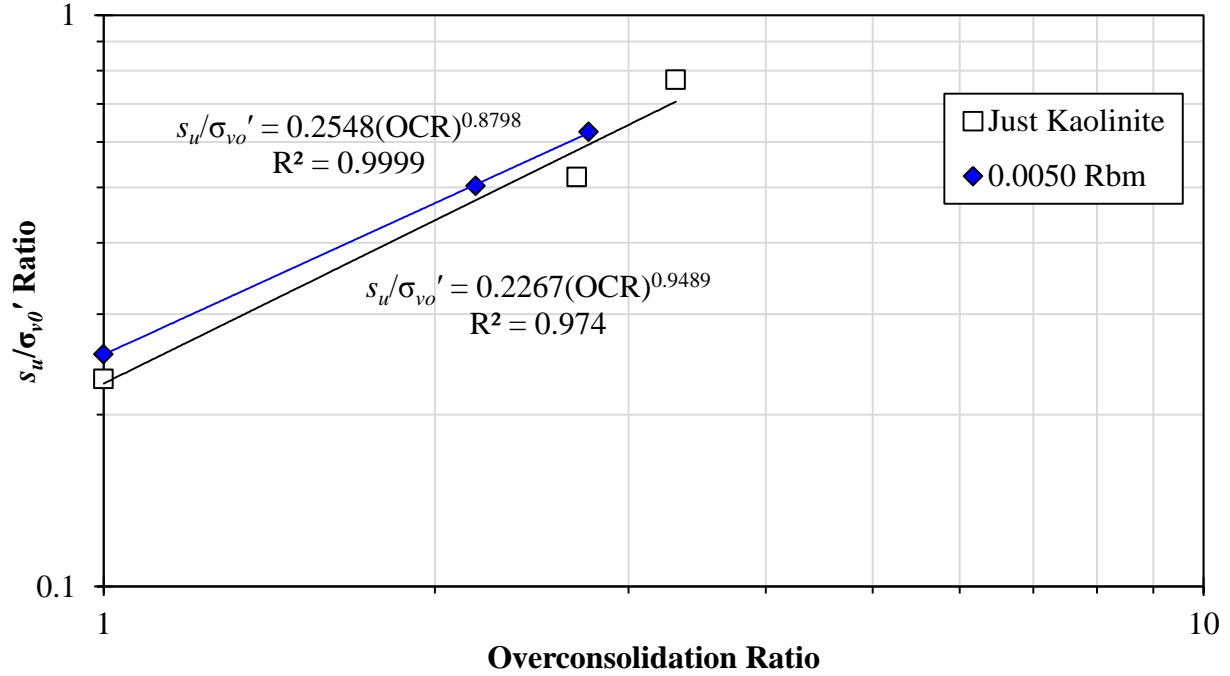


Figure 7.6: SHANSEP model determination for just kaolinite and 0.0050  $R_{bm}$  guar gum mixtures.

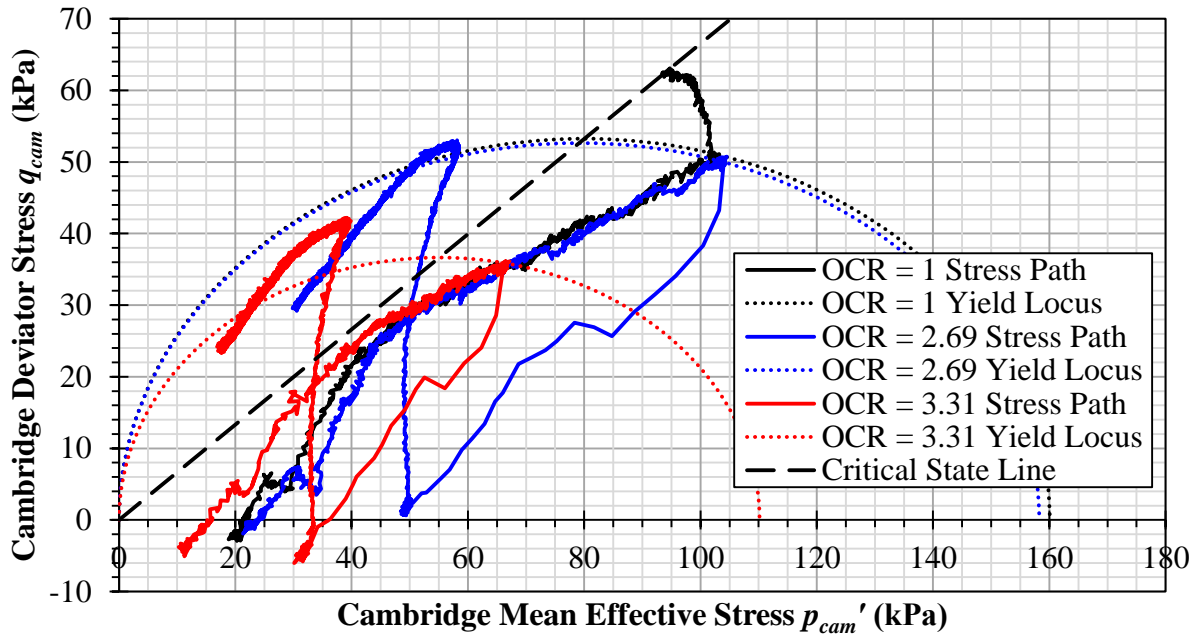


Figure 7.7: Cambridge stress paths and modified Cam clay predicted yield loci for tests performed on just kaolinite by OCR.

MIT stress paths, stress vs. strain curves, and excess pore water pressure during shear graphs are provided for the 0.0050  $R_{bm}$  mixtures in Figures 7.8, 7.9, and 7.10. Determination of SHANSEP constants is also shown in Figure 7.6 with values of 0.2548 for  $S$  and 0.8798 for  $m$  and a model  $R^2$  of 0.9999.

In general, the behavior of the guar gum and kaolinite mixtures was similar to the behavior of the kaolinite on its own. The normally consolidated shear strength of the 0.0050  $R_{bm}$  mixture was improved by 12.4%. This is demonstrated by the increase in the  $S$  constant. However, the improvement in shear strength due to overconsolidation was reduced.

One major deviation from the kaolinite only tests is the lack of decay in  $q$  as axial strain increases in Figure 7.9. This behavior was also predicted by Baudet and Stallebrass (2004) for a structured clay that strongly resists destructuring after reaching peak strength. This suggests that guar gum reinforces the structure of the kaolinite across the strains tested.

Stress paths for the kaolinite only, 0.0025  $R_{bm}$ , 0.0050  $R_{bm}$ , 0.0075  $R_{bm}$ , and 0.0100  $R_{bm}$  tests with OCR of approximately 2.7 are shown in Figure 7.11. Stress vs. strain curves for these same tests are shown in Figure 7.12. Figure 7.13 illustrates the excess pore water pressure during shear for these tests, as well.

Just as the highly linked clay-polymer network in 0.0050  $R_{bm}$  guar gum mixtures increased their consolidation stiffness (Nugent et al. 2011b), the triaxial tests show that the undrained shear strength of the 0.0050  $R_{bm}$  mixtures is increased by 12.5% for normally consolidated clay, 5.9% for 2.21 OCR clay, and 5.3% for 2.76 OCR clay when compared against the SHANSEP predicted strength of the kaolinite alone. Further, the  $C_c$  results from the triaxial tests reflect the same pattern of improvement demonstrated in Nugent et al. (2011b).

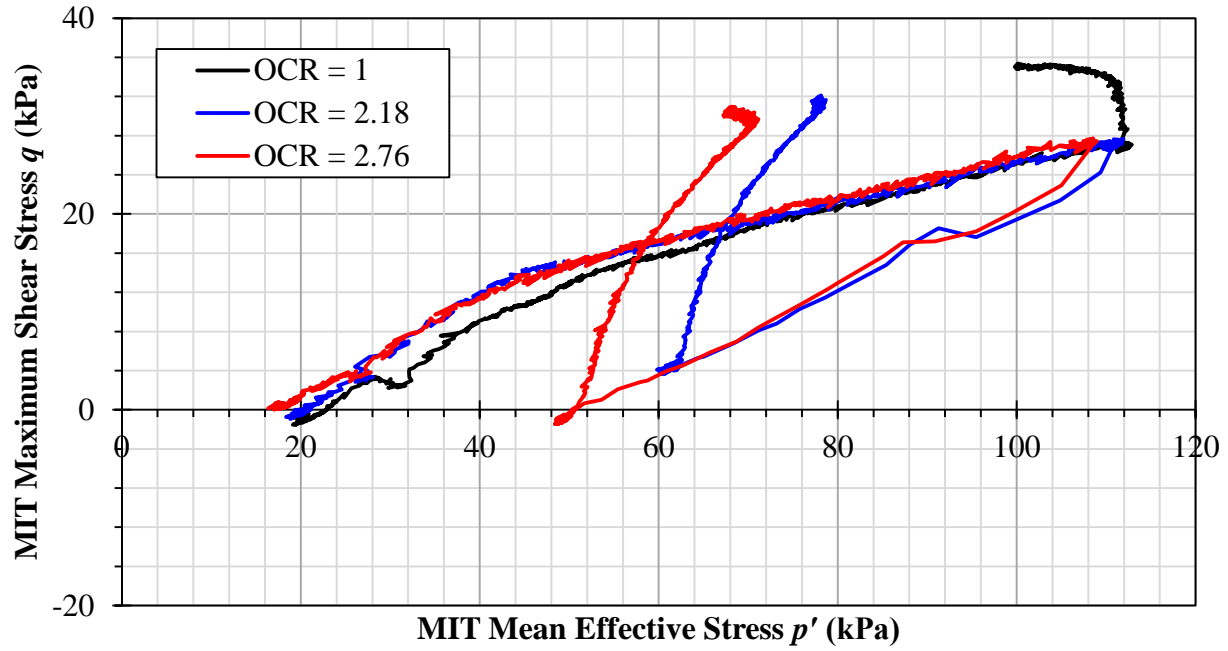


Figure 7.8: MIT stress paths for tests performed on 0.0050  $R_{bm}$  mixtures by OCR.

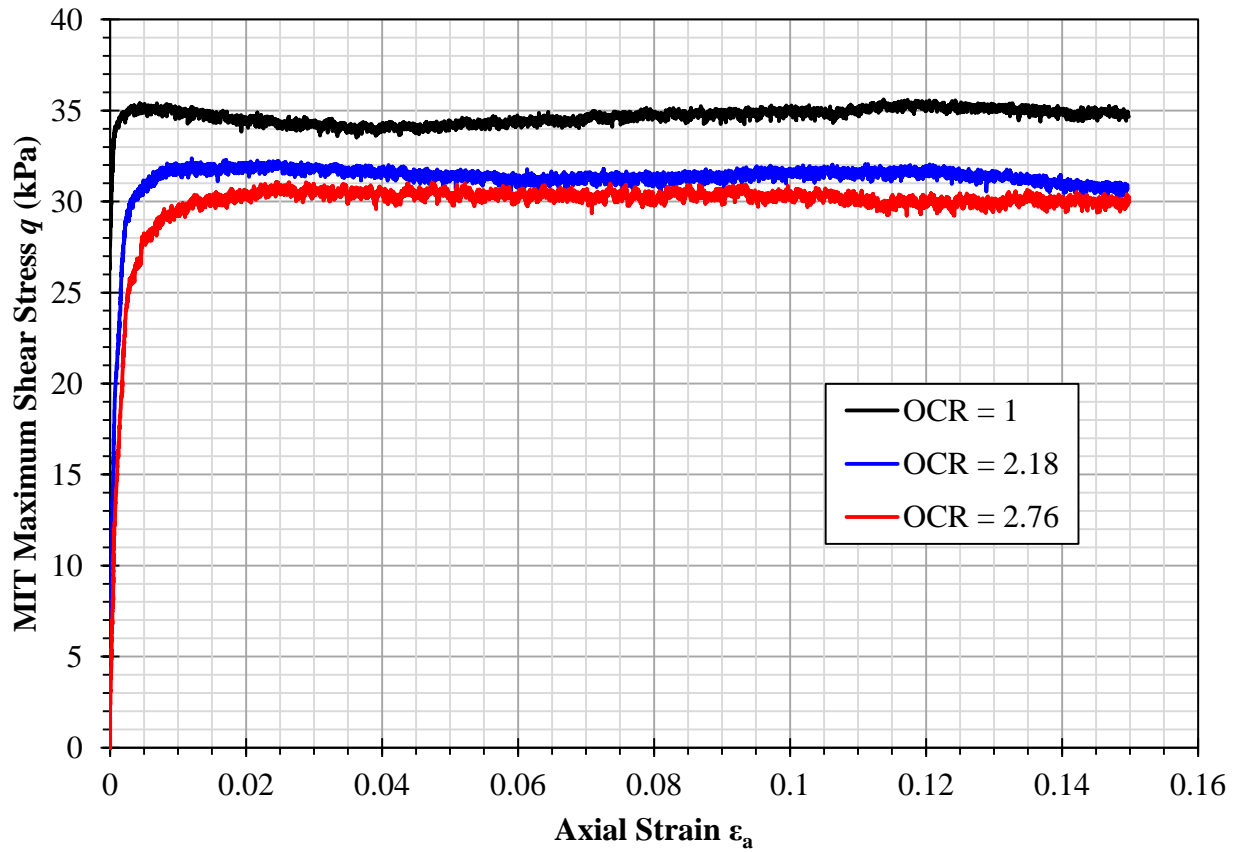
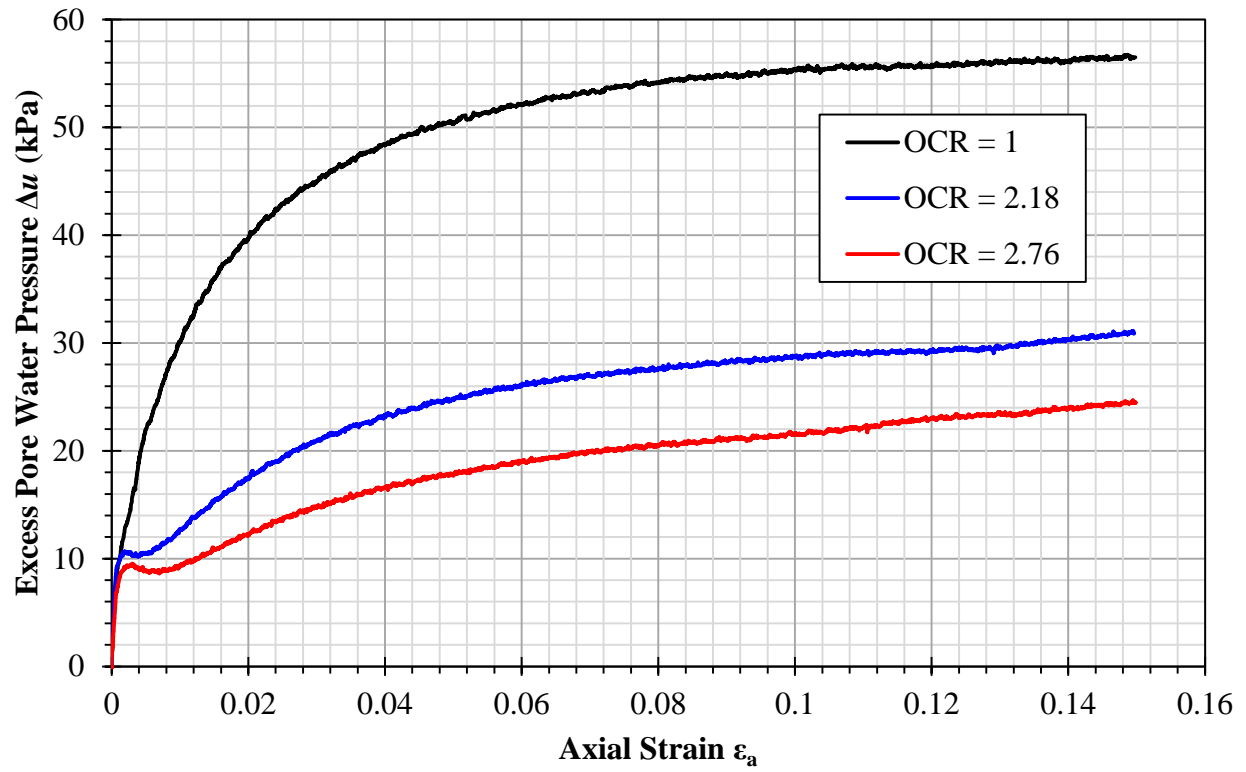
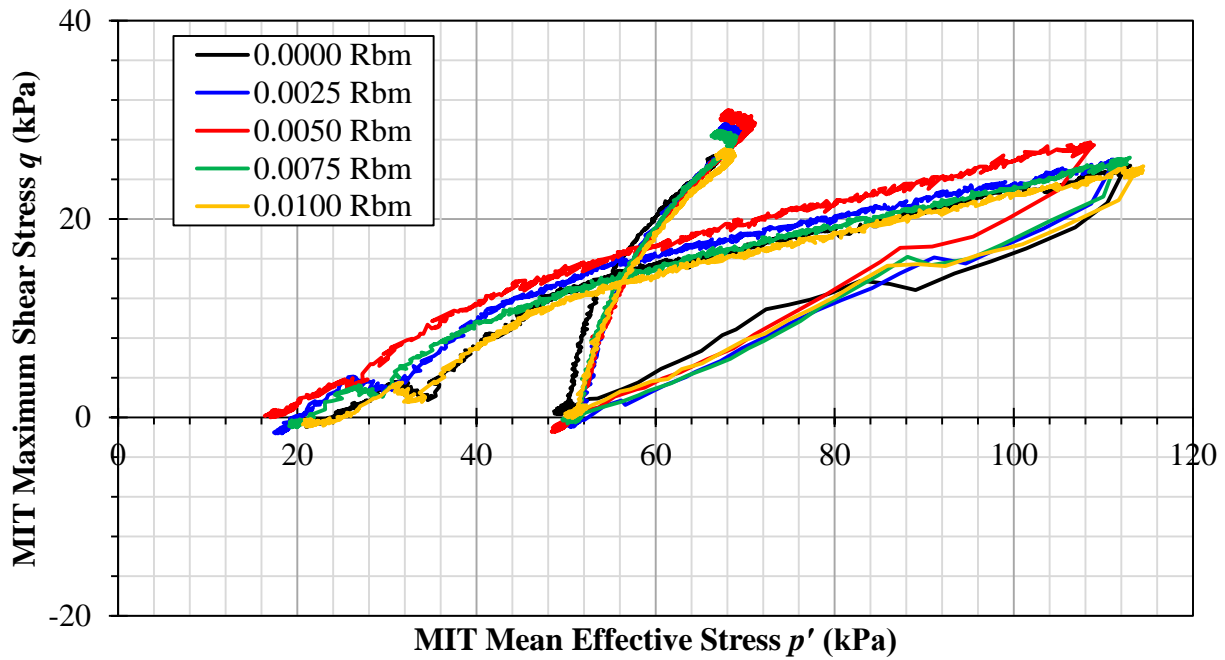


Figure 7.9: Stress vs. strain curves for tests performed on 0.0050  $R_{bm}$  mixtures by OCR.





**Figure 7.10: Excess pore water pressure during shear for tests performed on 0.0050  $R_{bm}$  mixtures by OCR.**



**Figure 7.11: MIT stress paths for tests performed on 2.7 OCR specimens by  $R_{bm}$ .**

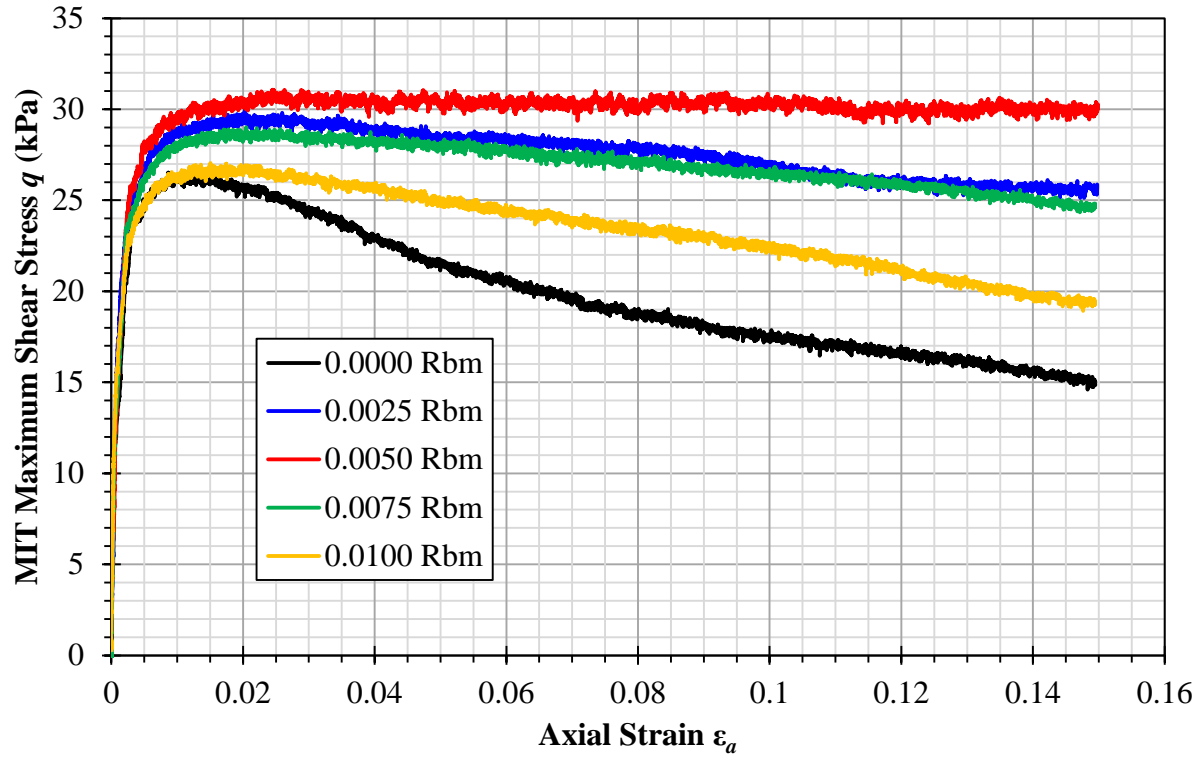


Figure 7.12: Stress vs. strain curves for tests performed on 2.7 OCR specimens by  $R_{bm}$ .

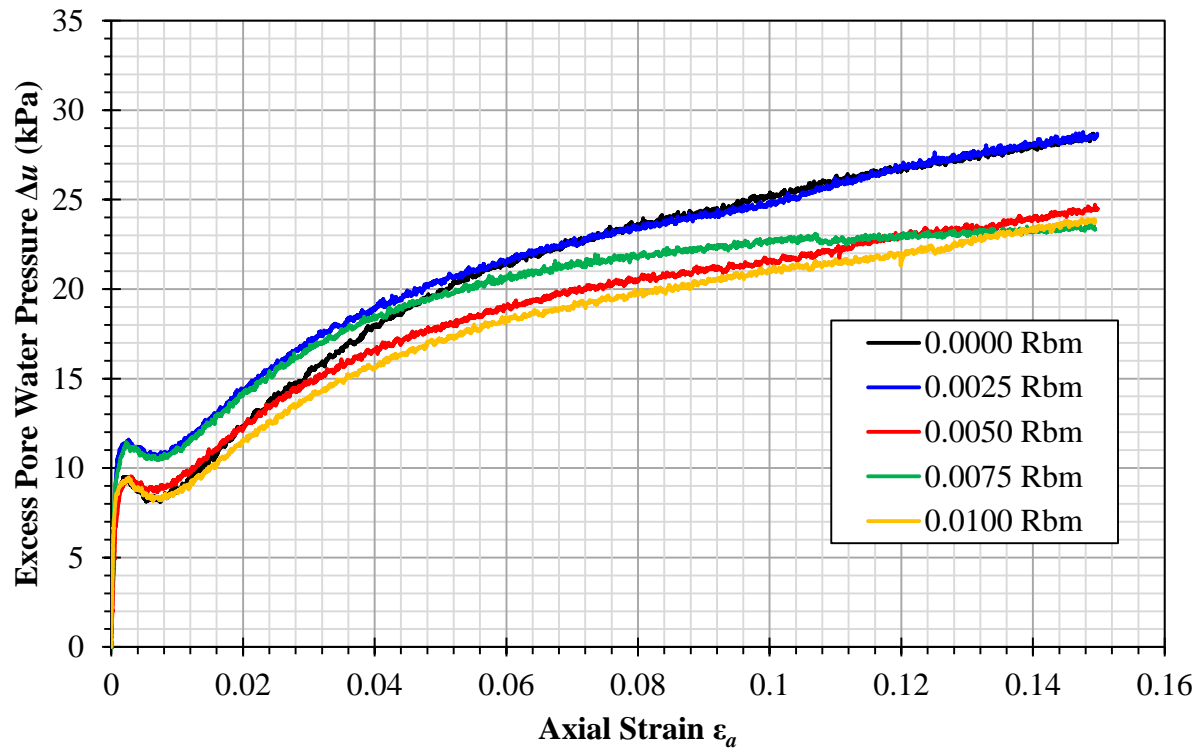


Figure 7.13: Excess pore water pressure during shear for tests performed on 2.7 OCR specimens by  $R_{bm}$ .

As suggested in Nugent et al. (2011b), at  $0.0050 R_{bm}$ , the guar gum should be able to establish hydrogen bonds between kaolinite particles that would otherwise not interact, raising the shear resistance of the mixture by acting as a kind of cement. However, as the guar gum concentration increases, strands of guar gum begin to displace kaolinite particles. As the shear resistance is largely the result of friction between clay particles in direct contact, replacing these direct kaolinite particle contact points with kaolinite to guar gum contacts appears to reduce the friction generated and the overall shear resistance. This is demonstrated by the 3.0% reduction in undrained shear strength of the  $0.0075 R_{bm}$  mixture and the 10.7% reduction of the  $0.0100 R_{bm}$  mixture when compared against the SHANSEP predicted strength of the kaolinite on its own.

Combining the improvement effect from hydrogen bonding with the detrimental effects of kaolinite particle displacement results in the downward inflected quadratic shape that is seen in Figure 7.14. When normalized based on the kaolinite only values,  $s_u/\sigma_{vo}'$  ratio and the inverse of  $C_c$  reflect a similar pattern of improvement due to the addition of guar gum. This pattern suggests that similar mechanisms are acting on both the stiffness and shear strength. However, further testing is needed to better develop the relationship.

The liquid limit results from Nugent et al. (2009) suggested that as the biopolymer concentration increases, the dynamic viscosity of the biopolymer solution in the clay pores increases, and the shear resistance of the mixture should increase, as well. However, this assertion is contradicted by the triaxial test results. Since the shear resistance of a viscous fluid is a function of the rate of strain, viscosity effects of the biopolymer solution become more important for rapidly applied loads. A Casagrande cup, which was used by Nugent et al. (2009) to measure liquid limits, applies rapid impact loads on fine-grained sediment, while the triaxial

tests applied a significantly slower rate of strain. This slower shearing made viscosity effects negligible.

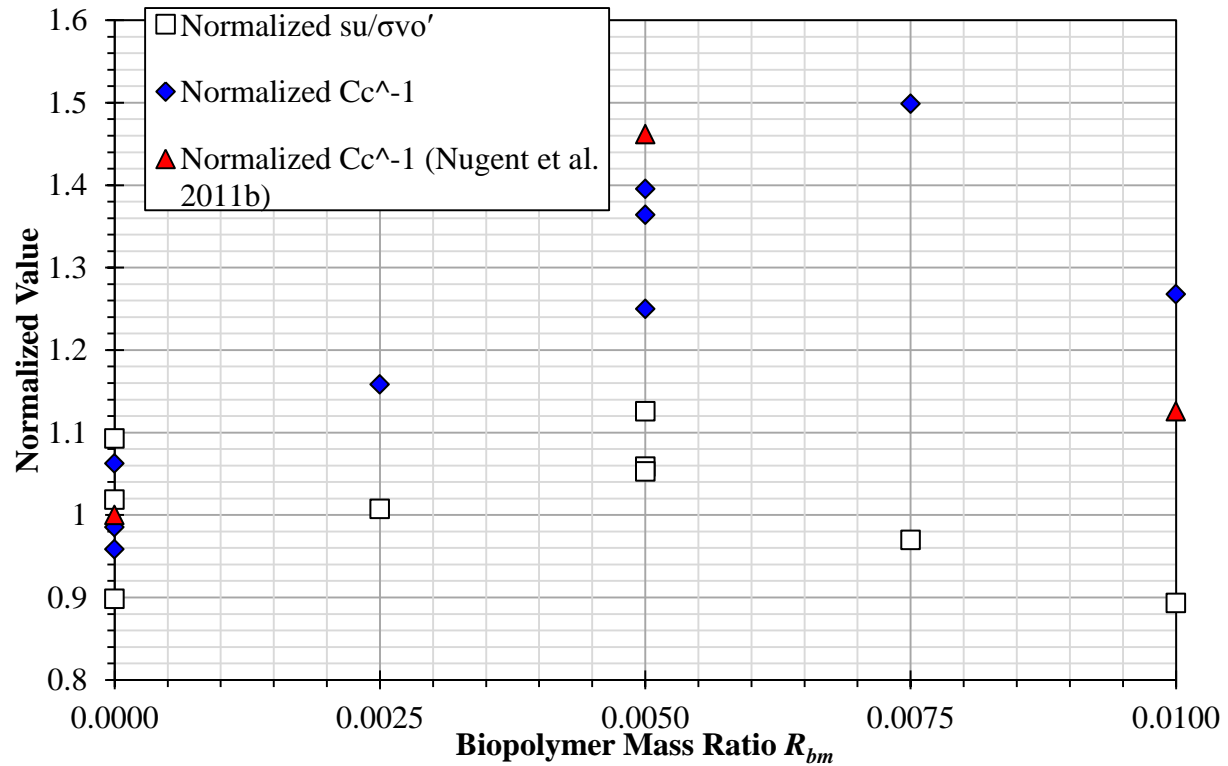


**Figure 7.14: Normalized  $C_c^{-1}$  and  $s_u/\sigma_{vo}'$  ratios vs. guar gum concentration. Three  $C_c^{-1}$  values are adapted from Nugent et al. (2011b).**

## 7.4 Practical Applications

Previous studies by Nugent et al. (2010; 2011a; 2011b) have shown that biopolymer amendment will improve the erosional resistance and reduce the compressibility of kaolinite. These studies suggest that guar gum added to hydraulically pumped dredged sediment could potentially improve resistance to erosion and subsidence in wetlands, while likely minimizing environmental damage. Guar gum's non-toxicity also allows plant growth that greatly stabilizes the soil (Wallace 1986). Results from this study demonstrate that undrained shear strength is also improved over the concentrations that reduce compressibility.

Further, the concentration that minimizes compressibility approximately corresponds with the concentration that maximizes improvement in the undrained shear strength. However, the improvement in shear strength was meager and comes at the cost of reducing the strength of the clay at high overconsolidation ratios. For the purpose of wetland restoration, guar gum concentrations that reduce subsidence will likely provide a small boost in the undrained shear strength of normally consolidated and lightly overconsolidated sediment. However, this improvement should be assumed to not occur in the interest of conservative design.

## **7.5 Conclusions**

In an effort to find the influence on undrained shear strength of a mixture caused by biopolymer and clay interactions, triaxial tests were performed on a kaolinite clay. This clay had differing concentrations of the EPS analogue guar gum, which is a plant polysaccharide that is electrostatically neutral. The following conclusions for guar gum and kaolinite mixtures can be made from the results of the tests:

- For normally consolidated and lightly overconsolidated material, kaolinite and guar gum form a hydrogen bonding network that at lower concentrations increases undrained shear strength by up to 12.5%.
- At higher guar gum concentrations, kaolinite particles are replaced with guar gum strands due to kaolinite particle displacement. This causes the reduction of shear resistance because the coefficient of friction between kaolinite and guar gum contacts are smaller than between kaolinite particle contacts. This reduction in shear resistance is greater than increases in shear resistance that is caused by hydrogen bonding at sufficiently high concentrations.

- Improvement in the undrained shear strength of the kaolinite and guar gum mixtures roughly follows the same trend of improvement in the compressibility of the mixtures with the concentrations of maximum improvement approximately corresponding for the two properties.

## **CHAPTER 8. EMPIRICAL MODELING OF THE IMPROVEMENT IN COMPRESSIBILITY AND UNDRAINED SHEAR STRENGTH DUE TO EXOPOLYMER ADDITION**

### **8.1 Introduction**

With the quantity of data provided by Chapters 5, 6, and 7, it is possible to develop an empirical model that ties together the results from the low concentration guar gum tests. Since it is the low concentration guar gum mixtures that consistently show improvement in stiffness and shear strength, the empirical behavior of these mixtures is of greatest interest to practicing engineers. This investigation involves combining previous  $C_c$ ,  $C_r$ ,  $S$ , and  $s_u/\sigma_{vo}'$  ratio values with additional  $C_c$ ,  $C_r$ , and  $S$  results to find relationships between the enhancement of stiffness and shear strength and the concentration of guar gum. The model produced will allow calculation of the optimum biopolymer concentration for soil improvement. It will also be possible to estimate the changes in hard and expensive to measure properties by using results from easier and cheaper tests.

### **8.2 Materials and Methods**

For the additional consolidation and direct shear tests, the kaolinite and guar gum that were described in Chapters 5, 6, and 7 were used. The procedures for the additional tests and the empirical modeling are described in the following sections.

#### **8.2.1 Consolidation Test Method**

Additional consolidation data were gathered to provide more points for the empirical model. The consolidation tests were performed primarily using the methods described in Sections 5.2.3 and 5.2.4. Concentrations of 0.0025, 0.0050, 0.0075, and 0.0100  $R_{bm}$  guar gum were used along with an extra kaolinite only test. A loading schedule of 23.94 kPa (500 psf), 47.88 kPa (1000 psf), 100 kPa (2088.6 psf), 191.52 kPa (4000 psf), 383.04 kPa (8000 psf),

191.52 kPa (4000 psf), 95.76 kPa (2000 psf), 191.52 kPa (4000 psf), 383.04 kPa (8000 psf), and 766.08 kPa (16000 psf) was used to determine both the normal compression index  $C_c$  and the recompression index  $C_r$ . Data for each load increment was analyzed using the log-time method.

### **8.2.2 Direct Shear Test Method**

Further additional data for the empirical model were collected by performing more direct shear tests. Again, the tests were largely performed according to the procedure described in Chapter 6. Four concentrations, kaolinite only,  $0.0025 R_{bm}$ ,  $0.0050 R_{bm}$ , and  $0.0075 R_{bm}$ , were tested.

For each concentration, the slurry was loaded into the direct shear machine and stiffened at 23.94 kPa (500 psf). Then it was consolidated to either 100 kPa (2088.6 psf), 119.70 kPa (2500 psf), 143.64 kPa (3000 psf), 167.58 kPa (3500 psf), or 191.52 kPa (4000 psf). Once the clay reached the end of primary consolidation, it was sheared as described in Section 6.2.1.

The kaolinite only and  $0.0050 R_{bm}$  mixture also had three additional runs. The kaolinite only had one extra test consolidated to 100 kPa (2088.6 psf) and two consolidated to 119.70 kPa (2500 psf). The  $0.0050 R_{bm}$  mixture also had one extra test consolidated to 100 kPa (2088.6 psf) and two consolidated to 167.58 kPa (3500 psf).

For each test, the undrained shear strength  $s_u$  was calculated. The SHANSEP model constant  $S$  was also calculated for each mixture.

### **8.2.3 Empirical Modeling Method**

Empirical relationships between the concentration of guar gum and the compressibility and shear strength of a kaolinite and guar gum mixture were created using Statistical Analysis Software (SAS). SAS can rapidly calculate many different forms of empirical equations, such as



linear, curvilinear, and polynomial. Also, SAS can test the terms that make up the equations for statistical significance.

Previous results from stiffness and shear strength testing suggested that there is a critical concentration where the improvement produced by guar gum is maximized. However, the compressibility results create a concave upwards curve, while the shear strength results produce a concave downwards curve. Because of this, the inverse of the normal compression index  $C_c^{-1}$  and the inverse of the recompression index  $C_r^{-1}$  were used in the model so that both types of results would be concave downwards.

Since the absolute values of the compressibility and shear strength data are quite different, they were normalized against the kaolinite only values. For the triaxial data sets, the average of the  $C_c$  and  $C_r$  for the kaolinite only tests was used for normalization of the consolidation data. The SHANSEP model was used to normalize the shear strength results. Values from the kaolinite only data for the consolidation and direct shear tests, described in Chapters 5 and 6, were used to normalize those previous test results, and the kaolinite only values from the additional tests were used for normalizing the new, additional data.

All of the results from just kaolinite tests were not averaged together since heterogeneities in the bulk kaolinite produce variance in the baseline kaolinite results. However, the improvement in the compressibility and shear strength of the kaolinite due to guar gum amendment is the primary interest and should be consistent regardless of the initial kaolinite response. Further, kaolinite heterogeneity effects are controlled over the course of a single test set. This is because the kaolinite for each test in a set comes from approximately the same location in the bulk kaolinite bucket.

A quadratic polynomial regression was used for model fitting, since it is the simplest model that reaches a maximum. Specifically, the following model was initially fitted:

$$Y = \beta_0 + \beta_1 R_{bm} + \beta_2 R_{bm}^2 + \beta_3 X_{Triaxial} + \beta_4 X_{Direct} \quad (\text{Eq. 8.1})$$

where  $Y$  is the normalized compressibility or shear strength value,  $R_{bm}$  is the guar gum concentration with an  $R_{bm}$  of 0 indicating kaolinite only,  $X_{Triaxial}$  is a flag variable that is 1 for triaxial tests and 0 for all other data,  $X_{Direct}$  is a flag variable that is 1 for direct shear data and 0 for other data, and  $\beta_0, \beta_1, \beta_2, \beta_3$ , and  $\beta_4$  are regression coefficients. The statistical significance of the overall model and the regressed coefficients was the main means of determining the strength of the model.

### 8.3 Results and Discussion

Table 8.1 contains the results of the additional consolidation and direct shear results. Figure 8.1 is the consolidation  $e$  versus  $\sigma_{vo}'$  graph, and Figure 8.2 is the direct shear  $s_u$  versus  $\sigma_{vo}'$  graph. Overall, the additional tests behave according to the same pattern of improvement that was described in Chapters 5, 6, and 7 with maximum improvement in the compressibility and shear strength occurring at 0.0050  $R_{bm}$ .

**Table 8.1: Additional test results for guar gum and kaolinite mixtures. Dash indicates that the value was not measured.**

$R_{bm}$	$C_c$	$C_r$	$C_c^{-1}$	$C_r^{-1}$	Normalized		$S$	Normalized $S$
					$C_c^{-1}$	$C_r^{-1}$		
0.0000	0.460	0.058	2.172	17.132	1.000	1.000	0.5227	1
0.0025	0.390	0.051	2.565	19.563	1.181	1.142	0.6062	1.159747465
0.0050	0.374	0.045	2.672	22.215	1.230	1.297	0.6484	1.240482112
0.0075	0.451	0.054	2.217	18.379	1.021	1.073	0.6131	1.172948154
0.0100	0.540	0.089	1.853	11.280	0.853	0.658	-	-

Results for the initial model described by Equation 8.1 are provided in Table 8.2. The residuals can be assumed to follow a normal distribution since the Shapiro-Wilk test has a

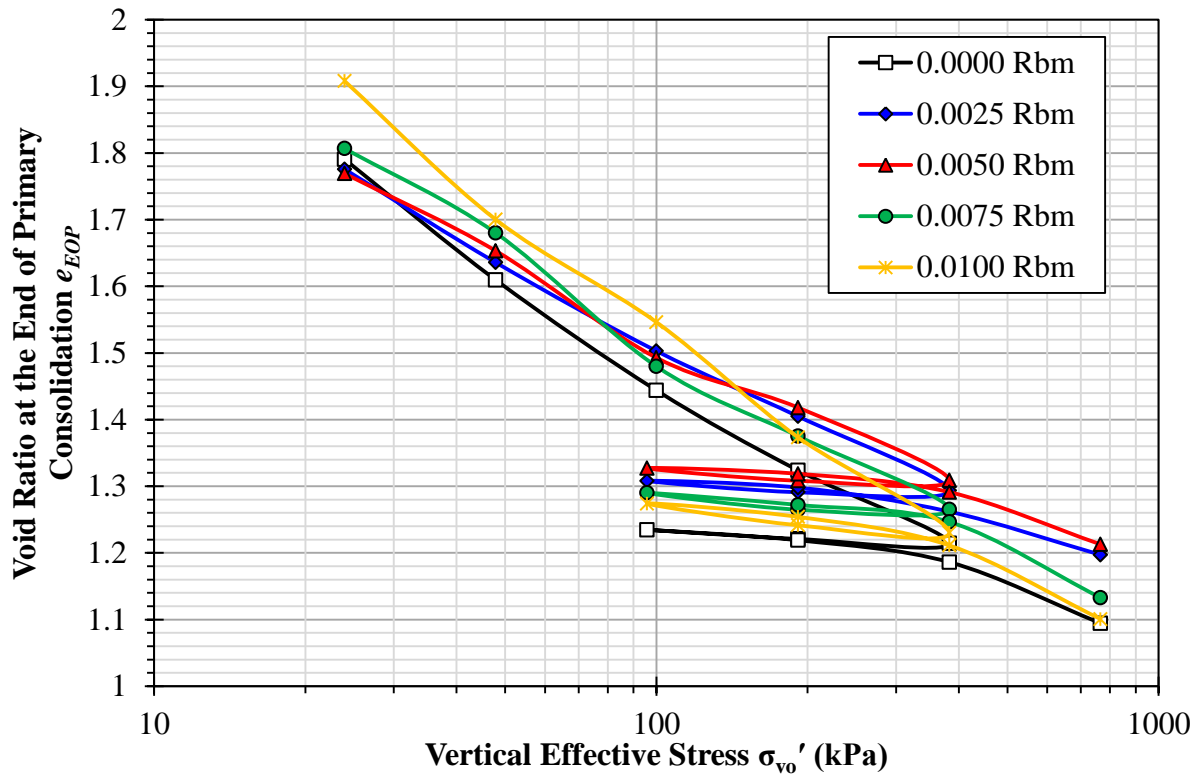


Figure 8.1: Void ratio vs. vertical effective stress for additional guar gum and kaolinite mixtures.

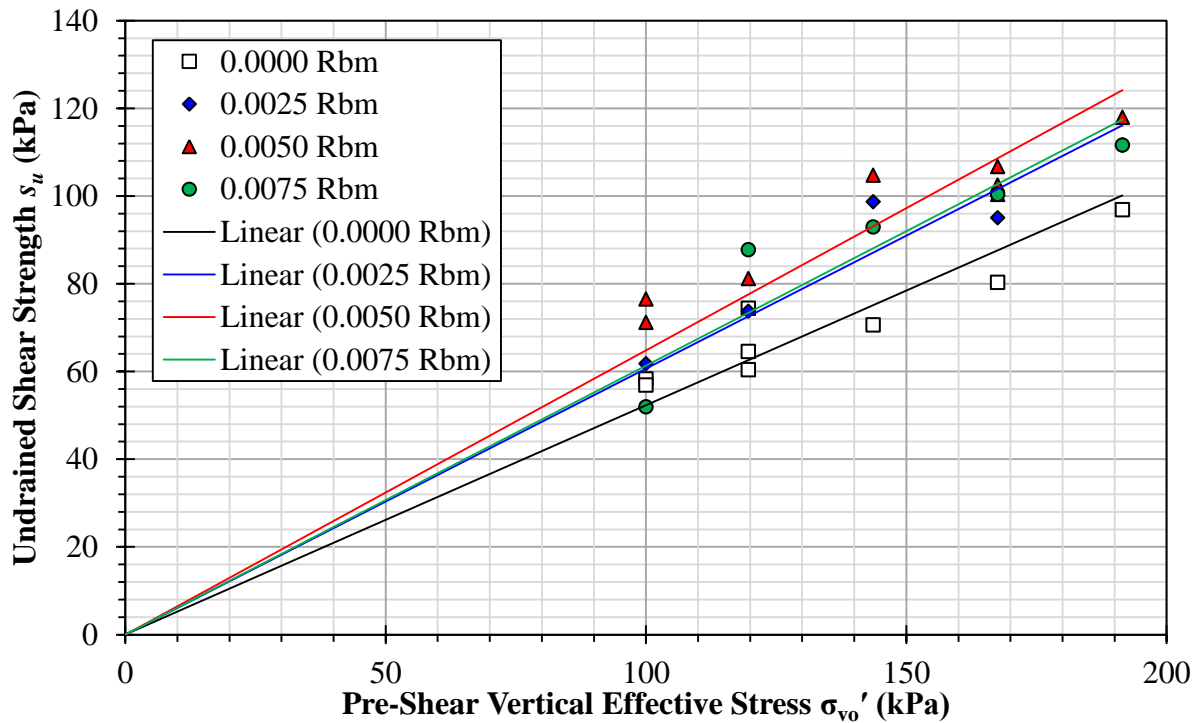


Figure 8.2: Undrained shear strength vs. pre-shear vertical effective stress for additional guar gum and kaolinite mixtures.

**Table 8.2: Results for the empirical models. D.F. stands for degrees of freedom, and dash means not applicable.**

	First Model (Eq. 8.1)			Second Model (Eq. 8.2)			Third Model (Eq. 8.3)		
	D.F.	Value	P-Value	D.F.	Value	P-Value	D.F.	Value	P-Value
$F$	4, 40	3.5	0.0153	3, 41	4.78	0.0060	2, 42	5.44	0.0079
$R^2$	-	0.2592	-	-	0.2591	-	-	0.2059	-
$\beta_0$	1	1.037	<.0001	1	1.0365	<.0001	1	1.01517	<.0001
$\beta_1$	1	65.83081	0.0024	1	65.82198	0.0021	1	65.65682	0.0026
$\beta_2$	1	-6959.81	0.0017	1	-6958.32	0.0015	1	-6866.59	0.0020
$\beta_3$	1	-0.09645	0.1038	1	-0.09595	0.0935	-	-	-
$\beta_4$	1	-0.00253	0.9686	-	-	-	-	-	-

p-value of 0.1426. Although the overall model p-value is 0.0153, the p-value of 0.9686 for  $\beta_4$  shows that the direct shear data does not follow a significantly different trend from the consolidation data. Thus,  $\beta_4$  was removed in order to make the following simplified model:

$$Y = \beta_0 + \beta_1 R_{bm} + \beta_2 R_{bm}^2 + \beta_3 X_{Triaxial} \quad (\text{Eq. 8.2})$$

For this second model, the residuals can be assumed to follow a normal distribution since the Shapiro-Wilk test has a p-value of 0.1360. A 0.0093 decrease in the  $F$  statistic p-value demonstrated that the model represented by Equation 8.2 is stronger overall compared to the initial model. Figure 8.3 graphs the second model against the data. Because the p-value for  $\beta_3$  was not very significant, it was also removed to produce the following third model:

$$Y = \beta_0 + \beta_1 R_{bm} + \beta_2 R_{bm}^2 \quad (\text{Eq. 8.3})$$

For this third model, the residuals can be assumed to follow a normal distribution since the Shapiro-Wilk test has a p-value of 0.5247. Removing  $\beta_3$  served to increase the  $F$  statistic p-value instead of decreasing it. When this is combined with the low, but not significant,  $\beta_3$  p-value, it appears that the triaxial data should have its own term in the model equation. Additional triaxial data would likely provide enough degrees of freedom to make  $\beta_3$  significant.

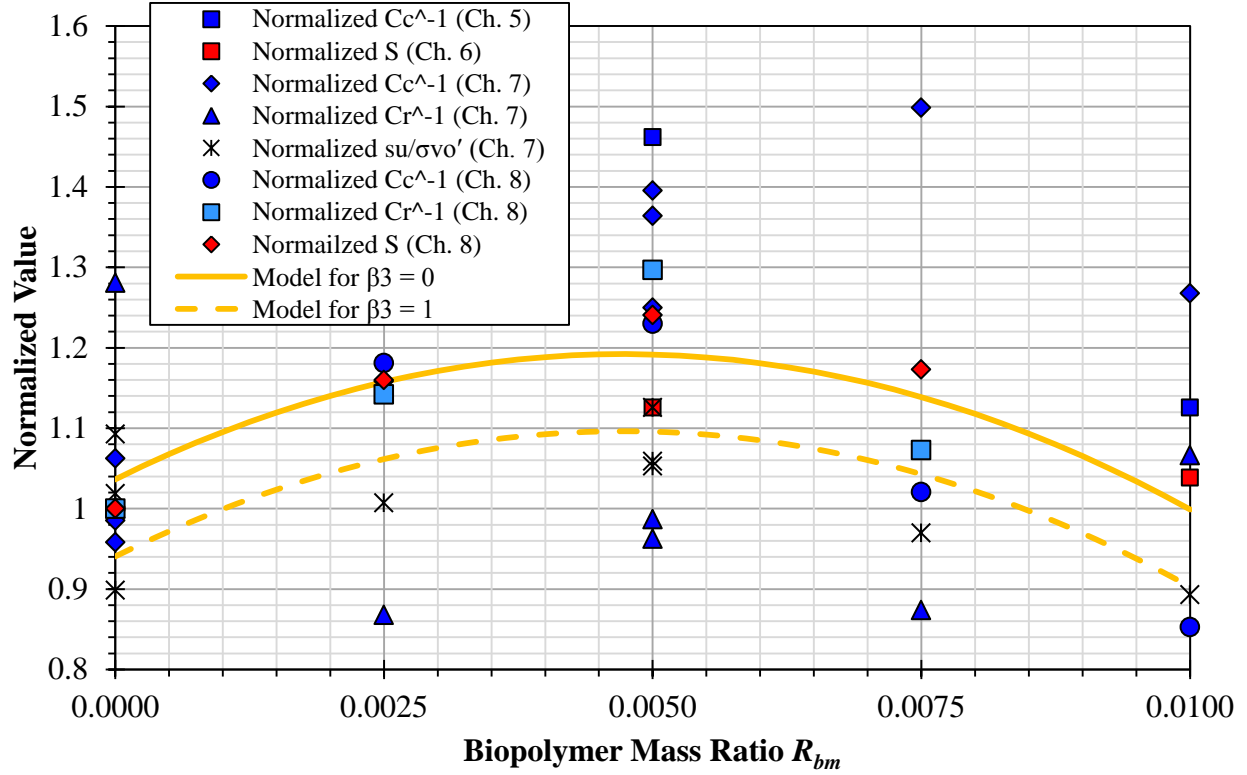


**Figure 8.3: Second empirical model plotted against all collected data.**

As model two is the most statistically significant of the models developed, it was selected as the final model. The maximum of the model occurs at 0.0047  $R_{bm}$ , which corresponds well with the maximum measured improvement occurring at 0.0050  $R_{bm}$  in the tests conducted. Predicted improvement in direct shear measured  $S$  and the inverse of compressibility at the model maximum is 19.22% with a standard deviation of 3.58%, and predicted improvement in the triaxial measured undrained shear strength at the model maximum is 9.62% with a standard deviation of 5.57%. Note that using the direct shear measured  $S$  as an estimate of the increase in the undrained shear strength is highly nonconservative.

The second model demonstrates two important relationships between the compressibility and shear strength of the kaolinite and guar gum mixtures. First, the maximum in the improvement in compressibility and shear strength occurs at the same guar gum concentration. In previous chapters, the mechanisms used to describe the changes in the compressibility and

shear strength of the mixtures were similar, so it stands to reason that these properties of the kaolinite and guar gum mixtures would be maximized at the same concentration. Second, the triaxial measured undrained shear strength will not be increased as much as the stiffness of the kaolinite and guar gum mixture. Thus, using consolidation data to predict the undrained shear strength of kaolinite and guar gum mixtures without correction will overestimate the amount of shear strength improvement.

#### **8.4 Practical Applications**

Performing a battery of triaxial tests to find the optimum concentration of guar gum for increasing undrained shear strength would be very expensive and time consuming. However, the empirical model developed in the previous section shows that the optimum concentration of guar gum can be determined through a set of 1D consolidation tests, although further testing is needed to validate this relationship for real sediments. 1D consolidation tests are faster and less expensive than triaxial tests, which makes locating the best concentration of guar gum more economical. Once the optimum concentration is found through the consolidation tests, triaxial tests can be performed on mixtures with this concentration to calculate the improvement of the undrained shear strength, or the normalized change in shear strength could be calculated by reducing the normalized change in the inverse of compressibility by 0.0962, as suggested by the model.

On the other hand, assuming that the shear strength is unchanged is more conservative. It is also a better choice given the high variance of the results and meager improvement in shear strength demonstrated in the triaxial results. Although direct shear tests can be used to get the optimum concentration, the increase in shear strength measured by direct shear tests is very nonconservative compared to values measured by triaxial tests.

Based on the model developed, the following procedure for finding the optimum concentration is recommended:

1. Run consolidation tests on a set of mixtures with 0.000, 0.002, 0.004, 0.006, 0.008, and 0.010  $R_{bm}$  guar gum.
2. Plot  $C_c$  versus  $R_{bm}$  and check that the points form a minimum within the range of concentrations tested. If the points do not reach a minimum, run additional tests on mixtures with higher concentrations until a minimum is found.
3. Fit a quadratic regression equation to the points in the plot made in step two. Calculate the minimum of this equation to find the optimum concentration.
4. Perform additional consolidation tests at and around this optimum concentration, if desired.

## 8.5 Conclusions

An empirical model that describes the relationship between normalized  $C_c^{-1}$ ,  $C_r^{-1}$ , direct shear calculated  $S$ , and  $s_u/\sigma_{vo}'$  ratio values from triaxial tests was determined for low concentration guar gum and kaolinite mixtures. Low concentration guar gum mixtures were the focus because practicing engineers would be most interested in the empirical behavior of clay and biopolymer mixtures that produce improvements in compressibility and shear strength.

Based on the empirical model developed, the following conclusions can be made:

- A quadratic regression equation readily fits the pattern of improvement in compressibility and shear strength created by guar gum at low concentrations.
- Both the compressibility and shear strength reach a maximum in improvement at the same guar gum concentration.

- Compressibility and shear strength have the same optimum concentration because the same mechanisms act on both.
- The 9.62% normalized improvement in the undrained shear strength at the optimum guar gum concentration is not as great as the 19.22% normalized improvement in the inverse of compressibility. Assuming the improvement in undrained shear strength will be the same as the improvement in compressibility will result in significant nonconservative errors.



## CHAPTER 9. CONCLUSIONS AND RECOMMENDATIONS

### 9.1 Conclusions

Casagrande cup, CSM, 1D consolidation, direct shear, and triaxial tests were performed on mixtures of kaolinite and two exopolymer analogues. These were guar gum, a neutral plant derived biopolymer, and xanthan gum, a negatively charged bacterial exopolymer. To perform these tests, methods for mixing and storing kaolinite and biopolymer mixtures were developed, and biopolymer mass ratio, or  $R_{bm}$ , was created to usefully describe the concentration of clay and biopolymer mixtures. SHANSEP and empirical models were applied to the results from previous tests. From this work, the following overall conclusions can be made:

- Guar gum forms an extensive hydrogen bonding network when mixed with kaolinite. This hydrogen bonding network induces the improvement that is seen in compressibility, shear strength, and erosional resistance.
- Although xanthan gum possesses the hydroxyl groups needed to form an extensive hydrogen bonding network, its negative charge repels negatively charged kaolinite particles and prevents the formation of a hydrogen bonding network in cation poor environments. As a result, kaolinite and xanthan gum mixtures without background cations do worse than kaolinite and guar gum mixtures in the tests performed.
- Adding background cations to xanthan gum and kaolinite mixtures balances electrostatic repulsion and can create cross-links. Substantial increases in liquid limits and erosional resistance result, compared to xanthan gum and kaolinite mixtures without background cations.
- For tests that rapidly deform kaolinite and biopolymer mixtures, such as Casagrande cup and CSM tests, increases in pore fluid viscosity result in increases in liquid limits and

erosional resistance because a rise in the pore fluid viscosity provides an improvement in the shear resistance of the pore fluid, and this leads to greater shear resistance of the overall material.

- Other tests that involve very slow deformation, like 1D consolidation, direct shear, and triaxial tests, do not display a significant pore fluid viscosity effect. Since fluid shear resistance is a function of both viscosity and the strain rate, tests that create rapid movement cause a significant viscous resistance effect.
- Tests with slow strain also show reductions in stiffness and shear strength at high biopolymer concentrations due to biopolymer displacement of kaolinite.
- Normalized improvement in the shear strength and the inverse of compressibility of low concentration guar gum and kaolinite mixtures both form concave down parabolas when plotted against biopolymer concentration. The maximums of these parabolas occur at the same biopolymer concentration because the same mechanisms act on both compressibility and shear strength.

## **9.2 Practical Applications**

Subsidence and erosion are major threats to Louisiana wetlands. Hydraulically pumped dredging is a common way to rebuild wetlands lost, but hydraulically pumped dredged sediment lacks the plant growth that provides significant improvement in erosional resistance and shear strength when initially deposited. The biopolymers tested in this dissertation are both able to significantly increase erosional resistance of kaolinite, and guar gum was demonstrated to be able to reduce compressibility and increase the undrained shear strength of both normally consolidated and lightly overconsolidated kaolinite. Thus, guar gum and xanthan gum that are

added to hydraulically pumped dredged sediment have the potential to improve resistance to erosion in wetlands, and guar gum is likely to reduce subsidence.

Both of these biopolymers are non-toxic, so they should not prevent plant growth that produces significant and long-term erosional resistance, and they should not have significant negative effects on wildlife. However, additional testing on real wetland sediments is needed to confirm the benefits suggested by this study. Even if the biopolymers degrade and do not produce long-term improvement, stabilizing the sediment in the short term to allow plants to establish themselves will increase the efficiency of marsh restoration efforts. Both biopolymers can easily be added to the sediment through a hydraulic dredge's slurry pump, where it can be completely mixed with the sediment by the turbulence of the slurry output pipe.

While the greatest improvement in compressibility and undrained shear strength occur at a relatively low concentration of guar gum, the greatest improvement in erosional resistance occurs at a high concentration. During dredging, the concentration of guar gum added could be kept low until the deposit area is almost filled. Guar gum concentration could then be increased to provide a high erosional resistance surface layer that protects the rest of the sediment from erosive flows.

### **9.3 Recommendations for Future Research**

Although the results for kaolinite provide a starting point for studying how exopolymers change the compressibility and shear strength of clays, there is still plenty of additional research needed. Investigating how exopolymers effect field collected wetland sediment would provide better estimates for the amount of improvement in compressibility and shear strength that could be produced in the field. Repeating the tests in this dissertation on other clays, such as bentonite, and on other biopolymers, such as chitosan, would help fill in the range of exopolymer and clay

interactions. These additional tests on other clays should especially focus on material representative of coastal sediments. Running 1D consolidation, direct shear, and triaxial tests on xanthan gum and kaolinite mixtures with background cations would also produce results that would better match the results expected for field application, since natural sediments would not be as cation poor as pure kaolinite mixed with DI water. Testing the speculative mechanisms proposed would reinforce the science behind the effects described in this work and pave the way towards developing theoretical models that describe exopolymer effects on compressibility and shear strength.

## REFERENCES

- Alkan, M., Demirbas, O., and Dogan, M. (2005). "Electrokinetic properties of kaolinite in mono- and multivalent electrolyte solutions." *Microporous and Mesoporous Materials*, 83(1-3), 51-59.
- Aslan, A. and Autin, W. (1998). "Holocene flood-plain soil formation in the southern lower Mississippi Valley: Implications for interpreting alluvial paleosols." *Geological Society of America Bulletin*, 110(4), 433-449.
- ASTM – American Society for Testing and Materials (2006). *Annual Book of ASTM Standards*, 04.08.
- de Baets, S., Poesen, J., Knapen, A., and Galinda, P. (2007). "Impact of Root Architecture on the Erosion-Reducing Potential of Roots during Concentrated Flow." *Earth Surface Processes and Landforms*, 32(9), 1323-1345.
- Baudet, B., and Stallebrass, S. (2004). "A constitutive model for structured clays." *Géotechnique*, 54(4), 269-278.
- Bolz, R. E., and Tuve, G. L. (1973). *Handbook of Tables for Applied Engineering Science*. CRC Press, Inc., Cleveland.
- Bruice, P. Y. (2004). *Organic Chemistry*. 4<sup>th</sup> ed., Pearson Education, Inc., Upper Saddle River, NJ.
- Budhu, M. (2000). *Soil Mechanics and Foundations*. W. Anderson, ed., John Wiley and Sons, Inc., Hoboken, NJ.
- Burland, J. B. (1990). "On the compressibility and shear strength of natural clays." *Géotechnique*, 40(3), 329-378.
- Çabalar, A. F., and Çanakci, H. (2005). "Ground Improvement by Bacteria." *Poromechanics – Biot Centennial (1905-2005)*. Abousleiman, Cheng, and Ulm, eds., Taylor and Francis Group, London, England, 707-712.
- Chandler, R. J. (2000). "Clay sediments in depositional basins: The geotechnical cycle." *Quarterly Journal of Engineering Geology and Hydrogeology*, 33, 7-39.
- Cheng, Y., Prud'homme, R. K., Chik, J., and Rau, D. C. (2002). "Measurement of forces between galactomannan polymer chains: Effect of hydrogen bonding." *Macromolecules*, 35(27), 10155-10161.
- Chenu, C., and Guérif, J. (1991). "Mechanical Strength of Clay Minerals as Influenced by an Adsorbed Polysaccharide." *Soil Science Society of America Journal*, 55(4), 1076-1080.

- Crowe, C. T., Elger, D. F., and Roberson, J. A. (2001). *Engineering Fluid Mechanics*. 7<sup>th</sup> ed., John Wiley and Sons, Inc., NY.
- Dade, W., Davis, J. D., Nichols, P. D., Nowell, A. R. M., Thistle, D., Trexler, M. B., and White, D. C. (1990). "Effects of Bacterial Exopolymer Adhesion on the Entrainment of Sand." *Geomicrobiology Journal*, 8(1), 1-16.
- Dontsova, K. M., and Bigham, J. M. (2005). "Anionic Polysaccharide Sorption by Clay Minerals." *Soil Science Society of America Journal*, 69(4), 1026-1035.
- Fischetti, M. (2001). "Drowning New Orleans." *Scientific American*, 285(4), 76-85.
- Flick, E. W. (1989). *Handbook of Adhesives Raw Materials*. 2<sup>nd</sup> ed., Noyes Publ., Park Ridge, NJ.
- Garrels, R. M. (1951). *A Textbook of Geology*, Harper, New York.
- Gerbersdorf, S. U., Jancke, T., and Westrich, B. (2007). "Sediment properties for assessing the erosion risk of contaminated riverine sites." *Journal of Soils and Sediments*, 7(1), 25-35.
- Goldberg, S., and Glaubig, R. A. (1987). "Effect of Saturating Cation, pH, and Aluminum and Iron Oxide on the Flocculation of Kaolinite and Montmorillonite." *Clay and Clay Minerals*, 35(3), 220-227.
- Goycoolea, F. M., Morris, E. R., and Gidley, M. J. (1995). "Viscosity of galactomannans at alkaline and neutral pH - evidence of hyperentanglement in solution." *Carbohydrate Polymers*, 27(1), 69-71.
- Guanghui, M. (2010). "The Strength and Deformation Behavior of a Residual Soil in Singapore." Ph.D. thesis, Nanyang Technological Univ., Nanyang, Singapore.
- Hassler, R. A., and Doherty, D. H. (1990). "Genetic Engineering of Polysaccharide Structure: Production of Variants of Xanthan Gum in *Xanthomonas campestris*." *Biotechnology Program*, 6(3), 182-187.
- Hernandez, M. E., and Mitsch, W. J. (2007). "Denitrification potential and organic matter as affected by vegetation community, wetland age, and plant introduction in created wetlands." *Journal of Environmental Quality*, 36(1), 333-342.
- Hunter, R. J. (1981). *Zeta Potential in Colloid Science: Principles and Applications*, Academic Press, London.
- Ivanov, V., and Chu, J. (2008). "Applications of Microorganisms to Geotechnical Engineering for Bioclogging and Biocementation of Soil in Situ." Review in *Environmental Science and Technology*, 7(2), 139-153.

- Ladd, C. C., and Foott, R. (1974). "New design procedure for stability of soft clays." *Journal of Geotechnical Engineering Division*, 100, 763-786.
- Li, S. Z., and Xu, R. K. (2008). "Electrical double layers' interaction between oppositely charged particles as related to surface charge density and ionic strength." *Colloids and Surfaces A-Physicochemical and Engineering Aspects*, 326(3), 157-161.
- Ma, C., and Eggleton, R. A. (1999). "Cation exchange capacity of kaolinite." *Clays and Clay Minerals*, 47(2), 174-180.
- Ma, X., and Pawlik, M. (2007). "Role of Background Ions in Guar Gum Adsorption on Oxide Minerals and Kaolinite." *Journal of Colloid and Interface Science*, 313, 440-448.
- Maier, R. M., Pepper, I. L., and Gerba, C. P. (2000). *Environmental Microbiology*. Academic Press, San Diego.
- Martin, G. R., Yen, T. F., and Karimi, S. (1996). "Application of Biopolymer Technology in Silty Soil Matrices to Form Impervious Barriers." *7<sup>th</sup> Australia New Zealand Conference on Geomechanics: Geomechanics in a Changing World: Conference Proceedings*. M. B. Jaksa, W. S. Kaggwa, and D. A. Cameron, eds., Barton, ACT: Institution of Engineers, Australia, National Conference Publ. 96/07, 814-819.
- Milas, M., Rinaudo, M., and Tinland, B. (1985). "The Viscosity Dependence on Concentration, Molecular Weight and Shear Rate of Xanthan Solutions." *Polymer Bulletin*, 14(2), 157-164.
- Mitchell, J. K., and Santamarina, J. C. (2005). "Biological Considerations in Geotechnical Engineering." *Journal of Geotechnical and Geoenvironmental Engineering*, 131(10), 1222-1233.
- Mitchell, J. K., and Soga, K. (2005). *Fundamentals of Soil Behavior*, 3<sup>rd</sup> ed., John Wiley & Sons, Inc., Hoboken, New Jersey.
- Nugent, R. A., Zhang, G., and Gambrell, R. P. (2009). "Effect of Exopolymers on the Liquid Limit of Clays and Its Engineering Implications." *Transportation Research Board: Journal of the Transportation Research Board*, 2101, 34-43.
- Nugent, R. A., Zhang, G., and Gambrell, R. P. (2010). "The Effect of Exopolymers on the Erosional Resistance of Cohesive Sediments." *Proc., 5<sup>th</sup> International Conference on Scour and Erosion*, ASCE, San Francisco, CA, 162-171.
- Nugent, R. A., Zhang, G., and Gambrell, R. P. (2011a). "The Effect of Exopolymers and Void Ratio on the Erosional Resistance of Cohesive Sediments." *Proc., Geo-Frontiers 2011*, ASCE, Dallas, TX, in press.

- Nugent, R. A., Zhang, G., and Gambrell, R. P. (2011b). "The Effect of Exopolymers on the Compressibility of Clays" *Proc., Geo-Frontiers 2011*, ASCE, Dallas, TX, in press.
- Ouhadi, V. R., and Goodarzi, A. R. (2006). "Assesment of the Stability of a Dispersive Soil Treated by Alum." *Engineering Geology*, 85, 91-101.
- Parker, G. G., and Jenne, E. A. (1967). "Structural failure of western U. S. highways caused by piping." *46<sup>th</sup> Annual Meeting of the Highway Research Board*. U. S. Geological Survey, Water Resources Division, WA.
- Phillips, G. O., and Williams, P. A. (2000). *Handbook of Hydrocolloids*. Woodhead Publishing Limited, Cambridge, England.
- Plummer, C. C., McGeary, D., and Carlson, D. H. (2003). *Physical Geology*. 9<sup>th</sup> ed., McGraw-Hill, NY.
- Podsiadlo, P., Kaushik, A. K., Arruda, E. M., Waas, A. M., Shim, B. S., Xu, J. D., Nandivada, H., Pumplin, B. G., Lahann, J., Ramamoorthy, A., and Kotov, N. A. (2007). "Ultralong and Stiff Layered Polymer Nanocomposites." *Science*, 318, 80-83.
- Rao, M. A. (2007). *Rheology of Fluid and Semisolid Foods: Principles and Applications*. 2<sup>nd</sup> ed., Springer Science + Business Media, NY.
- Reddi, L. N., and Bonala, M. V. S. (1997). "Critical Shear Stress and Its Relationship with Cohesion for Sand-Kaolinite Mixtures." *Canadian Geotechnical Journal*, 34, 26-33.
- Risica, D., Dentini, M., and Crescenzi, V. (2005). "Guar Gum Methyl Ethers, Part I. Synthesis and Macromolecular Characterization." *Polymer*, 46(26), 12247-12255.
- Roscoe, K. H., and Burland, J. B. (1968). "On the generalized stress-strain behavior of 'wet' clay." *Engineering Plasticity*, 535-609.
- Sandford, P. A., Cottrell, I. W., and Pettitt, D. J. (1984). "Microbial Polysaccharides: New Products and Their Commercial Applications." *Pure and Applied Chemistry*, 56(7), 879-892.
- Sharma, B., and Bora, P. K. (2003). "Plastic Limit, Liquid Limit and Undrained Shear Strength of Soil – Reappraisal." *Journal of Geotechnical and Geoenvironmental Engineering*, 129(8), 774-777.
- Sherard, J. L., Decker, R. S., and Ryka, N. L. (1972). "Piping in earth dams of dispersive clay." *American Society of Civil Engineers, Soil Mechanics and Foundation Conference*. Purdue University, Lafayette, IN, June 12-14.
- Sjötröm, E. (1993). *Wood Chemistry: Fundamentals and Applications*. Academic Press, San Diego.



- Sutherland, I. W. (2001). "Exopolysaccharides in biofilms, flocs and related structures." *Water Science and Technology*, 43(6), 77-86.
- Sutherland, I. W. (1994). "Structure-Function Relationships in Microbial Exopolysaccharides." *Biotech Advances*, 12(2), 393-448.
- Tengbeh, G. T. (1993). "The Effect of Grass Roots on Shear Strength Variations with Moisture Content." *Soil Technology*, 6(3), 287-295.
- Tolhurst, T. J., Black, K. S., Shayler, S. A., Mather, S., Black, I., Baker, K., and Paterson, D. M. (1999). "Measuring the *in situ* Erosion Shear Stress of Intertidal Sediments with the Cohesive Strength Meter (CSM)." *Estuarine, Coastal and Shelf Science*, 49, 281-294.
- Tombácz, E., and Szekeres, M. (2006). "Surface charge heterogeneity of kaolinite in aqueous suspension in comparison with montmorillonite." *Applied Clay Science*, 34 (1-4 SI), 105-124.
- Tomqvist, T. E., Wallace, D. J., Storms, J. E. A., Wallinga, J., Van Dam, R. L., Blaauw, M., Derksen, M. S., Klerks, C. J. W., Meijneken, C., and Snijders, E. M. A. (2008). "Mississippi Delta Subsidence Primarily Caused by Compaction of Holocene Strata." *Nature Geoscience*, 1(3), 173-176.
- Trhlíková, J., Mašín, D., and Boháč, J. (2009). "Modelling of cementation bonds in clay – laboratory and numerical model." *Proceedings of the 17<sup>th</sup> International Conference on Soil Mechanics and Geotechnical Engineering*, 151-154.
- U. S. Department of Agriculture (2007). *The Encyclopedia of Wood*. Skyhorse Publishing, Inc., NY.
- Wallace, A. (1986). "A Pollysaccharide (Guar) as a Soil Conditioner." *Soil Science*, 141(5), 371-373.
- Wang, Y. H., and Xu, D. (2007). "Dual Porosity and Secondary Consolidation." *Journal of Geotechnical and Geoenvironmental Engineering*, 133(7), 793-801.
- Wardhana, K., and Hadipriono, F. C. (2003). "Analysis of Recent Bridge Failures in the United States." *Journal of Performance of Constructed Facilities*, 17(3), 144-150.
- Watts, C. W., Tolhurst, T. J., Black, K. S., and Whitmore, A. P. (2003). "In situ measurements of erosion shear stress and geotechnical shear strength of the intertidal sediments of the experimental managed realignment scheme at Tollesbury, Essex, UK." *Estuarine, Coastal and Shelf Science*, 58, 611-620.
- Whistler, R. L., and Smart, C. L. (1953). *Polysaccharide Chemistry*. Academic Press, NY, NY.

- Whitcomb, P. J., Gutowski, J., and Howland, W. W. (1980). "Rheology of Guar Solutions." *Journal of Applied Polymer Science*, 25(12), 2815-2827.
- Widdows, J., Brinsley, M. D., Pope, N. D., Staff, F. J., Bolam, S. G., and Somerfield, P. J. (2006). "Changes in Biota and Sediment Erodability Following the Placement of Fine Dredged Material on Upper Intertidal Shores of Estuaries." *Marine Ecology Progress Series*, 319(1), 27-41.
- World Health Organization (1987). "Toxicological evaluation of certain food additives and contaminants." *WHO Food Additives Series*, No. 21, Cambridge University Press, Cambridge.
- World Health Organization (1975). "Toxicological evaluation of some food colours, thickening agents, and certain other substances." *WHO Food Additives Series*, No. 8, Geneva.
- Yallop, M. L., Paterson, D. M., and Wellsbury, P. (2000). "Interrelationships between Rates of Microbial Production, Exopolymer Production, Microbial Biomass, and Sediment Stability in Biofilms of Intertidal Sediments." *Microbial Ecology*, 39(2), 116-127.
- Zentar, R., Abriak, N.-E., and Dubois, V. (2009). "Fall Cone Test to Characterize Shear Strength of Organic Sediments." *Journal of Geotechnical and Geoenvironmental Engineering*, 135(1), 153-157.
- Zhang, G., Germaine, J. T., Whittle, A. J., and Ladd, C. C. (2004). "Index Properties of a Highly Weathered Old Alluvium." *Geotechnique*, 54(7), 441-551.
- Zhu, Jun-Gao, and Yin, Jian-Hua (2000). "Strain-rate-dependent stress-strain behavior of overconsolidated Hong Kong marine clay." *Canadian Geotechnical Journal*, 37, 1272-1282.

**APPENDIX A: LETTER OF PERMISSION FROM THE TRANSPORTATION  
RESEARCH BOARD**

from Rick Nugent <rnugen2@tigers.lsu.edu>  
to jawan@nas.edu  
date Fri, Oct 1, 2010 at 12:32 PM  
subject Fwd: PhD Permission Request for Rick Nugent  
mailed-by tigers.lsu.edu

Dear Javy Awan,

Below is the original permission request I sent. The TRB paper will become part of a much larger work. Again, I need permission to include the article in my dissertation, and LSU requires that there is explicit permission to make the work web viewable.

Sincerely,

Rick Nugent  
rnugen2@lsu.edu

----- Forwarded message -----

From: <TRBWeb4@nas.edu>  
Date: Tue, Sep 28, 2010 at 12:40 AM  
Subject: Rick Nugent has sent you a message.  
To: Phyllis Barber <pbarber@nas.edu>  
Cc: rnugen2@lsu.edu

Dear Phyllis Barber,

I am a PhD student at LSU, and I am currently writing my dissertation.

I recently published a paper in the Transportation Research Record ("Effect of Exopolymers on the Liquid Limit of Clays and Its Engineering Implications", Nugent, Zhang, and Gambrell, 2009). I would like copyright permission to use this paper in my dissertation. Specifically, I need a letter that provides permissions described in the following quote from the dissertation manual: "All previously copyright material included in the document must be web viewable and permission to use the material on the web must be included in the letter of permission."

Of course, acknowledgement of the TRB will be explicitly provided in my dissertation.

Sincerely,

Rick Nugent  
rnugen2@lsu.edu

from Awan, Javy <JAWAN@nas.edu>  
to Rick Nugent <rnugen2@tigers.lsu.edu>  
cc "Barber, Phyllis" <PBARBER@nas.edu>  
date Fri, Oct 1, 2010 at 1:23 PM  
subject RE: PhD Permission Request for Rick Nugent  
mailed-by nas.edu

To: Rick Nugent  
Louisiana State University

You have permission to include your paper, Effect of Exopolymers on the Liquid Limit of Clays and Its Engineering Implications, coauthored with Guoping Zhang and Robert P. Gambrell, in your PhD dissertation, which will be posted on the web.

Please include an acknowledgment of the paper's publication in Transportation Research Record: Journal of the Transportation Research Board, No. 2101, pp. 34-43 (a reference citation suffices), as well as a statement to the effect that permission was given "by the Transportation Research Board on behalf of the National Academy of Sciences."

Please let me know if you have any questions. Thank you for publishing your paper in TRB's journal. Every success with your dissertation and future research.

All the best,  
Javy Awan  
Director of Publications  
Transportation Research Board of the National Academies  
500 Fifth Street, NW - Keck 479  
Washington, DC 20001

## **APPENDIX B: LETTER OF PERMISSION FROM THE AMERICAN SOCIETY OF CIVIL ENGINEERS**

from Rick Nugent <rnugen2@tigers.lsu.edu>  
to permissions@asce.org  
date Thu, Sep 30, 2010 at 5:18 PM  
subject Use of Conference Papers in PhD Dissertation  
mailed-by tigers.lsu.edu

Dear ASCE,

I am a PhD student at LSU, and I am currently writing my dissertation.  
Recently, I have submitted three papers to two different ASCE  
conferences. These papers are as follows:

The Effects of Exopolymers on the Erosional Resistance of Cohesive Sediments  
R.A. Nugent, G. Zhang, R.P. Gambrell  
Proceedings for the Fifth International Conference on Scour and Erosion, 2010  
( <http://icse5.ce.gatech.edu/icse5status.htm> )

The Effect of Exopolymers on the Compressibility of Clays  
R.A. Nugent, G. Zhang, R.P. Gambrell  
Geo-Frontiers 2011 Proceedings

The Effect of Exopolymers and Void Ratio on the Erosional Resistance  
of Cohesive Sediments  
R.A. Nugent, G. Zhang, R.P. Gambrell  
Geo-Frontiers 2011 Proceedings

I would like copyright permission to use these papers in my  
dissertation. All of the papers have been reviewed and accepted for  
publication, but they are not currently in the ASCE digital library.  
For this reason, I am directly asking for permission. The permission  
letter must provide permissions as described in the following quote  
from the LSU dissertation manual: "All previously copyright material  
included in the document must be web viewable and permission to use  
the material on the web must be included in the letter of permission."

Of course, acknowledgement of the ASCE will be explicitly provided in  
my dissertation.

Sincerely,

Rick Nugent  
rnugen2@lsu.edu

from PERMISSIONS <permissions@asce.org>  
to Rick Nugent <rnugen2@tigers.lsu.edu>  
date Fri, Oct 1, 2010 at 9:08 AM  
subject RE: Use of Conference Papers in PhD Dissertation  
mailed-by asce.org

Hi Mr. Rick Nugent,

Thank you for your inquiry. You have our permission to use your paper "The Effects of Exopolymers on the Erosional Resistance of Cohesive Sediments" in your dissertation.

I have asked the ASCE Conference Dept to check for me that your two papers for Geo-Frontier have been accepted. It may take a few days. I will get back to you as soon as I have the confirmation from them.

Regards,

Xi Van Fleet  
Senior Manager, Information Services  
Publication Division  
American Society of Civil Engineers  
1801 Alexander Bell Drive  
Reston, VA 20191  
(703) 295-6278-FAX  
PERMISSIONS@asce.org

from PERMISSIONS <permissions@asce.org>  
to Rick Nugent <rnugen2@tigers.lsu.edu>  
date Tue, Oct 5, 2010 at 10:15 AM  
subject RE: Use of Conference Papers in PhD Dissertation  
mailed-by asce.org

Hi Mr. Nugent,

I have just received confirmation from the Conference Dept. that both of your papers have been accepted.

You have our permission to use three of your papers in your dissertation and to post it online, under the condition that the papers will not be reproduced exactly as the published versions.

Please add full credit lines to the material being reprinted: "With permission from ASCE" for the published paper, and "Posted Ahead of Print" (With permission from ASCE) for the yet to be published papers.

Regards,

Xi Van Fleet  
Senior Manager, Information Services  
Publication Division  
American Society of Civil Engineers  
1801 Alexander Bell Drive  
Reston, VA 20191  
(703) 295-6278-FAX  
PERMISSIONS@asce.org

## **VITA**

Rick Alton Nugent was born in 1985 at Baton Rouge, Louisiana. He earned the Bachelor of Science degree in Civil Engineering from Louisiana State University in May 2007. He earned his Engineering Intern license in June 2007. In addition to maintaining a 4.00 GPA as a high school, undergraduate, and graduate student, Rick scored in the top 1% on the ACT, SAT, and GRE exams, as well as scoring in the top 2% on the MCAT.

Since Rick has also been active in technical and professional societies, as well as service organizations, Rick has earned numerous awards. Some of his graduate awards include the LSU University Medal, LSU Engineering McLaughlin Dean's Medal, Donald W. Clayton Engineering Graduate Excellence Award, Vincent A. Forte Graduate School Fellowship, Tau Beta Pi Deuchler No. 28 Fellowship (without stipend), Alpha Lambda Delta Margaret Louise Cuninggim Fellowship, Middleton Scholarship, Dr. Louis J. Capozzoli Scholarship, and P.E. Engineering Graduate School Scholarship. His undergraduate awards include the Donald W. Clayton Engineering Undergraduate Excellence Award, LSU Alumni Top 100 Scholarship, Pegues Engineering Scholarship, TOPS Honors Scholarship, BR Teachers FCU Star Student Award, BR Downtown Kiwanis Outstanding Student Award, the national Tylenol Scholarship, LSU College of Engineering Outstanding Freshman and Sophomore awards, Louisiana Board of Regents Scholar, Advanced Placement Scholar with Distinction, United States Presidential Scholar Semi-finalist, Robert C. Byrd Honors Scholarship, and Boy Scouts of America Eagle Scout rank.

As a Graduate Research Assistant, Rick has done research in the area of biological soil improvement. Also, as an undergraduate, he worked in LSU's Chancellor's Future Leaders in Research program. He worked with Dr. Guoping Zhang in the Civil Engineering



Nanotechnology Lab, Dr. William G. Henk in the Veterinary Medicine's Electron Microscopy Lab, Dr. Marc L. Levitan in the Hurricane Center's Wind Tunnel Lab, and Dr. W. Todd Monroe in researching photoactivatable DNA.

As a culmination of Rick's research, he has one published journal paper and three conference papers that have been accepted for publishing. These include the following:

Nugent, R. A., Zhang, G., and Gambrell, R. P. (2009). "Effect of Exopolymers on the Liquid Limit of Clays and Its Engineering Implications." *Transportation Research Board: Journal of the Transportation Research Board*, 2101, 34-43.

Nugent, R. A., Zhang, G., and Gambrell, R. P. (2010). "The Effect of Exopolymers on the Erosional Resistance of Cohesive Sediments." *Proc., 5<sup>th</sup> International Conference on Scour and Erosion*, ASCE, San Francisco, CA, 162-171.

Nugent, R. A., Zhang, G., and Gambrell, R. P. (2011a). "The Effect of Exopolymers and Void Ratio on the Erosional Resistance of Cohesive Sediments." *Proc., Geo-Frontiers 2011*, ASCE, Dallas, TX, in press.

Nugent, R. A., Zhang, G., and Gambrell, R. P. (2011b). "The Effect of Exopolymers on the Compressibility of Clays" *Proc., Geo-Frontiers 2011*, ASCE, Dallas, TX, in press.

The degree of Doctor of Philosophy from Louisiana State University will be awarded to Rick at the May 2011 commencement.